

TRAF Regulation of Caspase-2-Dependent Apoptosis in Response to DNA Damage

by

Alexander Christian Robeson

Program in Molecular Cancer Biology
Duke University

Date: _____

Approved:

Sally Kornbluth, Supervisor

Kris Wood, Chair

Gerard Blobel

Jen-Tsan Chi

Christopher Newgard

Dissertation submitted in partial fulfillment of
the requirements for the degree of Doctor
of Philosophy in the Program in
Molecular Cancer Biology in the Graduate School
of Duke University

2016

ABSTRACT

TRAF Regulation of Caspase-2-Dependent Apoptosis in Response to DNA Damage

by

Alexander Christian Robeson

Program in Molecular Cancer Biology
Duke University

Date: _____

Approved:

Sally Kornbluth, Supervisor

Kris Wood, Chair

Gerard Blobe

Jen-Tsan Chi

Christopher Newgard

An abstract of a dissertation submitted in partial
fulfillment of the requirements for the degree
of Doctor of Philosophy in the Program in
Molecular Cancer Biology in the Graduate School of
Duke University

2016

Copyright by
Alexander Christian Robeson
2016

Abstract

The DNA of a cell operates as its blueprint, providing coded information for the production of the RNA and proteins that allow the cell to function. Cells can face a myriad of insults to their genomic integrity during their lifetimes, from simple errors during growth and division to reactive oxygen species to chemotherapeutic reagents. To deal with these mutagenic insults and avoid passing them on to progeny, cells are equipped with multiple defenses. Checkpoints can sense problems and halt a cell's progression through the cell cycle in order to allow repairs. More drastically, cells can also prevent passing on mutations to progeny by triggering apoptosis, or programmed cell death. This work will present two separate discoveries regarding the regulation of DNA damage-induced apoptosis and the regulation of the spindle checkpoint.

The protease caspase-2 has previously been shown to be an important regulator of DNA damage-induced apoptosis. In unstressed cells caspase-2 is present as an inactive monomer, but upon sensing a stress caspase-2 dimerizes and becomes catalytically active. The mechanisms that regulate this dimerization are poorly understood. The first research chapter details our development of a novel method to study dimerized caspase-2, which in turn identified TRAF2 as a direct activator of caspase-2. Specifically, we utilized the Bimolecular Fluorescence Complementation technique, wherein complementary halves of the Venus fluorophore are fused to

caspase-2: when caspase-2 dimerizes, the non-fluorescent halves fold into a functional Venus fluorophore. We combined this technique with a Venus-specific immunoprecipitation that allowed the purification of caspase-2 dimers. Characterization of the caspase-2 dimer interactome by MS/MS identified several members of the TNF Receptor Associated Factor (TRAF) family, specifically TRAF1, 2, and 3. Knockdown studies revealed that TRAF2 plays a primary role in promoting caspase-2 dimerization and downstream apoptosis in response to DNA damage. Identification of a TRAF Interacting Motif (TIM) on caspase-2 indicates that TRAF2 directly acts on caspase-2 to induce its activation. TRAF2 is known to act as an E3 ubiquitin ligase as well as a scaffold for other E3 ubiquitin ligases. Indeed, we identified three lysine residues in the caspase-2 prodomain (K15, K152, and K153) important for its ubiquitination and complex formation. Together these results revealed a novel role for TRAF2 as a direct activator of caspase-2 apoptosis triggered by DNA damage.

During mitosis, when the cell prepares to divide, great care is taken to ensure that the chromosomes are properly segregated between the two daughter cells by the mitotic spindle. This is primarily accomplished through the spindle checkpoint, which becomes activated when the mitotic spindle is not properly attached to each chromosome's kinetochore. When activated, the primary effector of the spindle checkpoint, the mitotic checkpoint complex (MCC), inhibits the anaphase-promoting complex (APC/C) by binding to the APC/C co-activator, CDC20. This prevents the

APC/C from targeting critical pro-mitotic proteins, like cyclin B and securin, to promote mitotic exit. Although the function of the MCC is well understood, its regulation is not, especially in regard to protein phosphatases. To investigate this, we activated the spindle checkpoint with microtubule inhibitors and then treated with a variety of phosphatase inhibitors, examining the effect on the MCC and APC/C. We found that two separate inhibitors, calyculin A and okadaic acid (1 μ M), were able to promote the dissociation of the MCC. This led to the activation of the APC/C, but the cells remained in mitosis as evidenced by high levels of Cdk1 activity and chromosome condensation. This is the first time that phosphatases have been shown to be essential to maintaining the MCC and an active spindle checkpoint.

Dedication

For my wonderful wife RiLee, my fellow Bio nerd, and my best friend – thank you for everything. You are amazing. And for my son and little buddy Sam, who brings so much joy and life to our home. I love you both so much - thank you for your unfailing support, without which I cannot imagine being able to get through this grad school craziness.

Contents

Abstract	iv
List of Tables	xii
List of Figures	xiii
Acknowledgements	xv
1. Introduction	1
1.1 The unifying theme	1
1.2 Apoptosis.....	1
1.2.1 The caspase family	3
1.2.2 From caspases to apoptotic morphology	6
1.2.3 Intrinsic apoptosis	8
1.2.4 Extrinsic apoptosis	12
1.2.5 Caspase-2.....	13
1.2.5.1 A brief overview of caspase-2	13
1.2.5.2 Caspase-2 mechanism of action	15
1.2.5.3 Monitoring caspase-2 activation: bimolecular fluorescence complementation	19
1.2.5.4 Caspase-2 localization	22
1.2.5.5 Caspase-2 activation platforms	24
1.3 TNF-Receptor Associated Factors.....	29
1.3.1 TRAFs as adaptor proteins.....	29
1.3.2 TRAFs as E3 ubiquitin ligases	30

1.3.2.1 RING domain and ubiquitination overview	30
1.3.2.2 TRAF2, ubiquitination, and caspase activation	32
1.4 Mitosis: where cells divide	32
1.4.1 Regulation of mitosis	35
1.4.1.1 Cyclin-dependent kinases and their partner cyclins.....	35
1.4.1.2 Mitotic phosphatases PP1 and PP2A	36
1.4.1.3 The anaphase promoting complex/cyclosome (APC/C).....	36
1.4.2 The spindle checkpoint.....	37
2. Materials and methods.....	40
2.1 Materials and methods for chapter 3.....	40
2.1.1 Reagents and cell culture.....	40
2.1.2 Antibodies	40
2.1.3 Plasmids.....	41
2.1.4 Generation of Tet system responsive caspase-2 BiFC expressing cell line.....	42
2.1.5 RNA interference.....	43
2.1.6 Immunoprecipitation.....	43
2.1.7 Microscopic or flow cytometric analysis of BiFC signal	44
2.1.8 BiFC dimer immunoprecipitation by GFP-Trap	45
2.1.9 Co-immunoprecipitation with BiFC dimer specific capture and mass spectrometry analysis of the protein complex	46
2.1.10 Apoptotic cell death detection by Annexin V or PI staining.....	47
2.1.11 Detection of ubiquitination of caspase-2.....	48

2.1.12 Recombinant protein production.....	49
2.1.13 <i>In vitro</i> binding assay of ubiquitinated caspase-2 and recombinant MBP-TRAF2	50
2.1.14 Salt titration assay to test the strength of caspase-2 dimer stability.....	50
2.1.15 VDVAase activity assay for caspase-2 purified from cells.....	51
2.1.16 Statistical analysis.....	52
2.2 Materials and methods for chapter 4.....	52
2.2.1 Reagents and cell culture.....	52
2.2.2 RNA interference.....	53
2.2.3 Plasmids.....	54
2.2.4 Antibodies, Western Blotting, and Co-Immunoprecipitation.....	54
2.2.5 qPCR.....	56
2.2.6 Chromosome spread.....	57
2.2.7 <i>In vitro</i> lambda phosphatase assay	57
3. Targeted immunoprecipitation of BiFC dimers reveals a novel role for TRAFs in regulating caspase-2 dimerization and apoptosis in response to DNA damage.....	58
3.1 Introduction.....	58
3.2 Results	61
3.2.1 Combining GFP-Trap with BiFC to immunoprecipitate caspase-2 dimers	61
3.2.2 TRAF1, 2, and 3 bind to dimerized, active caspase-2.....	66
3.2.3 TRAF2 is critical for caspase-2 activation and apoptosis in response to DNA damage.....	69

3.2.4 TRAF2 interacts directly with caspase-2 via a TRAF Interaction Motif (TIM) to promote dimerization.....	71
3.2.5 TRAF2-dependent ubiquitination of the caspase-2 prodomain is critical for dimer stability and fully enzymatic activity.....	73
3.3 Discussion.....	77
4. Mitotic phosphatase activity is required for MCC maintenance during the spindle checkpoint.....	83
4.1 Introduction.....	83
4.2 Results.....	87
4.2.1 Calyculin A and okadaic acid can override the spindle checkpoint to activate the APC/C.....	87
4.2.2 Phosphatase activity is required for MCC maintenance during the spindle checkpoint.....	90
4.2.3 Calyculin A and okadaic acid-induced APC/C activation does not lead to mitotic exit.....	95
4.3 Discussion.....	101
5. Conclusions and future directions.....	106
5.1 BiFC combined with GFP-Trap for the identification of novel regulators of active caspase-2.....	106
5.2 An unexpected role for protein phosphatase activity: promoting the MCC.....	111
5.3 Concluding remarks.....	113
References.....	114
Biography.....	132

List of Tables

Table 4.1 Mass spectrometry results showing Myc-Mad2 and Myc-BubR1 binding proteins.....	102
--	-----

List of Figures

Figure 1.1 Intrinsic apoptosis pathway as regulated by caspase-2.	11
Figure 1.2 Mechanism of caspase-2 activation.	17
Figure 1.3 Caspase-2 bimolecular fluorescence complementation.	21
Figure 3.1 GFP-Trap selectively immunoprecipitates Casp2pro BiFC dimers to the exclusion of monomers.	64
Figure 3.2 Caspase-2 stimuli do not induce expression of CASP2pro BiFC mRNA.	65
Figure 3.3 Workflow for mass spectrometry experiment.	66
Figure 3.4 TRAF1, 2, and 3 bind to active, dimerized caspase-2.	68
Figure 3.5 TRAF2 is required for cisplatin-induced, caspase-2-initiated apoptosis.	70
Figure 3.6 TRAF2 interacts directly with caspase-2 to induce activation.	72
Figure 3.7 Caspase-2 prodomain is ubiquitinated after dimerization at K15, K152, and K153.	75
Figure 3.8 Caspase-2 prodomain ubiquitination appears to be necessary for dimer stability and activity.	78
Figure 4.1 Calyculin A and okadaic acid (1 μ M) induce cyclin B degradation in spindle checkpoint-arrested cells via the APC/C ^{CDC20}	88
Figure 4.2 Calyculin A and okadaic acid (1 μ M) induce MCC dissociation during the spindle checkpoint.	91
Figure 4.3 MCC dissociation precedes the degradation of cyclin A and B.	93
Figure 4.4 Calyculin A-induced phosphorylation of CDC20 and BubR1 at mass spectrometry-identified sites is not necessary for MCC dissociation.	94
Figure 4.5 Calyculin A and okadaic acid (1 μ M) do not induce mitotic exit despite APC/C activation.	97

Figure 4.6 Knockdown of PPP family phosphatases did not induce cyclin degradation. 99

Figure 4.7 Knockdown of mass spectrometry-identified phosphatases did not induce cyclin degradation. 101

Acknowledgements

First, I want to thank my advisor, Sally Kornbluth. As a scientist, Sally exudes a combination of ingenuity, curiosity, and optimism, all of which are traits that I hope to emulate. As a mentor, Sally genuinely cares about her students, both before and after graduation. Her support and advice, especially when it was given in times of both professional and family crisis, has meant a lot to me. Thank you Sally. I also want to thank my past and present dissertation committee – Kris Wood, Ashley Chi, Gerry Blobel, Chris Newgard, and Jeff Rathmell – for their guidance and support.

And of course, there is the Kornbluth Lab. I am especially grateful to Kenkyo Matsuura for the opportunity to work closely with him over the last 5 years. Kenkyo is an excellent scientist and friend, and I have learned so much from his mentorship and example. I also want to thank Kelly Lindblom for the opportunity to work with her on Team TRAF, as well as Kristen Foss and Liguozhang, my collaborators on the spindle checkpoint phosphatase project. Nai-Jia Huang, Erika Segear Johnson, Kim Cocce, Chihsheng Yang, Bofu Huang, Jeff Wotjon, Chris Freel, Josh Andersen, Mike Thomenius, and more – thank you for your friendship, and for making the Kornbluth Lab a great place to work. And finally, a big thank you to Denise Ribar for her tireless work that keeps the lab running and lets us operate smoothly, and for being the best lab “mom” ever.

I also need to thank Will Thompson, Laura Dubois, and Sarah Mabbett of the Duke Proteomics and Metabolomics Shared Resources, Olga Ilkayeva and Chris Newgard of the Sarah W. Stedman Nutrition and Metabolism Center, and Mike Cook of the Flow Cytometry Shared Resource for their expertise and guidance. I also want to thank my DGSA, Jamie Baize-Smith, for her patience, consistent help, and advice over the years.

Finally, I want to thank the immense support that both my family and I have been given by our parents, siblings, friends, church, and broader community. In many ways, this was a collaborative effort, and this project would not have come to fruition without all of this amazing support.

1. Introduction

1.1 The unifying theme

This dissertation is composed of two separate projects: the first (chapter 3) on apoptosis in response to high levels of DNA damage induced by chemotherapeutic agents, and the second (chapter 4) on the maintenance of cell cycle arrest in response to mitotic spindle disruption. While these two subjects might at first seem disparate, both are focused on cellular safeguards that protect the integrity of genetic material. In fact, genetic insults often initially result in cell cycle arrest, giving cells time to address the issue and, if possible, repair it. However, when genetic integrity is irreparably compromised, such as in the case of persistent or extensive DNA damage, cells are able to initiate the final failsafe of programmed cell death. Both of these processes play critical roles in the response of healthy and cancerous tissues to frontline chemotherapeutic drugs. Thus, further studies that enable a better understanding of how cells respond to genetic insults could help develop better therapeutic strategies for targeting tumors with less side effects.

1.2 Apoptosis

Apoptosis is a form of programmed cell death, wherein a cell undergoes a genetically-encoded form of suicide. It was initially characterized by the distinct morphological changes exhibited by the dying cell, where the cytoplasm and nucleus,

with all of their components, are packaged into small, membrane-enclosed vesicles called apoptotic bodies (J F R Kerr 1972). Specifically, this packaging process includes the condensation of chromatin, fragmentation of DNA, breakdown of the nuclear envelope, shrinking of the cytoplasm, blebbing of the outer membrane, and exposure of an “Eat me” signal on the exterior of the membrane (Elmore 2007). The apoptotic bodies are in turn phagocytosed by other cells, such as macrophages, allowing for a neat and orderly removal of the dying cell. This prevents the exposure of the inner contents of the cell to the surrounding tissue, which would trigger an inflammatory response and secondary necrosis (Silva 2010). The purpose of such a process in multi-cellular organisms is to rid the organism of unnecessary or unhealthy cells without damaging the surrounding tissue.

Apoptosis takes place during normal development to shape tissues and as a homeostatic mechanism (Elmore 2007). The first apoptotic genes were discovered in *C. elegans* where they were determined to facilitate the timely removal of over 10% of the worm’s somatic cells during its development (Ellis 1986; Horvitz 1999). In mammals, apoptosis is known to shape the digits of the hand and prune nerve cells in the brain during development, as well as cull overabundant or autoreactive lymphocytes (Cecconi et al. 1998; Kuida et al. 1996; Green 2003; Nagata, Hanayama, and Kawane 2010). It is

also utilized by the immune system to clear infected cells, simultaneously eliminating the pathogen and its host environment necessary for its survival (Labbé and Saleh 2008).

Because apoptosis is commonly used to clear unhealthy and unwanted cells, it is not surprising that its misregulation can give rise to disease. For instance, some of the pathology of neurodegenerative diseases is attributed to the triggering of excessive apoptosis (Ghavami et al. 2014). Suppression of apoptosis, on the other hand, can lead to inappropriate proliferation of unhealthy cells and is known to contribute to autoimmune diseases and cancer (Elmore 2007; Letai 2008). Thus, the ability of a cell to balance between life and death is highly regulated at the molecular level.

1.2.1 The caspase family

There are a range of proteins involved in and impinging on the apoptotic pathway, but the core apoptotic factors are cysteine-dependent aspartyl-specific endoproteases, or caspases. This central role for caspases has been confirmed in genetic studies as well as through the use of various caspase inhibitors, which have been shown to block the effects of apoptosis. Caspases exist in unstressed cells as inactive zymogens and have a basic structure of an N-terminal prodomain followed by two catalytic domains, one large (p20) and one small (p10) (Riedl and Shi 2004). When caspases sense a pro-death signal and become activated, they go on to cleave a host of other signaling

and structural proteins (including other caspases), eventually leading to the orderly dismantling of the cell (Crawford and Wells 2011).

Apoptotic caspases can be divided into two main categories: initiator and executioner caspases. Initiator apoptotic caspases (like mammalian caspase-2, -8, -9, and -10) act as sensors of pro-death signals, controlling the initiation of the caspase signaling cascade. They are expressed in monomeric form and require dimerization for activation, which is facilitated by the binding of adaptor proteins to motifs in their long prodomains (Riedl and Shi 2004; Parrish, Freel, and Kornbluth 2013). Caspase-8 and -10 each contain two death effector domains (DEDs) in their prodomains that facilitate their binding to other DED containing proteins. Similarly, caspase recruitment domains (CARDs) in the prodomains of caspase-2 and -9 can interact with the CARD of adaptor proteins.

Executioner caspases (caspase-3, -6, and -7), on the other hand, have a short prodomain and even in their inactive state exist as dimers. Instead, their activation occurs initially through cleavage, primarily by initiator caspases (Riedl and Shi 2004; Turk and Stoka 2007; Parrish, Freel, and Kornbluth 2013). Their targets further differentiate these two classes of caspases: while initiator caspases primarily focus on activating executioner caspases, both directly and indirectly, executioner caspases target

hundreds of substrates (Riedl and Shi 2004; Luthi and Martin 2007; Tait and Green 2010; Crawford and Wells 2011).

A third category of caspases includes the non-apoptotic inflammatory human caspases-1, -4, -5, and -12 (McIlwain, Berger, and Mak 2013). Similar to caspase-2 and -9, these caspases all possess long CARD-containing prodomains that play a role in their activation (Shi et al. 2014; Shi et al. 2015; de Zoete et al. 2014). Inflammatory caspases have been demonstrated to play roles critical in the immune system and were classically defined as the enzymes that cleaved the cytokines IL-1 β and IL-18, leading to their secretion and consequent inflammation (de Zoete et al. 2014). Later studies have begun to tie these caspases to another form of cell death distinct from apoptosis called pyroptosis. Unlike apoptosis, pyroptosis results in the rupture of the plasma membrane and is inherently pro-inflammatory, playing a role in fighting microbial infections (Bergsbaken, Fink, and Cookson 2009). While investigation of such mechanisms is beyond the scope of this work, further studies in inflammatory caspases may well complement our understanding of the regulation and function of apoptotic caspases and should not be neglected.

1.2.2 From caspases to apoptotic morphology

Substrate cleavage could theoretically have a number of effects. It could inflict a simple loss of function on the substrate, or it could reveal a new function by removal of an inhibitory domain or by converting the substrate to a dominant negative isoform. However, it is also possible (indeed, likely) that a number of the hundreds of identified substrates are simply bystanders and do not play a significant role in apoptosis. Many of the current substrates have been identified through *in vitro* proteomics screens and not fully validated (Poreba et al. 2013). As such, much more effort is needed to determine the functional importance of the ever-growing list of caspase substrates.

There is, however, a subset of caspase substrates that have been tied directly to phenotypic changes that occur in the dying cell. In relation to nuclear changes, the condensation of the chromatin appears to be promoted by the protein Acinus after its cleavage by caspase-3, although the mechanism is not clear (Sahara et al. 1999; Joselin, Schulze-Osthoff, and Schwerk 2006). Caspase-3 and caspase-7 cleave the inhibitor of caspase-activated DNase (ICAD), leading to the release and activation of caspase-activated DNase (CAD). CAD then goes on to fragment the DNA for packaging into apoptotic bodies (Enari et al. 1998; Wolf et al. 1999). Also, the proteolysis of nuclear lamins by caspase-6 and caspase-3 helps lead to the breakdown of the nuclear envelope (Luthi and Martin 2007). Another DNA-related target of executioner caspases is the

DNA-repair enzyme Poly-ADP-ribose polymerase. Caspase-3 and -7 cleavage of PARP removes its DNA-binding domain and inhibits its ability to repair DNA (Sodhi, Singh, and Jaggi 2010).

In regards to apoptotic changes at the plasma membrane, blebbing is largely induced by the caspase-mediated activation of the serine/threonine kinase ROCK-1 (Riento and Ridley 2003). ROCK-1 mediates the activity of Rho-type GTPases in regulating dynamics of the actin cytoskeleton. Caspase cleavage of ROCK-1 removes a C-terminal autoinhibitory domain, resulting in constitutive activation and the blebbing phenotype.

The “Eat me” signal displayed on the plasma membrane was discovered over twenty years ago, but the caspase targets responsible for it remained elusive until just recently (Fadok et al. 1992; Segawa et al. 2014; Segawa, Kurata, and Nagata 2016). Phosphatidylserine is normally asymmetrically localized to the cytoplasmic leaflet of the cell membrane. This distribution of phosphatidylserine was found to be controlled by the proteins ATP11C and ATP11A, which function as ATP-dependent aminophospholipid translocases (or flippases), along with their chaperone CDC50. Both ATP11C and ATP11A are caspase substrates whose cleavage results in a loss of function flippase function (Segawa et al. 2014; Segawa, Kurata, and Nagata 2016). This leads to re-distribution of phosphatidylserine to the extracellular leaflet of the membrane, which

in turn is recognized by professional phagocytes (Nagata, Hanayama, and Kawane 2010).

1.2.3 Intrinsic apoptosis

There are two main caspase activation pathways in vertebrates: intrinsic and extrinsic apoptosis. Intrinsic apoptosis is cell autonomous, centers around the mitochondria, and is activated by internal death signals like metabolic stress, cytoskeletal disruption, and genotoxic stress. Activation promotes mitochondrial outer membrane permeabilization (MOMP) and the consequent release of a number of pro-apoptotic factors, including cytochrome *c*, from the mitochondrial intermembrane space (IMS). When released, cytochrome *c* goes on to bind the adaptor protein Apaf-1, which in turn binds and activates caspase-9. This complex, known as the apoptosome, cleaves and activates executioner caspase-3 and caspase-7 to begin the dismantling of the dying cell.

MOMP is largely considered to be a point of no return, as it results both in the triggering of the caspase cascade and extensive impairment of normal mitochondrial function (Tait and Green 2013). As such, it is highly regulated by a large family of proteins known as the Bcl-2 family, defined by possessing one or more Bcl-2 homology (BH) domains. There are generally three types of Bcl-2 family members: the anti-apoptotic Bcl-2 proteins, the pro-apoptotic effectors, and the BH3-only proteins. The core

effectors of MOMP are the pro-apoptotic proteins Bax and Bak, which when activated form pores in the outer mitochondrial membrane (OMM) (Tait and Green 2010). In unstressed cells, Bak is constitutively localized to the OMM, while Bax is normally localized to the cytoplasm (Chipuk et al. 2010). Upon activation, both Bax and Bak undergo extensive conformational changes that allow targeting to the OMM (Bax) and homo-oligomerization (Bax and Bak) to induce MOMP. While the mechanism and nature of the pores is currently unclear, the role of Bax and Bak as the primary inducers of MOMP has been firmly established (Lindsten et al. 2000; Wei et al. 2001).

Anti-apoptotic Bcl-2 proteins such as Bcl-2, Bcl-xL, and Mcl-1 oppose the activation of Bax or Bak. These proteins are generally localized to the mitochondria and act by directly binding and sequestering the effectors and BH3-only proteins. BH3-only proteins can function in one of two ways: they can either directly activate Bax or Bak (Bim and Bid) or they can bind anti-apoptotic Bcl-2 proteins, displacing them from interactions with Bax, Bak or the direct activators (Bad, Bik, Noxa, Puma, etc.). The BH3-only and anti-apoptotic Bcl-2 proteins display varying affinities for each other and the effector proteins, which allows for an intricate fine-tuning of the balance between life and death (Chipuk et al. 2010).

BH3-only proteins are regulated through a number of mechanisms. Noxa and Puma can be transcriptionally upregulated by p53 in the wake of DNA damage or

growth factor withdrawal (Oda et al. 2000; Nakano and Vousden 2001; Yu et al. 2001). Growth factors promote phosphorylation of Bad by Akt, leading to an inhibitory binding to 14-3-3 proteins (del Peso et al. 1997; Datta et al. 1997). This inhibitory interaction can be disrupted by JNK- or Cdc2-mediated phosphorylation at an adjacent site, allowing for Bad activation (Konishi et al. 2002; Donovan et al. 2002). Growth factors can also induce an Erk-dependent phosphorylation of Bim, which promotes its ubiquitination and degradation (Ley et al. 2003).

Bid is a unique member of the BH3-only protein subfamily. Unlike the other BH3-only proteins, which are intrinsically unstructured proteins, Bid maintains a globular structure similar to the effector and anti-apoptotic Bcl-2 proteins (Billen, Shamas-Din, and Andrews 2008; Chipuk et al. 2010). Bid is also unique in that it possesses an auto-inhibitory N-terminus that must be cleaved in order for Bid to become active (Tan, Tan, and Yu 1999). Upon cleavage, the C-terminal BH3 domain-containing portion of Bid, termed truncated Bid or tBid, translocates to the mitochondria where it can recruit and activate Bax or Bak and induce MOMP (Leber, Lin, and Andrews 2007). Bid cleavage can be induced by several proteases, including caspase-2 and caspase-8, the extrinsic apoptosis initiator caspase (Bonzon et al. 2006; Li et al. 1998; Luo et al. 1998) (Figure 1.1).

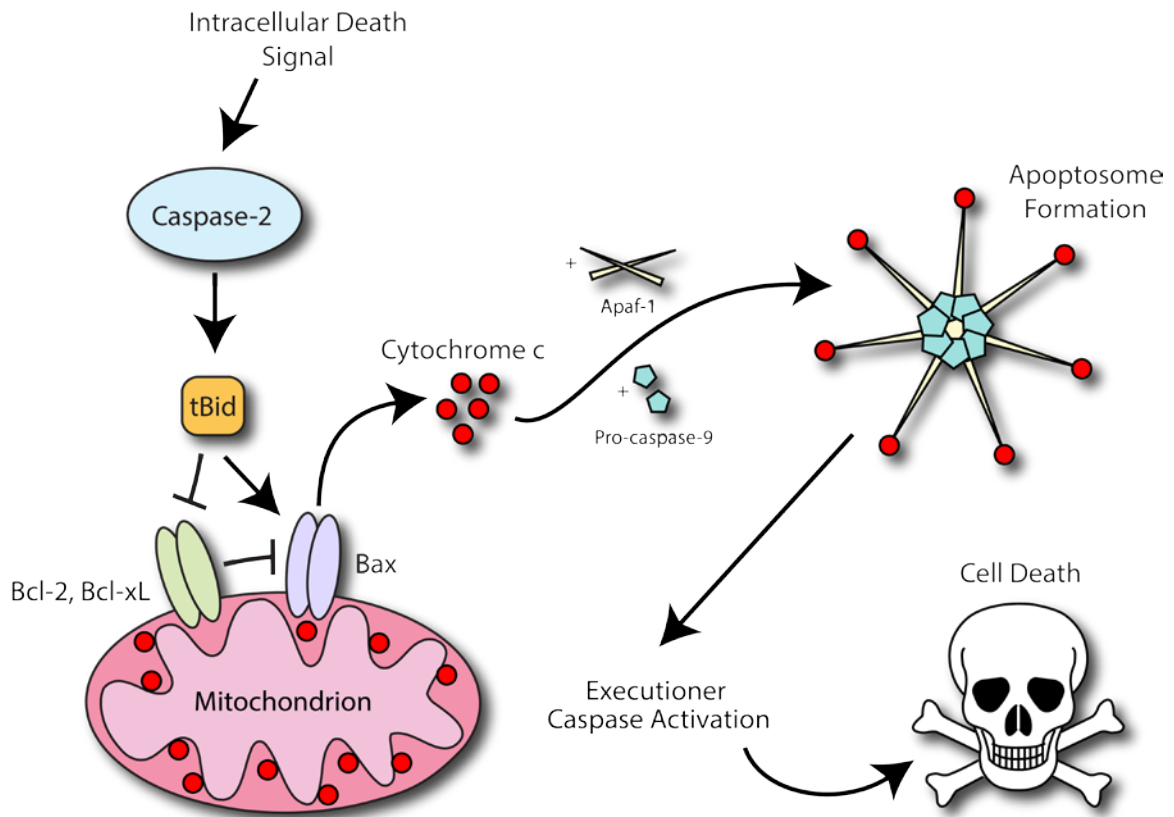


Figure 1.1 Intrinsic apoptosis pathway as regulated by caspase-2.

Caspase-2 can act as an initiator of intrinsic apoptosis by cleaving (truncating) the BH3-only protein Bid to convert it to its pro-apoptotic form (tBid). tBid can then directly activate the pro-apoptotic Bcl-2 protein Bax, which translocates to the mitochondrial outer membrane, oligomerizes, and induces the release of pro-apoptotic proteins from the mitochondrial intermembrane space. tBid is also able to inhibit the anti-apoptotic Bcl-2 proteins, such as Bcl-2 or Bcl-xL, thereby relieving Bax from inhibition. The most critical pro-apoptotic protein released is cytochrome c, which together with the adapter protein Apaf-1 induces the oligomerization of caspase-9 into a large caspase-9 activating complex. Caspase-9 then goes on to cleave and activate executioner caspases (-3 and -7), which in turn target a host of molecular substrates to facilitate apoptotic cell death.

1.2.4 Extrinsic apoptosis

As expected from its name, extrinsic apoptosis is regulated by members of the TNF superfamily of extracellular death ligands, such as CD95L/FasL and Apo2L/TRAIL. These cytokines are known to trigger the caspase cascade by binding and activating their respective death receptors. This interaction induces oligomerization of the receptor, which in turn is able to recruit and cluster the death domain (DD) containing protein FADD to its intracellular domain (Walczak 2013). Alongside the DD, FADD also possesses a DED, which allows it to recruit and promote proximity-induced dimerization and activation of caspase-8. Together, this complex is termed the death-inducing signaling complex (DISC).

Upon activation, caspase-8 can directly cleave and activate caspase-3 (Walczak 2013). In some cells, termed type I cells, this is a robust enough pathway to lead directly to apoptosis. However, other cells (type II) exhibit resistance to this direct activation, most likely through the action of X-linked inhibitor of apoptosis protein (XIAP), which can directly bind and inhibit caspase-3 (Jost et al. 2009). To induce apoptosis in these cells, caspase-8 triggers MOMP by cleaving and activating Bid. Beside cytochrome c, MOMP also releases the IAP inhibiting proteins Smac and HtrA2/Omi from the IMS. Once released, Smac can promote the autoubiquitination of XIAP, while HtrA2/Omi, a serine protease, cleaves and deactivates XIAP. Cytochrome c then goes on to promote

caspase-9 activation and the consequent apoptotic signaling cascade. Interestingly, while TNF was the founding member of this family of cytokines, it is a relatively weak inducer of extrinsic apoptosis compared to its family members (Walczak 2013). Instead, TNF signaling most often results in the intracellular activation of the NF- κ B family.

1.2.5 Caspase-2

1.2.5.1 A brief overview of caspase-2

Caspase-2 was the second caspase to be identified, with caspase-1 being the first (Kumar, Tomooka, and Noda 1992). It was first named Neural Precursor Cell Expressed, Developmentally Down-Regulated 2 (Nedd-2), as it was originally discovered to be expressed in the mouse brain in early development and then down-regulated in the adult mouse. A following paper renamed it Ice and ced-3 homolog (Ich-1) due to its sequence similarity to caspase-1 (Ice) and the nematode caspase CED-3 (Wang et al. 1994; Kumar et al. 1994). Both of these naming conventions were largely dropped when the expanding cysteine protease family was renamed to caspase (Alnemri et al. 1996). Interestingly, despite being discovered so early on and appearing to be highly conserved across species, our understanding of caspase-2 is still fairly limited.

It must be noted that the claim that caspase-2 can trigger apoptosis as an initiator caspase is controversial. Caspase-2 null mice were found to be developmentally normal, except for a moderate excess of oocytes (Bergeron et al. 1998). Furthermore, caspase-2 is

not able to cleave any other caspase except for itself, unlike other initiator caspases (-8 and -9) (Guo et al. 2002). And finally, caspase-2 can be cleaved and directly activated by caspase-3 (Harvey et al. 1996; Paroni et al. 2001; Slee et al. 1999). This led to the hypothesis that it functions primarily as part of a feed forward loop to promote further MOMP and accelerate apoptosis in response to a pro-death stimulus.

However, while these studies do shed light on caspase-2, they do not disqualify it from initiator caspase status. First, it does appear that caspase-2 is largely dispensible for early development, aside from regulating oocyte death ((Bergeron et al. 1998; Nutt et al. 2005; Nutt et al. 2009). This has led to the hypothesis that caspase-2 functions largely as a stress-induced initiator caspase. Furthermore, just as many other factors that act upstream of MOMP can have a functional niche, caspase-2 likely only acts as an initiator of apoptosis protein in a discrete set of circumstances.

Recent mouse work has provided intriguing insights into some of those circumstances. Although caspase-2 null mice do not spontaneously form tumors, when crossed into lymphoma-promoting mouse models (c-Myc overexpression, loss of ATM) loss of caspase-2 was found to enhance the lymphomagenesis (Ho et al. 2009; Manzl et al. 2012; Puccini et al. 2013). Deletion of caspase-2 was also found to potentiate breast cancer tumorigenesis in an MMTV/*c-neu* background (Parsons et al. 2013). Most recently, a study of chemically-induced (diethylnitrosamine) hepatocellular carcinoma found that

loss of caspase-2 also accelerates tumorigenesis. Furthermore, experiments in MEFs have shown that cells lacking caspase-2 are more resistant to genotoxic and cytoskeletal stresses (Dorstyn et al. 2012; Ho et al. 2009; Ho et al. 2008). Together, these studies provide substantial evidence that caspase-2 plays a tumor suppressor role in distinct tumorigenic scenarios.

Caspase-2 is also emerging as an important regulator of other pathologies. One study that helped reinvigorate the field showed that caspase-2 null mice experience an accelerated aging phenotype (Zhang et al. 2007). And in a twist, loss of caspase-2 was found to protect against obesity-related liver damage and metabolic disorders (Machado et al. 2015; Machado et al. 2016; Segear Johnson et al. 2013). Thus, it is clear that caspase-2 can play a significant role in specific physiological and pathological settings.

Unfortunately, the ability to gain further insight into caspase-2 function has been hampered by a lack of novel, precise tools to study its regulation. Researchers should focus on developing these tools to enable more robust research with the intent of developing a more concrete understanding of the physiological relevance of caspase-2.

1.2.5.2 Caspase-2 mechanism of action

As mentioned above, caspase-2 is classified as an initiator caspase. This is evidenced by its long CARD-containing prodomain, activation by dimerization, and ability to directly cleave and activate Bid to induce MOMP (Guo et al. 2002; Paroni et al.

2002; Bouchier-Hayes and Green 2012). As with other initiator caspases, caspase-2 dimerization was found to precede its autoproteolytic processing, and this depended on the prodomain (Butt et al. 1998). Also like other initiator caspases, overexpression of caspase-2 can lead to its spontaneous dimerization and activation (Butt et al. 1998; Colussi et al. 1998). The mechanism by which this occurs is unclear, but does require the CARD. Interestingly, one study found that by replacing the short caspase-3 prodomain with the long prodomain of caspase-2, caspase-3 acquired the capacity to autoactivate when overexpressed, an ability largely absent from wild type caspase-3 (Colussi et al. 1998).

Autoproteolytic processing, which occurs in stages at D333, D169, and finally D347, cleaves the caspase-2 proenzyme into three main peptides: prodomain, p19 catalytic domain, p12 catalytic domain (Harvey, Butt, and Kumar 1997; Harvey et al. 1996; Baliga, Read, and Kumar 2004) (Fig. The prodomain is eventually discarded, while the p19 and p12 catalytic domains together form a single catalytic site. Technically, the fully cleaved and activated caspase-2 dimer is a heterotetramer containing two p19/p12 dimers and thus two catalytic sites (Schweizer, Briand, and Grütter 2003) (Figure 1.2). A crystal structure of the fully processed heterotetramer reveals that it also possesses a unique disulfide bridge buried in the interface between the two p12 subunits (Schweizer, Briand, and Grütter 2003). The function of this interaction is unknown, but it

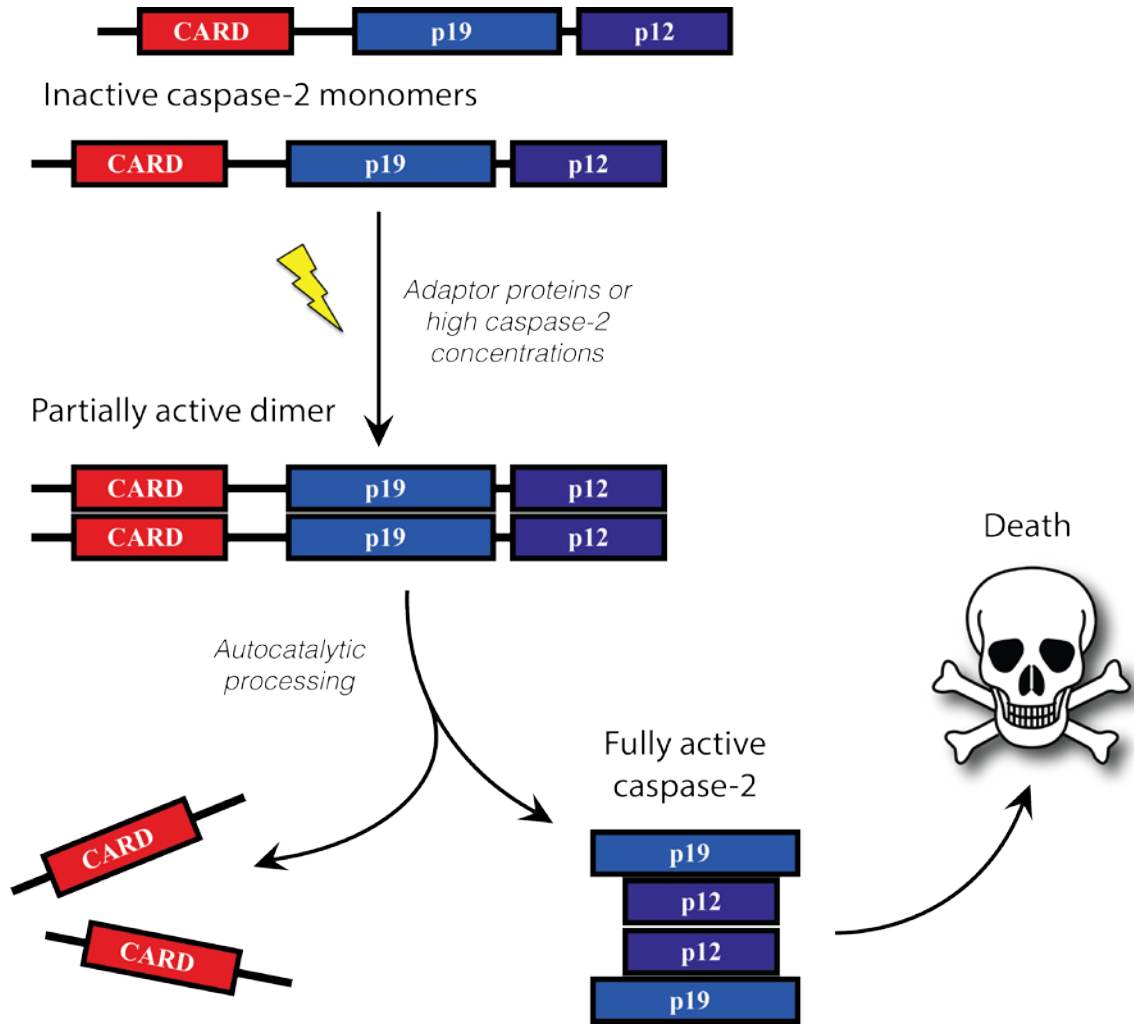


Figure 1.2 Mechanism of caspase-2 activation.

Caspase-2 exists in the cell under unstressed conditions as an inactive monomer. The initial step in its activation involves proximity-induced dimerization, which requires the CARD-containing prodomain and can be facilitated either by adapter proteins or high concentrations of caspase-2. This yields a partially active caspase-2 complex, which then goes on to induce autocatalytic processing, resulting in the formation of a fully active caspase-2 dimer of dimers, or heterotetramer, composed of two p12 and two p19 catalytic domains.

was proposed to help stabilize the mature caspase-2 heterotetramer. However, mutation of the relevant cysteine was found to have no effect on dimerization and processing (Baliga, Read, and Kumar 2004). Thus, further work is needed to determine its relevance.

Non-cleavable caspase substrates can be generated by mutating the critical aspartate residue found in the cleavage site to an alanine. Interestingly, mutation of the three main caspase-2 autocleavage sites prevents processing, but does not prevent either dimerization or the formation of an active protease (Baliga, Read, and Kumar 2004). However, this noncleavable caspase-2 dimer has a reduced catalytic activity when compared to fully processed enzyme and is not able to induce apoptosis at physiologically-relevant levels. This validates that proximity-induced dimerization of caspase-2 is the first step in its activation, followed by processing and the formation of a mature, death-inducing protease.

As a side note, the caspase-2 studies mentioned above utilized caspase-2 overexpression to initiate a spontaneous activation. These studies provided valuable insight into the importance of the caspase-2 prodomain and how it sets caspase-2 apart from executioner caspases in terms of its mechanism of activation. While it is unclear if induction of caspase-2 expression to such an extent can be triggered in a physiological setting, subsequent studies have validated the order of caspase-2 activation as occurring first through dimerization and second through cleavage.

1.2.5.3 Monitoring caspase-2 activation: bimolecular fluorescence complementation

Many of the early studies of caspase-2 sought to study its activation using cleavage as a readout. Unfortunately, as was mentioned above, caspase-2 is initially activated by dimerization, and cleavage can be induced by other proteases. Thus, using this readout has likely led to some confusing and conflicting reports on caspase-2. Other studies utilized a pentapeptide substrate composed of the sequence VDVAD. While caspase-2 does appear to prefer this substrate over others, other proteases, to include caspase-3, can also target this substrate (Talanian et al. 1997; Krumschnabel et al. 2008). This lack of specificity severely impairs the use of this technique in a complex cellular environment. A third technique that is more robust is the direct study of caspase-2 dimers and higher order oligomers using fast protein liquid chromatography (FPLC), or gel filtration. This technique has been used to study other initiator caspases to great success, but requires large amounts of protein per sample and has minimal capacity for scaling.

To overcome these limitations, Bouchier-Hayes and colleagues coopted a technique known as bimolecular fluorescence complementation (BiFC) in order to directly study the initial dimerization step of caspase-2 activation (Bouchier-Hayes et al. 2009). BiFC utilizes a split fluorophore system to monitor protein interactions. Specifically, the complementary (N-terminal and C-terminal) halves of a fluorophore are

fused to two proteins that are known to interact, and the resulting constructs are expressed in cells. When the two proteins interact, they bring the complementary halves together and allow them to refold into a functional fluorophore. Thus, the interaction of the proteins can be directly detected in live cells using flow cytometry or microscopy.

This technique is superior to previous caspase-2 activity monitoring methods for a number of reasons. First, it measures the initial step in caspase-2 activation in live cells. Second, experiments can be conducted in the presence of a cell-permeable pan-caspase inhibitor, such as Q-VD-OPh or zVAD-fmk. This eliminates the possibility that caspase-2 is being activated as part of an amplification loop by executioner caspases. Third, BiFC is easily quantifiable to a single cell level. Fourth, BiFC allows for more detailed studying of caspase-2 activation, such as localization of the dimers, temporal ordering compared to other apoptotic events (such as MOMP which can also be monitored by live-cell microscopy), and single cell dynamics in a cell population. Finally, this technique also lends itself more easily to the development of screens for the study of caspase-2 regulators and stimuli.

Bouchier-Hayes and colleagues chose to utilize split halves of the YFP variant mVenus, which is known to be exceptionally stable in a cellular context as well as efficient and rapid in its maturation (Bouchier-Hayes et al. 2009; Nagai et al. 2002). They went on to show that fusing only the prodomain of caspase-2 to the BiFC halves was

able to faithfully replicate the behavior of a full-length caspase-2 BiFC system (Figure 1.3). Using this system, they were able to validate a number of previously identified

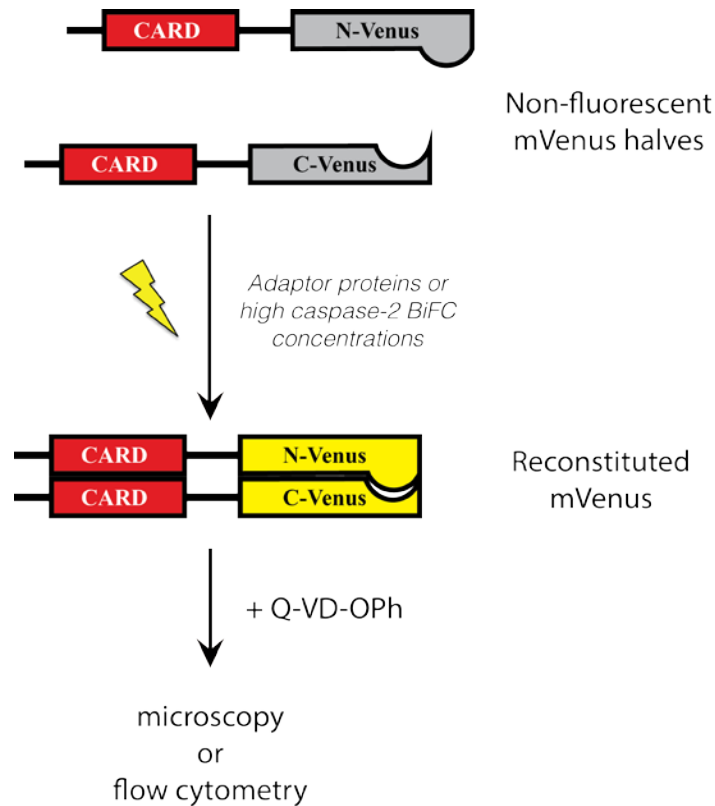


Figure 1.3 Caspase-2 bimolecular fluorescence complementation.

The initial step in caspase-2 activation, dimerization, can be directly observed using BiFC. Two complementary halves of the Venus fluorophore are fused to full length caspase-2 or the CARD-containing prodomains (pictured), which is responsible for facilitating caspase-2 dimerization. Cells expressing these caspase-2 BiFC constructs can then be treated with caspase-2 stimuli to observe both the timing and localization of caspase-2 activation. This is normally done in the presence of a pan-caspase inhibitor like Q-VD-OPh to both preserve fluorescence signal and to validate that dimerization is independent of caspase activity.

caspase-2 stimuli, to include cytoskeletal disruption, DNA damage, metabolic stress, and heat shock. They went on to study heat shock as a caspase-2 stimulus and found that dimerized caspase-2 localizes in an undetermined cytoplasmic, perinuclear region (Bouchier-Hayes et al. 2009).

1.2.5.4 Caspase-2 localization

Early studies of caspase-2 indicate that it can be localized to a number of subcellular contexts, to include the cytoplasm, nucleus, Golgi apparatus, mitochondria, and endoplasmic reticulum (ER) (Colussi, Harvey, and Kumar 1998; Baliga et al. 2003; Paroni et al. 2002; Mancini et al. 2000; Cheung et al. 2006). However, the nuclear and cytoplasmic localization have been the most studied and most clearly validated, while others have been clearly disputed (van Loo et al. 2002). For this reason, this section will focus primarily on nuclear and cytoplasmic localization.

Localization of caspase-2 to the nucleus is dependent on its prodomain (Colussi, Harvey, and Kumar 1998). Several separate studies have defined that the prodomain contains two distinct nuclear localization signals (NLSs) at opposite ends. The first to be identified was a bipartite NLS in the N-terminal portion of the prodomain, spanning residues 25-44 (Colussi, Harvey, and Kumar 1998). The second is a monopartite sequence spanning residues 149-156 near the C-terminus of the prodomain, and was specifically identified as being engaged by the importin α/β complex to translocate into

the nucleus (Baliga et al. 2003; Paroni et al. 2002). Both studies also found that overexpressed caspase-2 induced apoptosis from the nucleus.

Mutagenesis experiments of the monopartite sequence showed that caspase-2 could no longer be localized to the nucleus when NLS residue K152 (mouse) or residues K152 and K153 (human) was mutated to an alanine. This is in line with classic importin α/β complex mechanism of action, which normally relies on the basic lysine residue for binding. A less drastic mutation, where the lysine is instead mutated to arginine, another basic residue, might have a less drastic effect on caspase-2 localization. Interestingly, though, despite the inability to localize to the nucleus, both studies found that overexpression of the lysine-alanine mutants could still potently induce cell death (Paroni et al. 2002; Baliga et al. 2003).

This is in line with the Bouchier-Hayes and colleagues study that found dimerized caspase-2 localizes to a cytoplasmic, perinuclear region (Bouchier-Hayes et al. 2009). The earlier studies that identified a nuclear localization for activation of caspase-2 used overexpression to spontaneously induce caspase-2 activation, while Bouchier-Hayes and colleagues titrated the expression of the BiFC constructs to a low level of expression to ensure that they would not spontaneously dimerize without a stimulus. This, combined with the fact that nuclear localization is not required for activation, indicates that nuclear activation of caspase-2 may not be a physiological phenomenon.

However, it is also possible that different stimuli can promote distinct localization patterns for caspase-2 activation, and a nuclear activation of caspase-2 requires a different stimulus. Regardless, we can conclude that more caspase-2 localization studies are needed, using a combination of multiple techniques for validation such as BiFC, biochemical fractionation, and immunofluorescence.

1.2.5.5 Caspase-2 activation platforms

As mentioned above, initiator caspases are activated by proximity-induced dimerization, which is typically facilitated by adaptor proteins binding to the prodomain. The first putative caspase-2 adaptor protein to be identified was RIP-associated ICH1/CED3-homologous protein with a death domain (RAIDD), also known as CASP2 And RIPK1 domain containing adaptor with a death domain (CRADD) (Duan and Dixit 1997). RAIDD possesses both a CARD, which binds to the caspase-2 CARD in a homotypic fashion, and a DD. After the discovery of RAIDD, another study found that caspase-2 is recruited into a high molecular weight (HMW) complex (~700kDa) when cell lysates were incubated at 37°C, and that caspase-2 in these complexes appears to undergo autoproteolytic cleavage (Read et al. 2002). This indicated that dimerized caspase-2 is initiated by or recruited into a larger complex, similar to but distinct from the apoptosome. Two years later, the Tschopp lab determined that this HMW caspase-2 complex was also composed of RAIDD and the p53-induced protein

with a DD (PIDD), which bound to RAIDD through a homotypic DD interaction. This complex was termed the PIDDosome.

As its name suggests, PIDD is transcriptionally upregulated by p53; thus it was assumed that caspase-2 activation would be directly tied to p53-induced apoptosis. However, even from the beginning of its discovery the importance of this complex has been controversial. In the 2002 study that identified caspase-2 recruitment to a HMW fraction, Read and colleagues were unable to detect RAIDD co-migration (Read et al. 2002). Later studies of PIDD found that it could actually promote survival after DNA damage due to activation of the NF- κ B pathway (Janssens et al. 2005). This was explained by the discovery of a unique PIDD autocleavage event, via an intein-like mechanism, that sequentially produces two distinct C-terminal PIDD fragments (Tinel et al. 2007). The first cleavage event produces a C-terminal PIDD fragment termed C-PIDD (containing the DD) that activates NF- κ B via binding of receptor-interacting protein kinase 1 (RIPK1), while the second cleavage event produces a shorter C-terminal fragment termed CC-PIDD that preferentially binds caspase-2 via RAIDD (Tinel et al. 2007). This led to the proposal that PIDD acts as a switch, initially engaging pro-survival pathways in response to DNA damage for a limited window before eventually converting to a pro-death protein. However, while this highly detailed study provided a fascinating mechanism for PIDDosome activation and showed that activation of caspase-

2 by overexpression of PIDD required the formation of CC-PIDD, it did not show that the endogenous PIDDosome is required for activation of caspase-2 in response to DNA damage.

In fact, later studies of caspase-2 have largely called into question the role of the PIDDosome in promoting caspase-2 functions. Two separate groups generated PIDD null mice and found that caspase-2 was still effectively activated in response to a variety of stimuli (Manzl et al. 2009; Kim et al. 2009). A later report showed that neuronal caspase-2 activation and apoptosis in response to A β treatment or growth factor withdrawal was dependent on RAIDD but not PIDD (Ribe et al. 2012b). In regards to the tumor suppressor role of caspase-2, a 2012 study found that caspase-2 protection against c-Myc-driven lymphomagenesis was independent of PIDD, while a 2015 study from the same group found that RAIDD was also unimportant for this function (Manzl et al. 2012; Peintner et al. 2015).

Together, these findings seem to undermine the importance of the PIDDosome for caspase-2 function. It is possible that the PIDDosome, or even just RAIDD, functions as a caspase-2 activation platform in only certain cell types. Alternatively, PIDD and/or RAIDD might only act as a primary death-inducing platform in response to a subset of caspase-2 stimuli such as heat shock (Bouchier-Hayes et al. 2009; Tu et al. 2006). More

work will be needed to examine the importance of RAIDD and PIDD for activating caspase-2 in other scenarios, such as chemically-induced liver cancer or lipotoxicity.

Also, more efforts should be made to identify alternative caspase-2 activation platforms. Several candidates have already been identified, but either remain controversial or have not been extensively studied. For instance, one group found that treatment of human lymphocytes with the death ligand Fas leads to recruitment of caspase-2 (but not RAIDD) to the DISC where it undergoes cleavage (Lavrik et al. 2006). A second group complemented this study by identifying caspase-2 recruitment to the DISC in HCT-116 colon carcinoma cells in response to DNA damage by the reagent 5-fluorouracil (5-FU) (Olsson et al. 2009). These studies built on the work of an earlier group that found that caspase-2 was required for Fas induced apoptosis (Droin et al. 2001). However, the earlier report explicitly stated that it was unable to detect interaction of caspase-2 with the DISC and the complex remains poorly understood (Droin et al. 2001). Furthermore, no caspase-2 localization studies have indicated that caspase-2 is recruited to the plasma membrane where such a complex would exist.

Another study found that caspase-2 can interact with the TNF-receptor associated factors 1 and 2 as well as RIPK1, although the relevance of this complex is unknown (Lamkanfi et al. 2005). Interestingly, the authors found that overexpressed caspase-2 was able to induce NF- κ B signaling in a manner dependent on its prodomain

and independent of its catalytic activity. Co-immunoprecipitation experiments showed that overexpressed caspase-2 was able to bind both overexpressed TRAF1 and TRAF2 in 293T cells, and this was validated using a yeast two-hybrid approach. Overexpressed RIPK1 was also found to bind to overexpressed caspase-2 in a TRAF2-dependent manner. Finally, the authors showed that heating cell lysates to 37°C induced the formation of a HMW complex containing caspase-2, TRAF2, and RIPK1.

This study appears to be the only report of a caspase-2/TRAF2/RIPK1 complex. While it is certainly believable that caspase-2 interacts with these other proteins, especially when highly overexpressed, the functional significance of such a complex has not been studied. Despite the finding that overexpressed caspase-2 can induce NF- κ B activation, it is unknown if this can occur at more physiological levels or if PIDD also plays a role in this activation. Furthermore, the only other stimulus (besides overexpression) used to study this complex was the heating of cellular lysate, and as was mentioned above, it is unclear if this actually replicates any physiological stimuli. Clearly, further work is needed to explore how caspase-2 is activated in response to intracellular stresses. Such studies would not only enhance our understanding of this enigmatic caspase, but could also potentially lead to new insights for therapies in cancer and other pathologies.

1.3 TNF-Receptor Associated Factors

1.3.1 TRAFs as adaptor proteins

The TNF-receptor activated factor family of proteins is made up of seven members. The inclusion of TRAF7 in this group is controversial as it is missing one of the two subdomains that make up the class-defining C-terminal TRAF homology domain (Xie 2013). This domain is known to be responsible for facilitating TRAF oligomerization as well as mediating interactions with other proteins. As the name suggests, TRAF proteins were originally identified as signaling adaptors that bind to intracellular domains of TNF-R family members (Chung et al. 2002). Over time this adaptor signaling function has expanded to include acting downstream of receptors activated by critical immune system and cytokine receptors, such as toll-like receptors (TLRs), NOD-like receptors (NLRs), RIG-I-like receptors (RIRs), IL-17 receptor family members (IL-17Rs), and TGF β receptors (Xie 2013). Interestingly, these receptors exhibit a range of intracellular localizations: some can localize both the plasma membrane as well as intracellular organelles like endosomes (some RIRs and TLRs), while others are cytosolic (NLRs and RIRs). It is thus not surprising that, upon binding to receptor complexes, TRAF proteins can facilitate a wide range of signaling pathways controlling responses such as survival, proliferation, differentiation, and autophagy.

The most well studied pathway activated by TRAFs is the NF- κ B pathway induced downstream of TNF/TNF-R. Oligomerization of TNF-R by TNF recruits the adaptor protein TNF-R associated protein with a DD (TRADD), which in turn can recruit either FADD or TRAF2 (Oeckinghaus, Hayden, and Ghosh 2011). As alluded to earlier, recruitment of FADD leads to the activation of caspase-8. The recruitment of TRAF2, on the other hand, leads to the recruitment of cellular inhibitors of apoptosis (cIAP) 1 and 2, as well as RIPK1. This complex signals to induce the activation and cytoplasmic localization of the NF- κ B dimers, where they induce transcription of a host of genes. NF- κ B activation generally results in pro-survival and pro-proliferation signaling (Oeckinghaus and Ghosh 2009). Alternatively, TNF can also signal through TRAF2 to induce JNK activity, a kinase known to have both pro- and anti-apoptotic effects (Dhanasekaran and Reddy 2008; Oeckinghaus, Hayden, and Ghosh 2011; Tang et al. 2013).

1.3.2 TRAFs as E3 ubiquitin ligases

1.3.2.1 RING domain and ubiquitination overview

Aside from their C-terminal TRAF domain, all of the TRAFs except TRAF1 possess an N-terminal really interesting new gene (RING) finger domain (Xie 2013). The RING finger domain is found in a host of E3 ligases, enzymes responsible for catalyzing

the post-translational attachment of ubiquitin to target proteins (Metzger, Hristova, and Weissman 2012).

Ubiquitin is a 76 amino acid protein that can be covalently attached to other proteins, typically at a lysine residue, as either a monomer or a polyubiquitin chain. Ubiquitin proteins have seven lysine residues to which other ubiquitins can be added to form these chains, and each of these seven types of lysine chains can theoretically have a distinct signaling function (Swatek and Komander 2016). Ubiquitin chains linked by the K48 residue are the best-characterized and most common type of linkage in the cell, and are used to target substrates for degradation by the ubiquitin-proteasome system (UPS). Other chains, like the K63-linked chain, are non-degradative and can promote signaling, often by serving as scaffolds that are bound by ubiquitin binding domain (UBD) containing proteins (Chen and Sun 2009).

Theoretically, all of the TRAF proteins except TRAF1 could function as E3 ligases. However, specific reports of E3 ligase activity have been primarily limited to TRAF2, TRAF3, TRAF5, and TRAF6 (Xie 2013). Most of these reports focus on non-degradative K63-linked ubiquitination. For instance, TRAF2 was reported to catalyze K63-linked ubiquitination of RIPK1 in order to promote NF- κ B signaling (Alvarez et al. 2010).

1.3.2.2 TRAF2, ubiquitination, and caspase activation

Recently, TRAF2, along with cIAP1 and 2, has also been found to induce K63-linked ubiquitination of the inflammatory caspase-1, directly promoting its activation (Labbé et al. 2011). It is unclear if TRAF2 catalyzes this ubiquitination directly, as both cIAP1 and 2 are also E3 ubiquitin ligases. It is also unclear how K63-linked ubiquitination promotes caspase-1 activity. However, this is not the first study to tie K63-linked ubiquitination to caspase activation. In 2009, Jin and colleagues demonstrated that caspase-8 is ubiquitinated in response to Apo2L signaling, and that this ubiquitination promotes caspase-8 signaling (Jin et al. 2009). This ubiquitination occurs while caspase-8 is at the DISC and results in the binding of the ubiquitin binding protein p62, or sequestosome. The authors found that p62 remains bound to caspase-8 as it undergoes autoproteolytically processing and displaces from the DISC, promoting its stability as a dimerized enzyme as well as aggregation into large foci that appear to be critical for caspase-8 activation.

1.4 Mitosis: where cells divide

The cell division cycle is the process through which cells grow and divide, passing on their genetic material to daughter cells. It can be broken down into two main stages: mitosis, or cell division, and interphase, when cells prepare for mitosis by acquiring nutrients, growing, and doubling their chromosomes (Vermeulen, Van

Bockstaele, and Berneman 2003). These stages occur through incremental steps: a new daughter cell starts in interphase with a growth phase called Gap 1 (G1), followed by S phase where the DNA is replicated, followed by another growth phase called Gap 2 (G2), which is followed ultimately by mitosis.

Mitosis is characterized primarily by massive re-organization events that occur in the cell, particularly in the nucleus, as the cell prepares to physically divide its contents. These events are centered on the preparation and partitioning of the chromosomes, which were copied in S phase. This partitioning is physically accomplished by the microtubule-based mitotic spindle, which emanates from the centrosomes.

Mitosis can be broken down into five stages: in order, they are prophase, prometaphase, metaphase, anaphase, and telophase. During prophase, the chromosomes are condensed and the mitotic spindle begins to form as the centrosomes move to opposite sides of the cell. These chromosomes are made up of two sister chromatids (each chromatid being a copy of the chromosomal sequence) joined together at a special chromatin structure termed the centromere and its protein counterpart, the kinetochore. The sister chromatids are also bound together by protein complexes called cohesins that form loops. Together, these structures ensure that the sister chromatids

remain bound until the cell is ready to separate them, thus ensuring that each daughter cell receives an identical copy of each chromosome.

After prophase comes prometaphase where the nuclear envelope is broken down, allowing the cytosolic mitotic spindle to begin to engage the chromosomes. Specifically, microtubules grow and retract from the two centrosomes located at opposite sides of the cell, seeking attachment to each chromatid's kinetochore. After attachment of the spindle to the chromatids, the cell progresses into metaphase where the chromosomes are aligned along a central axis termed the metaphase plate, an imaginary dividing line between the daughter cells. At this point the cell is primed to undergo the last stages of the cell cycle where the chromosomes are partitioned. When ready, the cell transitions into anaphase. As anaphase begins, the cohesin loops are cleaved and the sister chromatids are pulled to opposite ends of the cell by the mitotic spindle. This is followed by telophase, during which the mitotic spindle is dismantled and nuclear envelopes are reformed around the partitioned sets of chromosomes. Finally, this is followed by cytokinesis where the cell is cleaved in two to form the two new daughter cells.

Cells take great care to ensure the integrity of their genetic material as they pass through the cell cycle. This is manifested by temporal signaling checkpoints that occur at critical moments during the cell cycle. These checkpoints allow the cell to arrest in the

cell cycle until certain conditions meant to ensure proper cell divisions are met. One of these checkpoints occurs at the metaphase to anaphase transition, when the cells are ready to finally divide the genetic material. This checkpoint is called the spindle checkpoint, or the spindle assembly checkpoint.

1.4.1 Regulation of mitosis

Given the centrality of the cell cycle, it is not surprising that it is highly regulated by a number of mechanisms and pathways. However, there is a core set of signaling enzymes that control the process, primarily through post-translational modifications: serine/threonine kinases called cyclin-dependent kinases (CDKs), protein phosphatases, and E3 ligases like the anaphase promoting complex/cyclosome (APC/C).

1.4.1.1 Cyclin-dependent kinases and their partner cyclins

Of these three general classes of enzymes, the CDKs are the main drivers of the process. As their name suggests, the activity of CDKs depends on binding partners called cyclins (Morgan 1997). Cyclin levels, in turn, oscillate throughout the cell cycle, with different cyclins being required for different stages (Malumbres and Barbacid 2009). This oscillation is controlled primarily through transcription followed by proteasomal degradation. For instance, to drive cells into mitosis, first cyclin A (which also participates in S and G2 phase) and then cyclin B are required to bind and activate the mitotic CDK1. Conversely, in order for cells to exit mitosis, cyclin A and B must be

degraded to shut off CDK1 activity. This degradation takes place after the cell commits to entering into anaphase (Malumbres and Barbacid 2009; Malumbres 2014).

1.4.1.2 Mitotic phosphatases PP1 and PP2A

The activity of CDK1 is also counteracted by two main protein phosphatases, PP1 and PP2A (Manchado et al. 2010; Johnson and Kornbluth 2012). Aside from CDK1 activity, inhibition of these phosphatases is also required for entry into mitosis, and this inhibition is mediated by the kinase Greatwall, also known as microtubule associated serine/threonine kinase like (MAST-L) (Johnson and Kornbluth 2012). Greatwall maintains this inhibition until the cell is ready to transition out of mitosis, at which point PP1 and PP2A dephosphorylate CDK1 mitotic-promoting targets (Manchado et al. 2010). PP1 and PP2A have also been shown to play a key role in silencing the spindle checkpoint to facilitate exit (Nijenhuis et al. 2014b; Vanoosthuyse and Hardwick 2009b).

1.4.1.3 The anaphase promoting complex/cyclosome (APC/C)

The third major regulator of mitotic progression is the multi-protein E3 ligase known as the anaphase promoting complex/cyclosome (APC/C). As an E3 ligase, the APC/C functions by conjugating degradative K11- and K48-linked ubiquitin chains to its substrates, promoting their degradation via the ubiquitin proteasome system (Sivakumar and Gorbsky 2015). The APC/C also requires a co-activator that enables targeting of specific targets. During mitosis, this co-activator is the protein cell division

cycle 20 (CDC20). The main mitotic substrates of the active APC/C^{CDC20} are cyclin A and B, as well as a protein called securin. As mentioned above, proteasomal degradation of cyclin A and B leads to a loss of CDK1 activity, allowing the cell to exit. Securin, on the other hand, is an inhibitor of a protease called separase. When securin is targeted for degradation, this releases separase to target the cohesin complex binding the sister chromatids together, which in turn allows for their separation in anaphase. In order to prevent premature degradation of these important mitotic proteins during prometaphase and metaphase when the mitotic spindle is attaching to and positioning the chromosomes for division, the APC/C^{CDC20} is held in a suppressed state. This is accomplished by the spindle checkpoint.

1.4.2 The spindle checkpoint

The spindle checkpoint monitors the attachment of the mitotic spindle to the kinetochores and prevents the cell from progressing into anaphase until the chromosomes are properly engaged. Specifically, the kinetochores of both sister chromatids must be properly engaged by spindle poles from opposite poles (bi-orientation) in order for the checkpoint to be satisfied (Pinsky and Biggins 2005). Given that this process is fairly complicated and random, it is not surprising that initial engagement of a microtubule to a kinetochore does not always result in a stable attachment. Rather, it is a dynamic process that is at least partially regulated by proteins

at the kinetochore that can weaken microtubule attachments when they sense a lack of bi-orientation (Foley and Kapoor 2013). The kinase Aurora B plays a critical role in this destabilization process, and is opposed by the phosphatase PP2A (Foley and Kapoor 2013; Foley, Maldonado, and Kapoor 2011b).

Spindle checkpoint monitoring is highly sensitive: a single unengaged kinetochore is enough to activate it and prevent progression to anaphase (Lara-Gonzalez, Westhorpe, and Taylor 2012b). This is critical as failure of just one chromatid to segregate properly results in aneuploidy, which in turn can lead to tumorigenesis (Pinsky and Biggins 2005). A number of proteins converge on regulating the spindle checkpoint. However, the primary effector of the checkpoint is the mitotic checkpoint complex, or MCC (Musacchio and Salmon 2007b). This is made up of the proteins Mad2, BubR1, and Bub3, which form an inhibitory complex that binds to CDC20 and prevents it from activating the APC/C^{CDC20}.

The mechanism by which the MCC is generated is still being uncovered, but it appears that it initiates at the unattached kinetochore (Sivakumar and Gorbsky 2015). There, Mad1-Mad2 dimers recruit other Mad2 proteins and induce them to undergo a conformational change that enables binding to CDC20. This Mad2-CDC20 complex can then bind BubR1 and Bub3 to complete the generation of the MCC, which is then able to dissociate from the kinetochore (Foley and Kapoor 2013).

A paradigm that has emerged over the last decade is that phosphorylation plays a critical role in initiating and maintaining the spindle checkpoint, with kinases (phosphorylation events) generally being thought to promote the checkpoint and phosphatases (dephosphorylation) generally being thought to silence the checkpoint (Foley and Kapoor 2013). The kinase Mps1 has been shown to play a critical role in activating the checkpoint by promoting recruitment of checkpoint components to unattached kinetochores, while the kinases Aurora B and Plk1 are also known to play similar roles (Maciejowski et al. 2010b; Musacchio and Salmon 2007b; Ditchfield et al. 2003b). Furthermore, both PP1 and PP2A have been implicated in silencing the checkpoint (Vanoosthuyse and Hardwick 2009a; Nijenhuis et al. 2014b). In fact, it has been proposed that the spindle checkpoint primes phosphatases for silencing in a negative feedback loop that allows for a rapid response once all of the sister chromatids are properly engaged by the spindle (Nijenhuis et al. 2014b).

2. Materials and methods

2.1 Materials and methods for chapter 3

2.1.1 Reagents and cell culture

GFP-Trap_A (cat. no. gta-20) was from ChromoTek. Cisplatin (cat. no. P4394), doxycycline hydrochloride (cat. no. D3072), Phosphatase Inhibitor Cocktail 2 (cat. no. 5726), Phosphatase Inhibitor Cocktail 3 (cat. no. 0044), and Anti-Flag M2 Affinity Gel (cat. no. A2220) were from Sigma. Etoposide (cat. no. E-4488) and paclitaxel (cat. no. P-9600) were from LC Laboratories. Q-VD(OMe)-OPh (cat. no. A8165) was from APEXBio. Pierce Silver Stain Kit for Mass Spectrometry (cat. no. 24600) was from Thermo Scientific. AlexaFluor488 conjugated Annexin V (cat. no. A13201) was from Thermo Fisher Scientific/Molecular Probes. X-tremeGENE 9 DNA Transfection Reagent (cat. no. 06365809001) was from Roche. Amylose resin (cat. no. E8021) was from New England Biolabs. Caspase-2 Substrate Ac-VDVAD-pNA (cat. no. 1072-1000) was from BioVision).

2.1.2 Antibodies

Antibodies used in this study are as follows: caspase-2 mouse monoclonal (G310-1248, cat. no. 551093, BD Biosciences), caspase-2 rat monoclonal (11B4, cat. no. MAB3507, Millipore), actin rabbit polyclonal (I-19-R, cat. no. sc-1616-R, Santa Cruz Biotechnology), RAIDD mouse monoclonal (4B12, cat. no. M056-3, MBL), TRAF1 rabbit monoclonal (45D3, cat. no. 4715, Cell Signaling Technology), TRAF2 mouse monoclonal (cat. no. 558890, BD Biosciences), TRAF2 rabbit polyclonal (C192, cat. no. 4724, Cell Signaling

Technology), TRAF3 rabbit polyclonal (cat. no. 18099-1-AP, ProteinTech), GFP rabbit polyclonal (FL, cat. no. sc-8334, Santa Cruz Biotechnology), GFP rat monoclonal (3H9, cat. no. 3h9-100, ChromoTek), Flag mouse monoclonal (M2, cat. no. F1804, Sigma), Flag rabbit polyclonal (cat. no. PA1-984B, Thermo Scientific), Myc mouse monoclonal (9E10, cat. no. sc-40, Santa Cruz Biotechnology), Myc mouse monoclonal (9B11, cat. no. 2276, Cell Signaling Technology), caspase-3 rabbit monoclonal (8G10, cat. no. 9665, Cell Signaling Technology), active Bax mouse monoclonal (6A7, cat. no. 556467, BD Biosciences), Bax rabbit polyclonal (cat. no. 2772, Cell Signaling Technology), (N-20, cat. no. sc-493, Santa Cruz Biotechnology), BID rabbit polyclonal (cat. no. 2002, Cell Signaling Technology), ubiquitin rabbit polyclonal (cat. no. 3933, Cell Signaling Technology), ubiquitin mouse monoclonal (P4D1, cat. no. sc-8017, Santa Cruz Biotechnology), PARP rabbit polyclonal (cat. no. 9542, Cell Signaling Technology).

2.1.3 Plasmids

pBiFC-VN173 and pBiFC-VC155 were gifts from Dr. Chang-Deng Hu (Addgene plasmid # 22010 and # 22011, respectively). cDNA encoding caspase-2 prodomain (amino acids 1-169) or caspase-2 full length C320A (amino acids 1 - 452) was inserted into the multiple cloning site of pBiFC-VN173 or pBiFC-VC155 to generate plasmid encoding caspase-2 prodomain or caspase-2 (C320A) fused with VN173 or VC155. For the inducible caspase-2 prodomain BiFC system, cDNA encoding caspase-2 prodomain with VN173 or VC155 was inserted into pTRE-Tight-BI vector (Clontech, cat. no.

631068). A bidirectional Tet-responsive promoter in pTRE-Tight-BI enables simultaneous induction of both caspase-2pro-VN173 and caspase-2pro-VC155 in response to the presence (Tet-On system) or absence (Tet-Off system) doxycycline.

mVenus-N1 was a gift from Dr. Michael Davidson (Addgene plasmid # 54640). The cDNA sequence of caspase-2 prodomain was inserted into the multiple cloning site of mVenus-N1 to generate plasmid encoding C-terminal mVenus-tagged caspase-2pro.

Site-directed mutagenesis was performed by PCR-based method using QuikChange II Site-Directed Mutagenesis Kit (Agilent Technologies).

Plasmids encoding TRAF1, TRAF2, TRAF3, TRAF5, and TRAF6 were kindly provided from Dr. Tomohisa Kato (Kyoto University, Japan). Plasmids encoding TRAF2 wild-type and TRAF2 RING deletion mutant were kindly provided from Dr. Vishva Dixit (Genentech, USA).

2.1.4 Generation of Tet system responsive caspase-2 BiFC expressing cell line

HeLa Tet-Off cells were transfected with both pTRE-Tight-BI/caspase-2pro-VN173/caspase-2pro-VC155 and Linear Hygromycin Marker (Clontech, cat. no. 631625). The cells were then re-plated at low density and selected by 200 µg/mL hygromycin B for 15 days until formation of single cell colonies. Stably transfected clones were screened based on BiFC fluorescent signal and caspase-2pro-BiFC protein expression was confirmed by immunoblotting analysis.

2.1.5 RNA interference

siRNA sequences used in this study are as follows. siCtrl: AllStars Neg. Control siRNA (cat no. 1027281) was purchased from Qiagen. ON-TARGETplus siRNA (SMARTpool) for both TRAF2 and TRAF3 was purchased from Dharmacon. Silencer Select siRNA for TRAF1 (s224753) was purchased from Thermo Fisher Scientific. siRNA transfection was performed following manufacturer's protocol of Lipofectamine RNAiMAX Transfection Reagent. A final concentration of 20 nM siRNA was used.

Lentivirus encoding shRNA was generated by using pLKO.1-based plasmids. shNT for scramble shRNA was from Addgene (plasmid 1864). shTRAF2 #1 (TRCN0000004573), shTRAF2 #2 (TRCN0000004571), shCASP2 #1 (TRCN0000003508), and shCASP2 #2 (TRCN0000003509) were obtained from Duke Functional Genomics Shared Resource. pLKO.1 plasmid and plasmids encoding gag, pol, tat, or VSV-G were transfected into HEK293T cells with PEI (polysciences). Two days later, cell culture supernatant containing lentivirus was collected and filtered through 0.45 μ m filter. Lentivirus was concentrated by ultracentrifugation at 19,500 rpm for 3 h at 4°C. Cells were infected with the lentivirus and selected with 2 μ g/mL puromycin for at least 4 days before functional analysis.

2.1.6 Immunoprecipitation

Anti-FLAG: Constructs were transfected into HeLa Tet-Off cells using X-tremeGENE 9. After 48 h, cells were harvested by trypsinization and pelleted by 3 min

centrifugation at 500 x g at 4°C. Pellets were washed once with PBS, then lysed in Triton X-100 lysis buffer (40 mM HEPES (pH 7.4), 1 mM EDTA, 120 mM NaCl, 0.4% Triton X-100, 10 µg/mL each aprotinin and leupeptin, 1 mM PMSF) by incubating on ice for 20 min, followed by 15 min centrifugation at 15,000 x g at 4°C. Equal amounts of protein were incubated with anti-FLAG M2 affinity gel for 1 h under constant rotating at 4°C. After incubation, affinity gel was washed three times with Co-IP Lysis Buffer, followed by two more times with Co-IP Lysis Buffer supplemented with 120 mM NaCl. Then samples were resolved by SDS-PAGE for immunoblotting.

Anti-Bax(6A7): Cells were treated for 18 h with 20 µM cisplatin, then lysed similar to anti-FLAG IP but with CHAPS lysis buffer (1% CHAPS, 150 mM NaCl, 10 mM HEPES, 10 µg/mL each aprotinin and leupeptin, 1 mM PMSF). Anti-Bax(6A7) antibody was prebound to protein G agarose, washed with CHAPS lysis buffer, then incubated with equal amounts of protein for 1 h under constant rotating at 4°C. After incubation, sepharose beads were washed five times with CHAPS lysis buffer. Samples were resolved by SDS-PAGE for immunoblotting.

All figures are representative results of experiments that were repeated at least three times.

2.1.7 Microscopic or flow cytometric analysis of BiFC signal

HeLa Tet-Off CASP2pro-BiFC cells were plated on glass bottom dish at ~30% confluence. Expression of the caspase-2 BiFC fragments was induced by washing with

PBS and culturing cells in DMEM containing 10% Tet System Approved FBS (Clontech, cat no. 63110) for 24 h before treatment. Cells were treated with 20 μ M cisplatin in the presence of 10 μ M Q-VD(OMe)-OPh for 24 h. Caspase-2-BiFC signal was observed by Leica SP5 inverted confocal microscope with 40x objective lens. Images were analyzed by Leica LAS AF software.

For detection of BiFC for full length caspase-2 dimerization, HeLa cells were transiently transfected with a pair of plasmids encoding CASP2(C320A)-VN173 and CASP2(C320A)-VC155. 24 h post transfection, cells were treated with 20 μ M cisplatin in the presence of 10 μ M Q-VD(OMe)-OPh for 24 h. Cells were collected by trypsinization, and caspase-2 BiFC signal was analyzed by FACScan analyzer for BiFC fluorescent signal detection. All figures show mean \pm s.e.m of at least three independent experiments. Data were analyzed by unpaired two-tailed Student's t-test.

2.1.8 BiFC dimer immunoprecipitation by GFP-Trap

Cells were trypsinized with 0.05% or 0.25% trypsin/EDTA. A portion of cell suspension was analyzed by FACScan Analyzer or FACSCalibur for BiFC fluorescent signal. Cells were collected by centrifugation and lysed in lysis buffer (0.5% TritonX-100, 20 mM Hepes (pH 7.4), 150 mM NaCl, 1.5 mM MgCl₂, 2 mM EGTA, 2 mM DTT) or RIPA buffer (1% NP-40, 0.1% SDS, 0.1% sodium deoxycholate, 50 mM Tris (pH 7.4), 150 mM NaCl, 1mM EDTA) supplemented with aprotinin, leupeptin, PMSF, and phosphatase inhibitor cocktail 2 and 3 (Sigma). GFP-Trap_A was pre-washed with lysis buffer, lysate

was added, and incubated for 1 - 2 h under constant rotation at 4°C. GFP-Trap_A beads were washed with lysis buffer three times and captured protein was eluted in SDS sample buffer by boiling for 5 min. Immunoprecipitated protein was analyzed by immunoblotting. All figures are representative results of experiments that were repeated at least three times.

2.1.9 Co-immunoprecipitation with BiFC dimer specific capture and mass spectrometry analysis of the protein complex

HeLa Tet-Off CASP2pro-BiFC cells were plated at ~60% confluence for next day. Cells were thoroughly washed with PBS five times to completely washout residual doxycycline and cultured in DMEM with Tet system approved FBS for the induction of caspase-2 BiFC. For control cells, 0.1 mg/mL doxycycline was added to suppress caspase-2 BiFC expression, and 1 µg pair of pBiFC-VN173 and pBiFC-VC155 were transfected for overexpression of VN173 and VC155 proteins. After 24 h to allow for protein induction, cells were treated with DMSO, 20 µM cisplatin, 50 µM etoposide, or 100 nM paclitaxel in the presence of 10 µM Q-VD(OMe)-OPh. 24 h post-treatment, cells were collected by trypsinization and washed with cold PBS twice. Cell pellets were lysed in co-immunoprecipitation lysis buffer (0.5% TritonX-100, 20 mM Hepes (pH 7.4), 150 mM NaCl, 1.5 mM MgCl₂, 2 mM EGTA, 2 mM DTT) supplemented with aprotinin, leupeptin, PMSF, and phosphatase inhibitor cocktail 2 and 3. Cell lysates were cleared by centrifugation at 12,000 rpm for 15 min, and the supernatant was diluted with dilution buffer (20 mM Hepes (pH 7.4), 400 mM NaCl, 1.5 mM MgCl₂, 2 mM EGTA, 2

mM DTT) to reduce TritonX-100 concentration to 0.2% and to increase NaCl concentration to 300 mM. Protein concentration was measured by Bradford Assay (Bio-Rad), and 4.4 mg of total protein was used for co-immunoprecipitation by 13 mL slurry of GFP-Trap_A beads. At this step, control sample lysates from each treatment were mixed and used for GFP-Trap_A co-immunoprecipitation. The lysate GFP-Trap_A mixture was incubated under constant rotation at 4°C for 2 h. Then, GFP-Trap_A beads were washed 7 times with wash buffer (1% TritonX-100, 20 mM Hepes (pH 7.4), 300 mM NaCl, 1.5 mM MgCl₂, 2 mM EGTA, 2 mM DTT) supplemented with proteinase inhibitors and phosphatase inhibitors and 3 times with 50 mM ammonium bicarbonate. Samples were analyzed by direct on-resin digestion and mass spectrometry for interaction proteomics at Duke Proteomics and Metabolomics Core Facility.

2.1.10 Apoptotic cell death detection by Annexin V or PI staining

Regarding Annexin V staining: medium containing floating cells and cells trypsinized from culture dish were combined. Cells were collected by centrifugation and washed with PBS once. Washed cells were resuspended in 50 µL of Annexin V binding buffer (10 mM HEPES, 140 mM NaCl, and 2.5 mM CaCl₂, pH 7.4) 2.5 µL of Annexin V, Alexa Fluor 488 conjugate and incubated at room temperature for 15 min. Annexin V binding buffer 200 µL was added and Annexin V positive cells were detected by flow cytometry.

Regarding PI staining: following control or apoptosis-inducing stimulus, cell media was collected, cells were washed with PBS and PBS was collected, and cells were harvested after incubation with 0.25% Trypsin-EDTA (Gibco by Life Technologies). Cells were centrifuged at 4°C at 500 xg for 5 minutes and cells were resuspended in 1 µg/ml propidium iodide (PI) (dissolved in PBS), and kept on ice until analysis. PI staining was quantitated using a three color FACScan analyzer from BD Biosciences and BD's Cell Quest acquisition and analysis software.

All figures show mean \pm s.e.m of at least three independent experiments. Data were analyzed by unpaired two-tailed Student's t-test.

2.1.11 Detection of ubiquitination of caspase-2

HEK293T cells were transfected with plasmid encoding CASP2pro-mVenus (wild-type or KR mutant) or mVenus-N1 as control. 24 h post transfection, cells were collected and lysed in RIPA buffer supplemented with proteinase inhibitors, phosphatase inhibitors, and 10 mM N-ethylmaleimide. Cell debris was sheared by sonication and lysates were cleared by centrifugation. Caspase-2pro-mVenus (or mVenus) protein was captured by GFP-Trap_A under constant rotation at 4°C for more than 1 h. Beads were washed 3 times with harsh wash buffer (PBS containing 8M urea and 0.2% SDS) to washout any other ubiquitinated protein associating with caspase-2pro-mVenus. The samples were analyzed by SDS-PAGE, and immunoblotted with anti-

ubiquitin antibody for ubiquitinated caspase-2pro-mVenus. All figures are representative results of experiments that were repeated at least three times.

2.1.12 Recombinant protein production

TRAF2 sequence was amplified by PCR and inserted into pMAL-c2X (New England Biolabs) to obtain a construct encoding N-terminal MBP-tagged TRAF2 (pMAL/MBP-TRAF2). Rosetta2(DE3)pLysS competent cells (EMD Millipore) were transformed with pMAL/MBP-TRAF2 and transformant was cultured in LB medium at 37°C overnight. 0.1 mM of IPTG was added to induce recombinant protein production and the bacteria was further cultured at 30°C for 6 h. Bacteria was collected by centrifugation and resuspended in Buffer A (20 mM Hepes-KOH, pH 7.5, 10 mM KCl, 1.5 mM MgCl₂, 1 mM EDTA, 1 mM EGTA, 1 mM dithiothreitol, 0.1 mM PMSF, and aprotinin/leupeptin). Debris was sheared by sonication and lysates were cleared by centrifugation at 10,000 rpm for 30 min. Recombinant MBP-TRAF2 protein was captured by using glutathione sepharose beads (GE Healthcare) at constant rotation at 4°C for 1 h. Beads were washed with Buffer A containing 1 M NaCl 5 times, and Sequential elution of the recombinant protein was performed with Buffer A containing 10 mM glutathione (pH 8.0). The elution fraction containing high amount of MBP-TRAF2 was monitored by SDS-PAGE following coomassie brilliant blue (CBB) staining, and dialyzed in Buffer A at 4°C overnight. Purity and concentration of the recombinant protein was examined by SDS-PAGE and CBB staining.

2.1.13 *In vitro* binding assay of ubiquitinated caspase-2 and recombinant MBP-TRAF2

HeLa cells were transfected with plasmid encoding CASP2pro (wild type or 3KR) -mVenus. 2 days later, cells were collected and lysed in RIPA buffer (1% NP-40, 0.1% SDS, 0.1% sodium deoxycholate, 50 mM Tris (pH 7.4), 150 mM NaCl, 1mM EDTA) supplemented with aprotinin, leupeptin, PMSF, phosphatase inhibitor cocktail 2 and 3, and 10 mM N-ethylmaleimide. Cell pellets were sheared by sonication following centrifugation to clear the lysate. One mg of recombinant MBP or MBP-TRAF2 protein was added to the lysate and incubated on ice for 2 h. MBP proteins were retrieved by 20 mL slurry of amylose resin (New England Biolabs; cat. no. E8021) at constant rotation for 2 h and washed 4 times with RIPA buffer. Samples were analyzed by immunoblotting.

2.1.14 Salt titration assay to test the strength of caspase-2 dimer stability

HeLa cells, plated in 10 cm dish, were transfected with 20 ng pair of plasmids encoding C-terminal mVenus-tagged or N-terminal myc-tagged caspase-2 prodomain (wild type or 3KR). In order to induce caspase-2 dimerization, cells were treated with 20 μ M cisplatin in the presence of 10 μ M Q-VD(OMe)-OPh and cultured for 24 h. Cells were collected and lysed in lysis buffer (1% NP-40, 20 mM Hepes (pH 7.4), 50 mM NaCl, 2 mM EDTA) supplemented with aprotinin, leupeptin, PMSF, phosphatase inhibitor cocktail 2 and 3, and 10 mM N-ethylmaleimide. Lysates were cleared by centrifugation and high salt lysis buffer (1% NP-40, 20 mM Hepes (pH 7.4), 2 M NaCl, 2 mM EDTA)

was added to increase NaCl concentration up to 150, 300, 500, or 750 mM. Caspase-2pro-mVenus and protein binders were captured by GFP-Trap_A under constant rotation at 4°C for 1.5 h. GFP-Trap_A beads were washed 4 times with lysis buffer with 50, 150, 300, 500, or 750 mM NaCl, and once with lysis buffer. Captured proteins were analyzed by immunoblotting and stability of caspase-2pro dimer was assessed by dissociation of myc-caspase-2pro from caspase-2pro-mVenus with increasing concentration of NaCl.

2.1.15 VDVADase activity assay for caspase-2 purified from cells

HEK293T cells, plated in 10 cm dish, were transfected with plasmid encoding C-terminal mVenus-tagged caspase-2 (wild type, 3KR, C320A, or 3KR/C320A). The amount of plasmid for transfection was 75 ng which did not induce cell death 24 h post transfection. Cells were collected and lysed in lysis buffer (1% NP-40, 20 mM Hepes (pH 7.4), 50 mM NaCl, 2 mM EDTA) supplemented with aprotinin, leupeptin, phosphatase inhibitor cocktail 2 and 3, and 10 mM N-ethylmaleimide. Cell debris was sheared by sonication. Caspase-2-mVenus was purified from cleared lysates with GFP-Trap_A under constant rotation for 2 h at 4°C. Beads were washed 4 times with lysis buffer and once with PBS. Caspase-2-mVenus was eluted with 0.2 M glycine-HCl (pH 2.5) under constant vortex for 30 sec following immediate neutralization with 1 M Tris-HCl (pH 10.5). This step was repeated to increase elution efficiency. The elution was mixed with caspase-2 Substrate Ac-VDVAD-pNA in caspase assay buffer (50 mM Hepes (pH7.4), 0.1 M NaCl, 0.1% Chaps, 1 mM EDTA, 10% glycerol). The reaction was prepared in 96 well

plate and caspase-2-mVenus activity was measured as cleaved pNA signal at OD 405 nm under 37°C incubation up to 90 min. The equal amount of caspase-2-mVenus protein in elution was confirmed by immunoblotting.

2.1.16 Statistical analysis

Data from flow cytometry-based experiments were shown as mean \pm s.e.m of at least three experiments. Data were analyzed by unpaired two-tailed Student's t-test.

2.2 Materials and methods for chapter 4

This section is adapted from a published co-first author manuscript (Foss et al. 2016)

2.2.1 Reagents and cell culture

HeLa Tet-Off cells were a kind gift from Donald McDonald (Duke University, Durham, NC). All cultures were maintained in Dulbecco's modified Eagle medium (Invitrogen) supplemented with 10% fetal bovine serum (Invitrogen) at 37°C and 5% CO₂. HeLa Tet-Off cells were double thymidine blocked using 2.5 mM thymidine (Sigma), washed twice with PBS, and released into medium containing 100 ng/mL nocodazole (Calbiochem) or 100 nM taxol (LC Laboratories) for 16 hours to arrest cells at the spindle checkpoint. Phosphatase inhibitors were then added for two hours before collection. In certain experiments, MG132 or the APC/C inhibitor proTAME was added for one hour prior to phosphatase inhibitor treatment. For mitotic exit assays, nocodazole or taxol-arrested cells were washed twice with PBS and re-plated in media containing an inhibitor or DMSO. The following inhibitors were used: okadaic acid

(0.1 μ M or 1 μ M, Enzo), fostriecin (10 μ M, Enzo), FK506 (10 μ M, Enzo), cyclosporin A (10 μ M, Enzo), calyculin A (20nM, Calbiochem), MG132 (20 μ M, Enzo), proTAME (12 μ M, Boston Biochem), and roscovitine (10 μ M, Calbiochem).

2.2.2 RNA interference

siRNAs were synthesized by Sigma or Invitrogen and transfected using Lipofectamine RNAiMax (Invitrogen) per the manufacturer's instructions immediately prior to synchronization. Luciferase or AllStars Negative Control (Qiagen, 1027281) siRNA were used as controls. esiRNAs (Sigma) were used to knockdown the six phosphatases identified by mass spectrometry: DUSP6 (EHU123191), NUDT5 (EHU013191), PNKP (EHU132321), PPP1R12A (EHU072171), PPA1 (EHU109021), and DCTPP1 (EHU042641). Sigma's pLKO.1 lentiviral shRNA constructs were used for PP4 and PP6, and the control pLKO.1 shRNA construct is from Addgene (1864).

The following siRNA sequences were used:

Luciferase: UCGAAGUAUCCGCGUACG

CDC20: CGGAAGACCUGCCGUUACA

PP1 α : SIHP0511-250PMOL, Sigma

PP1 β -1: AAAUGCGAUUGAUGCUAGC

PP1 β -2: AUUCAGUCCACCAUACUGG

PP1 γ : SIHP0518-250PMOL, Sigma

PP2A: CAACGUGCAAGAGGUUCGAUGUCCA

PP5-1: AACAUAUUCGAGCUCAACGGU

PP5-2: CUCAACAUAUUCGAGCUCA

The following shRNAs were used:

PP4-1: TRCN0000002760

PP4-2: TRCN0000002761

PP4-3: TRCN0000002762

PP6-1: TRCN0000002764

PP6-2: TRCN0000002765

PP6-3: TRCN0000002766

2.2.3 Plasmids

Stratagene's site-directed mutagenesis kit was used to mutate serine and threonine residues to alanine in pCS2-HA-CDC20 and pcDNA3-Myc-BubR1 per the manufacturer's instructions. pCS2-HA-CDC20, pcDNA3-Myc-BubR1, and pCS2-Myc-Mad2 plasmids were transfected using X-tremeGENE 9 DNA Transfection Reagent (Roche) 48 hours before collection.

2.2.4 Antibodies, Western Blotting, and Co-Immunoprecipitation

The following antibodies were used for immunoprecipitations and immunoblotting: anti-cyclin A (sc-751), anti-cyclin B (sc-952), anti-actin (sc-1616-R), anti-

CDC20 (sc-5296), anti-CDC20 (Abcam, ab26483), anti-Mad2 (sc-6329), anti-BubR1 (Abcam, ab54894), anti-Bub3 (BD Transduction Lab, 611730), anti-PP1 α (sc-6104), anti-PP1 β (Abcam, ab53315), anti-PP1 γ (sc-6108), anti-PP2Ac (Millipore, 05-421), anti-PP5 (BD transduction Lab, 611020), anti-vinculin (Sigma, V9131), anti-myc (sc-789), anti-HA (sc-805), anti-MPM2 (Millipore, 05-368), and anti-phospho-histone H3 (Cell Signaling, 9701). The following secondary antibodies were used: Alexa Fluor 680 goat anti-rabbit (Life Technologies, A21076), IRDye 800CW goat anti-mouse (LI-COR, 926-32210), and IRDye 800CW donkey anti-goat (LI-COR, 926-32214). Co-immunoprecipitation was carried out as previously described.(Zhang et al. 2012) Briefly, mitotic cells were lysed in Co-IP buffer (150 mMNaCl, 20 mM HEPES pH 7.4, 0.5% Triton X-100, 1.5 mM MgCl₂, 2 mM EGTA, 5ug/mL aprotinin, 5ug/mL leupeptin) at 4°C for 30 minutes, followed by centrifugation at 16,000xg for 15 minutes. Lysates containing equal amounts of protein were incubated with CDC20 antibody for 4 hours at 4°C. Proteins were collected by adding Protein G Sepharose beads for another 1 hour at 4°C. The beads were washed four times with Co-IP buffer + 150mM NaCl, boiled in SDS sample buffer, and analyzed by SDS-PAGE and immunoblotting. For Myc-Mad2 and Myc-BubR1 co-immunoprecipitations, DSP crosslinking was performed in lysates prior to immunoprecipitation as previously described.(Zlatic et al. 2010) Anti-c-Myc Agarose Affinity Gel (Sigma, A7470) was used to pull down Myc-tagged proteins.

2.2.5 qPCR

RNA was isolated using Sigma's GenElute Mammalian Total RNA Miniprep Kit (RTN70), and cDNA was generated using BioRad's iScript cDNA Synthesis Kit (170-8891). qPCR was performed using BioRad's iQ SYBR Green Supermix (170-8882). All samples were amplified in triplicate. GAPDH was used for normalization of mRNA levels.

The following primers were used:

PP4: Forward 5- ATCAAGGAGAGCGAAGTCAAG -3; Reverse 5-
CCTACTCTGAACAGCTCTTTGAG -3

PP6: Forward 5- CCTGAAGGTGAGCCCTATTTG -3; Reverse 5-
ACAAACGTAGTCACATAGCCG -3

GAPDH: Forward 5- ACATCGCTCAGACACCATG -3; Reverse 5-
ATGACAAGCTTCCCGTTCTC -3

PPP1R12A: Forward 5- GAGACGGACCTCGAGCCT -3; Reverse 5-
CATCAATGCAAGCCTGGTGC -3

DUSP9: Forward 5- TTCCGGTGGCGTTAGGCTG -3; Reverse 5-
GATCGGCTCCCTACACGCTG -3

PNKP: Forward 5- ACCGGTTTCGAGAGATGACG -3; Reverse 5-
TCGAACTGCTTCCTGTAGCC -3

PPA1: Forward: 5- TGGA ACTATGGTGCCATCCC -3; Reverse 5-
CACCTCTTGCACATACCTTGC -3

DCTPP1: Forward 5- AGCTGGCAGAACTCTTTCAGTG -3; Reverse 5-
AGGACGTCACTAAGCTCCTCT -3

NUDT5: Forward 5- TCTCCAGCGGTCTGTATGGA -3; Reverse 5-
CTCTCCATCCCCTGGCTTTG -3

GAPDH (#2): Forward 5- CTCCTGTTGACAGTCAGCC -3; Reverse 5-
ACCAAATCCGTTGACTCCGAC -3

2.2.6 Chromosome spread

Mitotic cells were swelled in a prewarmed hypotonic solution containing 75 mM KCl for 20 min at 37°C. Cells were adjusted to a density of 2×10^5 /ml and fixed with methanol:acetic acid (v/v=3:1) for 15 min at room temperature. Cells were dropped onto microscope slides, dried at room temperature and stained with Hoechst 33258 (Molecular Probes) for 5 min. The slides were washed, sealed and viewed using a using a Leica SP5 confocal scanning microscope.

2.2.7 *In vitro* lambda phosphatase assay

To assess the phosphorylation status of CDC20 and BubR1, whole cell lysates or immunoprecipitated endogenous proteins were incubated with 1ul lambda phosphatase (New England Biolabs) for 1 hour at 30°C.

3. Targeted immunoprecipitation of BiFC dimers reveals a novel role for TRAFs in regulating caspase-2 dimerization and apoptosis in response to DNA damage

This chapter is adapted from a manuscript soon to be submitted for publication.

3.1 Introduction

Protein interactions often result in multimeric complexes that induce signaling to significantly alter cellular biology. As such, these protein complexes are tightly controlled by a number of factors such as protein expression or post-translational modifications like phosphorylation or ubiquitination. Studying the biochemistry of these complexes can provide critical insights into biological and pathological developments. However, this research is often limited by the availability of quality tools specific to the known components of the complexes.

One example is the cysteine protease caspase-2. Caspase-2 was one of the earliest caspases to be identified and has increasingly been established as an important modulator of the cellular response to insults such as genotoxic (Sidi et al. 2008; Ho et al. 2009; Olsson et al. 2009; Shalini et al. 2016), metabolic (Nutt et al. 2005; Segear Johnson et al. 2013; Yang et al. 2014), and cytoskeletal stress (Ho et al. 2008). Furthermore, its emerging role as a tumor suppressor (Parsons et al. 2013; Ho et al. 2009; Shalini et al. 2016; Manzl et al. 2012) and a promoter of metabolic disorders (Segear Johnson et al. 2013; Machado et al. 2015; Machado et al. 2016) indicates that modulating its activity

could have therapeutic potential. However, the molecular regulation of caspase-2 activation has remained largely obscure.

Apoptotic caspases can be divided into two camps: initiator caspases that begin the apoptotic signaling cascade and executioner caspases that propagate this signal. Caspase-2 is generally classified as an initiator caspase; like some other initiator caspases, caspase-2 contains a long amino-terminal prodomain with a caspase recruitment domain (CARD), and its activation initially occurs through dimerization (Butt et al. 1998; Baliga, Read, and Kumar 2004). The CARD plays a critical role in promoting this dimerization, most likely by forming a docking site for an activation platform (Colussi et al. 1998; Butt et al. 1998; Duan and Dixit 1997; Chou et al. 1998). The original caspase-2 activation platform was identified over a decade ago and consisted of PIDD and RAIDD (Tinel and Tschopp 2004). However, subsequent studies have shown that caspase-2 activation can occur independently of PIDD and RAIDD (Manzl et al. 2012; Ribe et al. 2012a; Peintner et al. 2015).

Identification of other regulators of caspase-2 activation has been limited by a lack of suitable reagents. To address this shortcoming, Bouchier-Hayes and colleagues cleverly adopted the method of bimolecular fluorescence complementation (BiFC) to study caspase-2 dimerization (Bouchier-Hayes et al. 2009). In BiFC, complementary N-terminal and C-terminal halves of a fluorophore are fused to two interacting proteins. When the proteins of interest interact they bring the fluorescent halves into close

proximity and allow them to fold into a functional fluorophore. Thus, BiFC allowed for the identification of caspase-2 activating stimuli and insight into the timing and localization of caspase-2 dimers. Furthermore, by combining caspase-2 BiFC with small molecule inhibitor or siRNA libraries, the upstream regulation of caspase-2 could be investigated in a targeted or even unbiased screen. Unfortunately, such screens can be cost prohibitive and prone to artifacts.

In this study we leveraged the BiFC system to develop a novel method for isolating protein dimers, and in particular caspase-2. Specifically, we isolated caspase-2 BiFC dimers by targeting the properly folded BiFC fluorophore with GFP-binding nanobodies (GFP-Trap). We combined this technique with a caspase-2 BiFC inducible expression system to study caspase-2 dimerization at near endogenous levels. Interestingly, we discovered that caspase-2 dimers interact with TRAF1, TRAF2, and TRAF3, with TRAF2 being of particular importance for DNA damage-induced caspase-2 dimerization and subsequent apoptosis. We determined that TRAF2, which has been shown to possess E3 ligase activity, binds directly with caspase-2 and that this is necessary for TRAF2 to promote caspase-2 activation. Finally, we identified three lysine residues in the caspase-2 prodomain that are targeted by ubiquitination, a step that appears to stabilize the caspase-2 dimer and promote its full activity.

3.2 Results

3.2.1 Combining GFP-Trap with BiFC to immunoprecipitate caspase-2 dimers

In order to identify novel regulators of caspase-2 activation, we turned to the caspase-2 BiFC method. We hypothesized that we could exploit this method to isolate the active, dimerized form of caspase-2 with a targeted pull down of the fluorophore itself. This in turn would allow us to detect proteins that interact with the caspase-2 dimer, as these are likely to regulate its activation.

Towards this end, we first sought a GFP-targeting tool that would selectively capture the dimerized, refolded BiFC Venus to the exclusion of the monomeric BiFC Venus halves. Specifically, we used mVenus residues 1-172 (VN173) for the N-terminal BiFC half and mVenus residues 155-238 (VC155) for the C-terminal BiFC half (hereafter referred to as VN and VC, respectively). While researching available options we came upon GFP-Trap, a resin that binds GFP and GFP derivatives. GFP-Trap utilizes a small (~15kDa) antigen-binding domain, termed a nanobody, which is derived from an alpaca monoclonal antibody. The antibody was designed against full length GFP, and structural analysis of the GFP-Trap:GFP complex indicates that the nanobody recognition site spans both the VN and VC regions of the GFP molecule (Kubala et al. 2010). This led us to believe that it might selectively isolate dimerized BiFC Venus.

In order to test this, we transiently expressed the caspase-2 prodomain composed of residues 1-169 (caspase-2pro) fused with VN or VC, both individually and together, in

293T cells. High caspase-2 protein levels are known to promote its spontaneous dimerization and activation in a manner dependent on its CARD-containing prodomain (Butt et al. 1998; Wang et al. 1994; Kumar et al. 1994; Colussi et al. 1998). Thus, when the complementary caspase-2 BiFC fragments were co-overexpressed, caspase-2 BiFC signal was detected by flow cytometry, while the expression of caspase-2pro-VN or caspase-2pro-VC alone did not show fluorescent signal. (Figure 3.1A). The cells were lysed and incubated with GFP-Trap, and the resultant precipitates analyzed by Immunoblot. Excitingly, we found that GFP-Trap immunoprecipitated both fragments when they were co-overexpressed, but was unable to pull down either fragment alone (Figure 3.1B). This indicated that GFP-Trap only bound the reconstituted BiFC Venus, recognizing an epitope that is absent in the constituent fragments. Thus, by combining GFP-Trap with BiFC, we were able to specifically isolate caspase-2 dimers to the exclusion of caspase-2 monomers.

Because of the link between high caspase-2 protein levels and spontaneous activation, we decided to construct a cell line with inducible expression of the caspase-2 BiFC system. The CASP2pro-VN and CASP2pro-VC coding sequences were cloned into a bidirectional tetracycline-inducible plasmid (pTRE-Tight-BI), which in turn was stably transfected into HeLa Tet-Off cells. We then tested the cell line (hereafter referred to as CASP2pro-BiFC cells) for its ability to detect more physiological levels of caspase-2 dimerization through BiFC. Under non-stressed conditions (PBS) caspase-2 dimerization

was not detected (Figure 3.1C). However, treatment with the DNA damaging agent cisplatin induced a significant BiFC Venus signal, which in turn could be blocked by shutting off the expression of the BiFC fragments with doxycycline.

Using this cell line, we then tested to see if GFP-Trap could immunoprecipitate caspase-2 BiFC dimers when expressed at low levels. CASP2pro-BiFC cells were released from doxycycline and then treated with various caspase-2 activating stimuli for the indicated times. Lysates of treated cells were probed with GFP-Trap and analysed by immunoblot. Importantly, protein levels of the caspase-2 BiFC fragments were similar to endogenous caspase-2, and treatment induced BiFC dimers were readily precipitated by GFP-Trap (Figure 3.1D). Caspase-2 BiFC fragment levels were moderately increased when BiFC signals were observed, but the mRNA levels remained unchanged, or even decreased as in the case of cisplatin treatment (Figure 3.2). We also observed that co-expression of the caspase-2 BiFC fragments yielded a similar increase in protein levels compared to individual overexpression of the constructs, indicating that the fragments are likely stabilized by dimerization (Figure 3.1B).

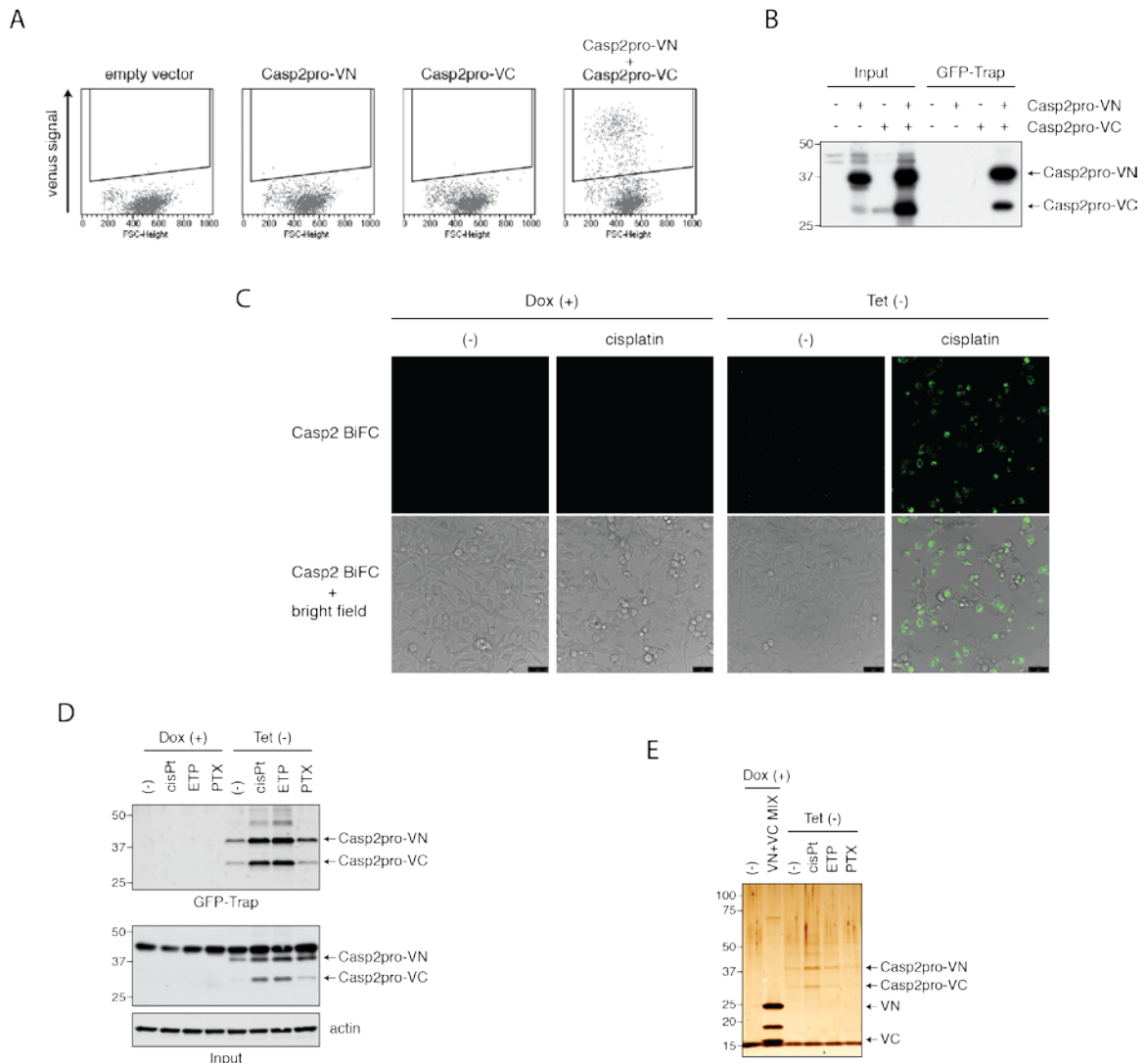


Figure 3.1 GFP-Trap selectively immunoprecipitates Casp2pro BiFC dimers to the exclusion of monomers.

(A) HEK293T cells transfected with empty plasmid, CASP2pro-VN or/and CASP2pro-VC for 48 h, followed by flow cytometry. (B) Lysates from (A) were immunoprecipitated (IP) using GFP-Trap followed by anti-caspase-2 (G310-1248) immunoblot (IB). (C) Representative confocal images of CASP2pro-BiFC cells treated with or without doxycycline (0.1 $\mu\text{g}/\text{mL}$) for 24 h, followed by 24 h with or without cisplatin (20 μM) and pan-caspase inhibitor Q-VD(OMe)-OPh (10 μM). (D) CASP2pro-BiFC cells treated with mock, cisplatin (20 μM), etoposide (50 μM), or paclitaxel (100 nM) for 24 h in presence of

Q-VD(OMe)-OPh (10 μ M), followed by GFP-Trap IP and anti-caspase-2 (G310-1248) IB. (E) CASP2pro-BiFC cells treated as in (D) followed by GFP-Trap IP and silver stain.

Thus, this seemed to be an optimal system to characterize and study the interactome of dimerized caspase-2 using a proteomics approach. CASP2pro-BiFC cells were again treated with caspase-2 activating stresses, lysed, and incubated with GFP-Trap. To control for BiFC Venus-targeting artifacts we overexpressed VN and VC, which can drive spontaneous dimerization, in CASP2pro-BiFC cells treated with doxycycline. These cells were treated similar to the experimental samples, lysed, and then combined before GFP-Trap immunoprecipitation (Figure 3.3). The resulting precipitates were then analyzed by LC-MS/MS for protein identification (Figure 3.1E).

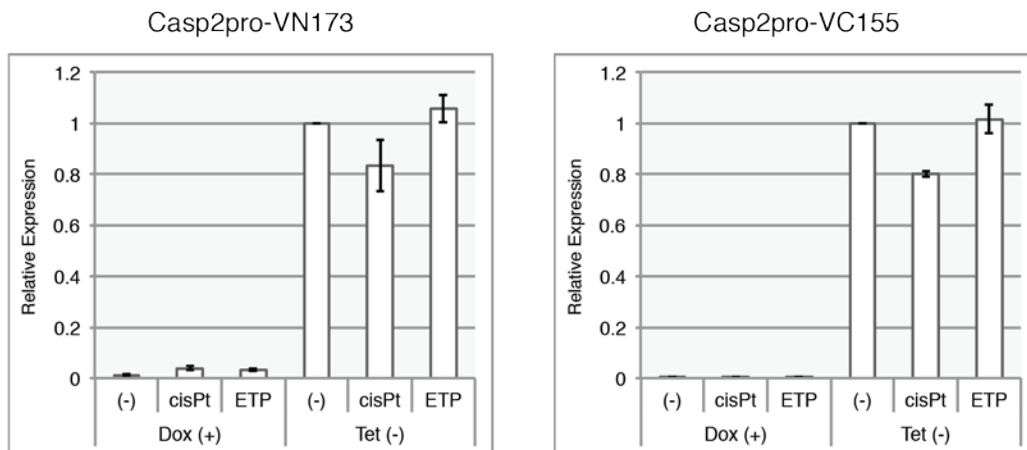


Figure 3.2 Caspase-2 stimuli do not induce expression of CASP2pro BiFC mRNA.

qPCR assay of CASP2pro BiFC fragment mRNA after treatment with caspase-2 stimuli. Cells were treated with or without doxycycline (0.1 μ g/mL) for 24 h, followed by mock, cisplatin (20 μ M), or etoposide (50 μ M) for 24 h in presence of Q-VD(OMe)-OPh (10 μ M).

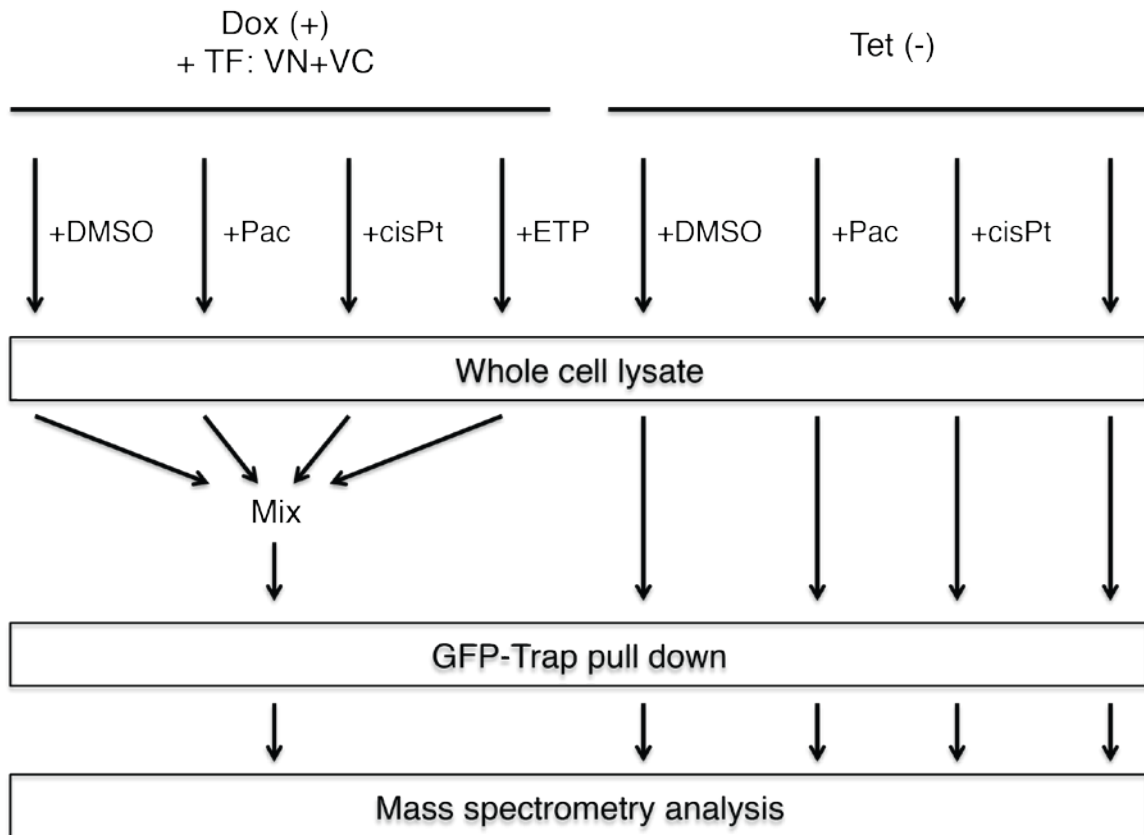


Figure 3.3 Workflow for mass spectrometry experiment.

CASP2pro-BiFC cells treated with mock, paclitaxel (100 nM), cisplatin (20 μ M), or etoposide (50 μ M) for 24 h in presence of Q-VD(OMe)-OPh (10 μ M) followed by GFP-Trap and submission for protein characterization by mass spectrometry. Note the control: CASP2pro BiFC expression was prevented with doxycycline (0.1 μ g/mL), and instead unconjugated BiFC VN and VC were transfected into cells before treating with caspase-2 stimuli, similar to experimental samples. Control lysates were then pooled before GFP-Trap.

3.2.2 TRAF1, 2, and 3 bind to dimerized, active caspase-2

This strategy identified several apoptosis-related proteins as putative caspase-2 binders: RAIDD, TRAF1, TRAF2, TRAF3, HtrA2/Omi, and cIAP1. The identification of

RAIDD, a well-known caspase-2 binding partner, was confirmation of the efficacy of the approach. Interestingly, PIDD was not identified by our proteomics screen of caspase-2 interactors, suggesting that the PIDDosome is not involved in caspase-2 dimerization in this context. Due to the prevalence of TRAF family members binding to caspase-2, and since TRAF proteins are known to act as adaptor proteins for signaling complexes, we decided to focus our efforts on TRAF1, 2, and 3.

To confirm our mass spectrometry results, we once again utilized the GFP-Trap system. Immunoblot analysis validated that endogenous TRAF1, 2, and 3 bind to caspase-2 BiFC dimers (Figure 3.4A). There are seven members of the TRAF family (Xie 2013); in order to determine the exclusivity of TRAF1, 2, and 3 in caspase-2 regulation we co-transfected a full-length caspase-2-Myc, in which the catalytic cysteine was mutated to alanine (C320A) to prevent induction of cell death, with each of the seven TRAFs and then immunoprecipitated by anti-Myc agarose beads. Immunoblot analysis revealed that only TRAF1, 2, and 3 bound significantly to caspase-2 (Figure 3.4B). We then transfected FLAG-caspase-2(C320A) alone, followed by anti-FLAG immunoprecipitation, and found that overexpressed caspase-2 bound endogenous TRAF1, TRAF2, and TRAF3 (Figure 3.4C). We performed the reverse experiment and transfected FLAG-TRAF1, 2, and 3 into HeLa Tet-Off cells, lysed the samples, and conducted anti-FLAG immunoprecipitation. In this case, we found that only TRAF2

bound strongly to endogenous caspase-2, possibly indicating an order of importance over the other TRAFs in caspase-2 regulation (Figure 3.4D).

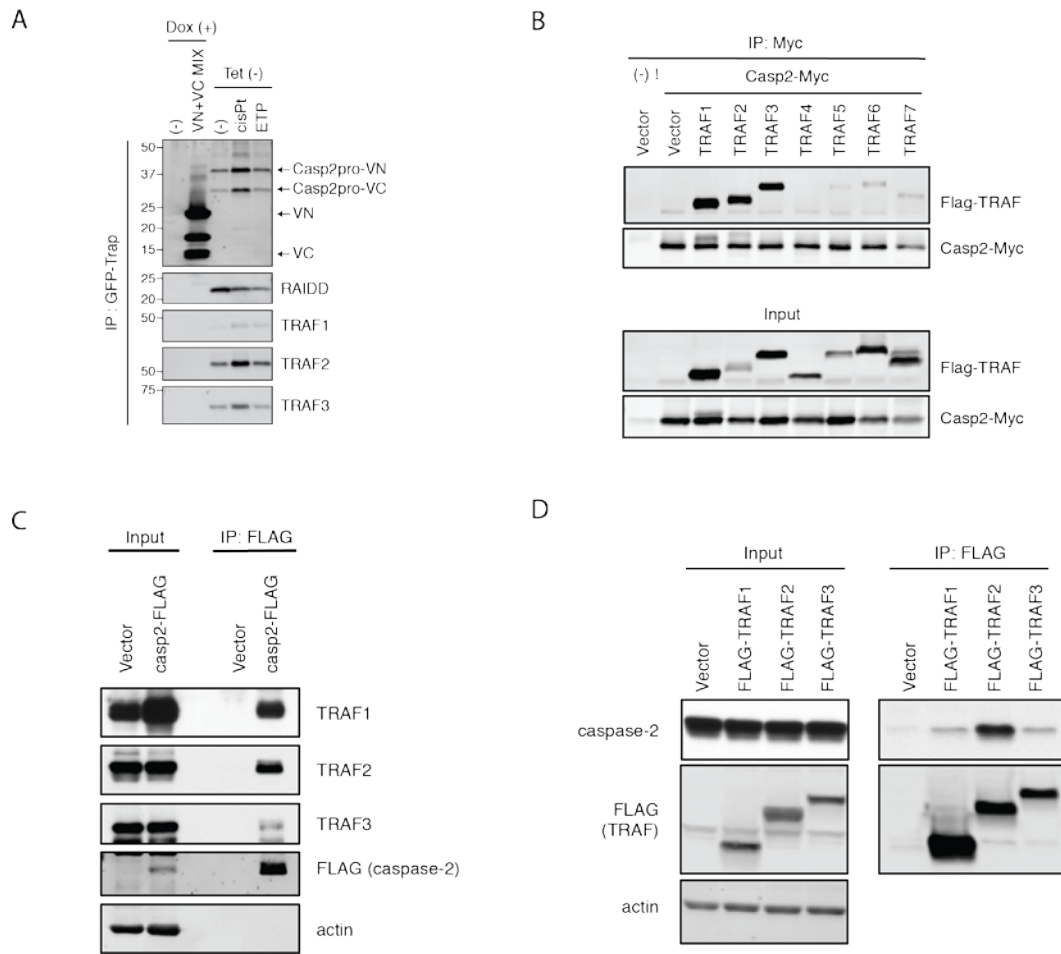


Figure 3.4 TRAF1, 2, and 3 bind to active, dimerized caspase-2.

(A) CASP2pro-BiFC cells treated with or without doxycycline (0.1 μ g/mL) for 24 h, followed by mock, cisplatin (20 μ M), or etoposide (50 μ M) for 24 h in presence of Q-VD(OMe)-OPh (10 μ M) followed by GFP-Trap and IB. BiFC fragments were detected with anti-GFP IB (B) CASP2-Myc and FLAG-TRAF1-7 panel co-expressed in HEK293T cells for 48 h, followed by α Myc IP and IB. (C) CASP2-FLAG transfected into HeLa Tet-Off cells 48 h, followed by α FLAG (M2) IP and IB. (D) FLAG-TRAF1-3 transfected into HeLa Tet-Off cells followed by α FLAG (M2) IP and IB.

3.2.3 TRAF2 is critical for caspase-2 activation and apoptosis in response to DNA damage

In order to understand the functional relevance of these caspase-2/TRAF interactions, we knocked down each of the TRAFs in the CASP2pro-BiFC cells and looked at the effect on DNA damage-induced caspase-2 BiFC. TRAF2 knockdown significantly decreased caspase-2 dimerization in response to cisplatin (Figure 3.5A). However, TRAF3 knockdown only partially reduced caspase-2 dimerization, while loss of TRAF1 slightly increased it. We then looked at how absence of the TRAFs affected DNA damage-induced apoptosis. Stable knockdown of TRAF2 using two separate shRNA significantly blocked cisplatin-induced apoptosis (Figure 3.5B). Stable knockdown of caspase-2 yielded similar results (Figure 3.5C). However, knockdown of TRAF3 only partially blocked cell death (Figure 3.5D), while targeting TRAF1 had no effect (data not shown). The effect of TRAF2 knockdown on cisplatin-induced apoptosis was confirmed by a reduction in the cleavage of the executioner caspase-3 (Figure 3.5E). Critically, TRAF2 knockdown also prevented the formation of active Bax and the cleavage of Bid to its pro-apoptotic form, tBid (Figure 3.5F and 3.5G). Together, these data indicate that TRAF2 controls the initiation of cisplatin-induced apoptosis by promoting mitochondrial outer membrane permeabilization (MOMP) via caspase-2 cleavage of tBid, while TRAF3 and TRAF1 play a lesser role.

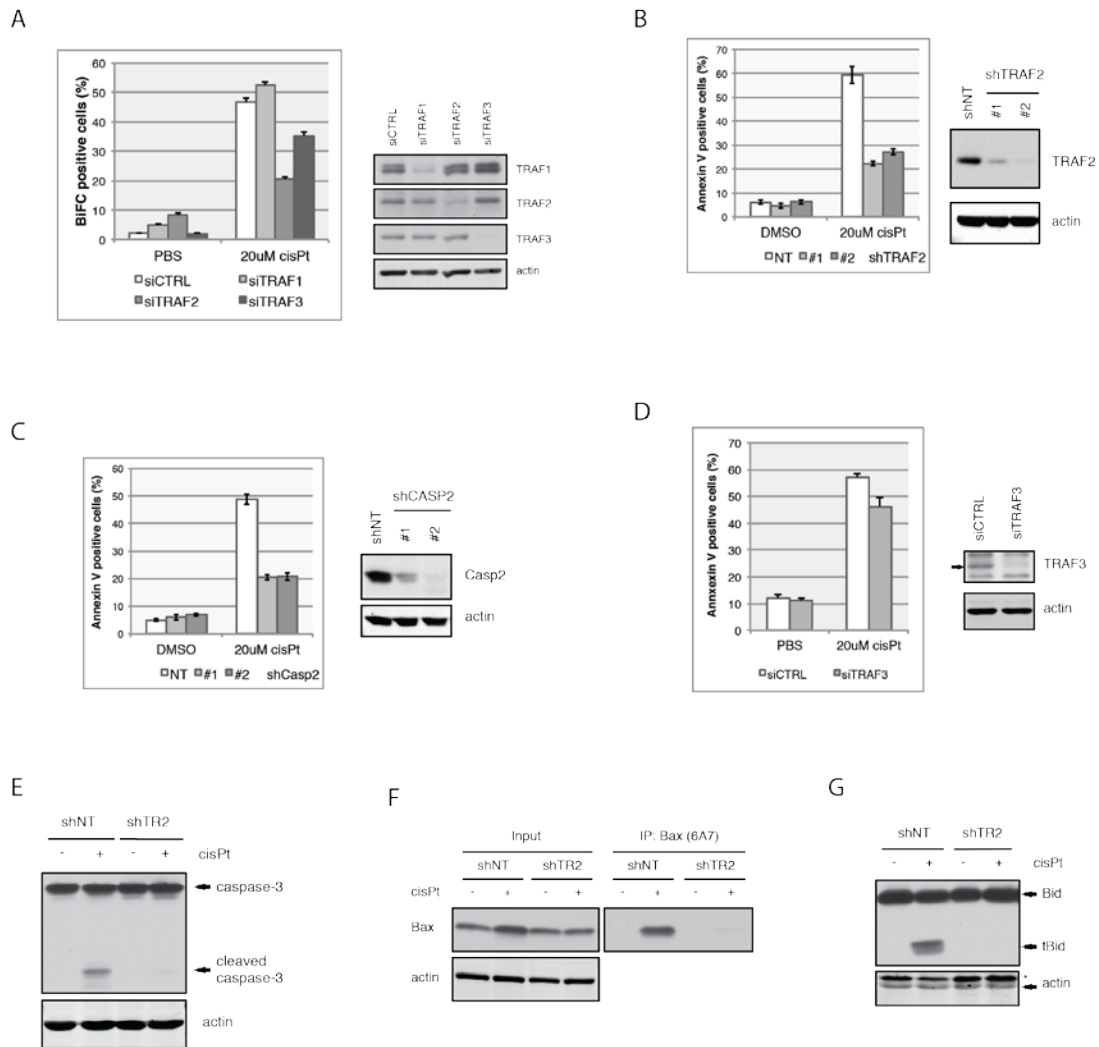


Figure 3.5 TRAF2 is required for cisplatin-induced, caspase-2-initiated apoptosis.

(A) CASP2pro-BiFC cells were transfected with siRNA for 48 h, followed by cisplatin (20 μ M) for 24 h in presence of Q-VD(OMe)-OPh (10 μ M), then flow cytometry to detect BiFC. (B) snNT (non-targeting) or shTRAF2 HeLa cells treated with cisplatin (20 μ M) for 24 h, followed by annexin V staining and flow cytometry. (C) shNT or shCASP2 HeLa cells treated as in (B). (D) HeLa Tet-Off cells transfected with siRNA for 48 h, followed by cisplatin (20 μ M) for 24 h, then stained with annexin V and analyzed by flow cytometry. (E-G) shNT or shTRAF2 #2 HeLa cells treated with cisplatin (20 μ M) for (E) 24 h, (F) 18 h, (G) 18 h, followed by IB.

3.2.4 TRAF2 interacts directly with caspase-2 via a TRAF Interaction Motif (TIM) to promote dimerization

A scan of the caspase-2 sequence revealed a putative TRAF-interacting motif (TIM) at residues 247-251 (TAQEM) (Ye et al. 1999). To investigate the importance of this sequence we constructed a caspase-2 mutant where all of the TIM residues were changed to alanine (hereafter referred to as caspase-2(TIM)). We then examined how this mutation affected the ability of caspase-2 to bind to TRAF1, 2, and 3. FLAG-caspase-2 or FLAG-caspase-2(TIM) was transfected into HeLa Tet-Off cells for 48h, after which caspase-2 was immunoprecipitated with anti-FLAG beads. Immunoblot analysis revealed that the mutation of the TIM completely disrupted caspase-2 binding to all three TRAFs (Figure 3.6A-C). To examine the effect of the loss of the TIM on caspase-2 activity, HeLa Tet-On cells were infected with retroviral particles containing tetracycline-inducible constructs of caspase-2(wild type) and (TIM). Induction of caspase-2(wild type) readily induced cell death but induction of caspase-2(TIM) had no effect (Figure 3.6D). Furthermore, we constructed full length, catalytically inactive caspase-2 BiFC fragments with a mutant TIM and examined the effect on dimerization. HeLa cells were carefully transfected with low amounts of the plasmids to reduce spontaneous dimerization and then treated with cisplatin. We found that mutation of the TIM significantly reduced cisplatin-induced caspase-2 dimerization (Figure 3.6E).

Furthermore, because we observed that overexpressed TRAF2 was able to bind to endogenous caspase-2, we speculated that it was possible for TRAF2 to actively

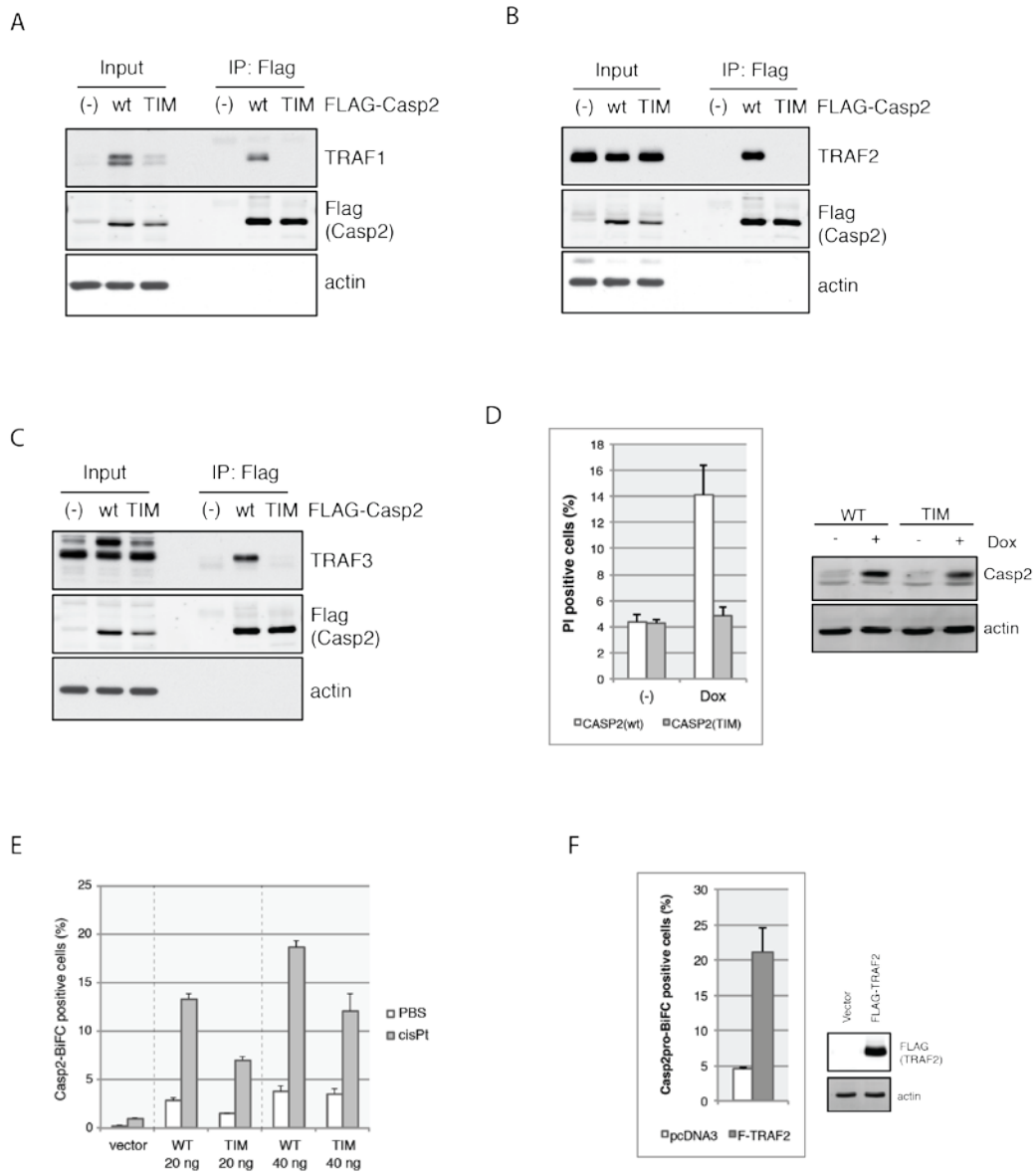


Figure 3.6 TRAF2 interacts directly with caspase-2 to induce activation.

(A-C) CASP2-FLAG constructs expressed in HeLa Tet-Off cells 48 h followed by α FLAG (M2) IP and IB. (D) Catalytically active caspase-2 was induced in HeLa Tet-On cells with doxycycline (0.1 μ g/mL) for 24 h, followed by PI stain and flow cytometry. (E) Indicated amounts of CASP2 (full length, catalytically inactive) BiFC constructs were transiently transfected for 24 h followed by cisplatin (20 μ M) in presence of Q-VD(OMe)-OPh (10 μ M) for 24 h, then flow cytometry to detect BiFC. (F) CASP2pro-BiFC cells were transfected with FLAG-TRAF2 and allowed to express 24 h, then washed out to allow

caspase-2pro BiFC expression for 24 h, followed by treated with Q-VD(OMe)-OPh (10 μ M) for another 24 h, then analyzed by flow cytometry to detect BiFC.

promote caspase-2 dimerization. To test this, we overexpressed TRAF2 in CASP2pro-BiFC cells and observed the effect by flow cytometry. Indeed, TRAF2 overexpression induced strong caspase-2 dimerization (Figure 3.6F). Together with the previous data this indicates that TRAF2 action is necessary and perhaps sufficient for promoting caspase-2 activation in response to DNA damage, and that this occurs through a direct interaction.

3.2.5 TRAF2-dependent ubiquitination of the caspase-2 prodomain is critical for dimer stability and fully enzymatic activity

TRAF2 is known to act as a scaffold that recruits other proteins, but it also possesses an amino-terminal RING domain, which has been shown to confer E3 ligase activity (Alvarez et al. 2010; Gonzalez et al. 2012). Indeed, ubiquitin was identified by mass spectrometry as one of the major proteins pulled down with the caspase-2 BiFC dimers. Furthermore, when we performed GFP-Trap immunoprecipitation on CASP2pro-BiFC cell lysates after cisplatin treatment, we found that the caspase-2 BiFC fragments were ubiquitinated (Figure 3.7A). We also observed ubiquitination of overexpressed caspase-2 prodomain, which in turn was diminished by TRAF2 knockdown (Figure 3.7B).

This led us to hypothesize that TRAF2 acts on caspase-2 to promote its activation through non-degradative ubiquitination of the prodomain. We thus created arginine mutants for each lysine residue in the prodomain in order to determine which of them contribute to caspase-2 ubiquitination. Two mutants yielded a significant phenotype: the K152/153R mutation dramatically reduced the ubiquitination of caspase-2 prodomain, while the K15R mutation had a more moderate effect (Figure 3.7C). When all three lysines were mutated in the same protein (hereafter referred to as 3KR), caspase-2 prodomain ubiquitination was almost completely abolished (Figure 3.7D). Interestingly, we found that the 3KR mutation partially diminished the binding of caspase-2 to endogenous TRAF2 (Figure 3.7E). To test more directly whether ubiquitination of caspase-2 affects binding of TRAF2, an *in vitro* binding assay was performed. In this assay, we overexpressed mVenus tagged caspase-2 prodomain to promote its ubiquitination, purified it with GFP-Trap, and mixed it with bacterially-expressed recombinant MBP tagged TRAF2. TRAF2 was then retrieved by amylose resin and the binding of caspase-2 was assessed. Wild type caspase-2 bound recombinant MBP-TRAF2, but the 3KR mutant of caspase-2 showed much weaker binding (Figure 3.7F). Together these findings indicate that the ubiquitination of caspase-2 itself contributes to TRAF2 binding.

(A) CASP2pro-BiFC cells were treated with or without doxycycline (0.1 $\mu\text{g}/\text{mL}$) for 24 h, followed by cisplatin (20 μM) for 24 h in presence of Q-VD(OMe)-OPh (10 μM), followed by GFP-Trap IP and IB to detect ubiquitination. Caspase-2 BiFC fragments were detected with anti-caspase-2 IB. (B) HEK293T cells were transfected with TRAF2 siRNA for 48 h, then transfected with CASP2pro-mVenus for 48 h, followed by GFP-Trap IP and IB. (C) HEK293T cells transfected with various CASP2pro-mVenus constructs for 48 h, followed by GFP-Trap IP and IB. mVenus tag was detected with anti-GFP IB. (D) HEK293T cells treated as in (C). (E) HeLa cells transfected with CASP2fl(C320A)-mVenus constructs for 48 h, followed by GFP-Trap IP and IB. mVenus tag was detected with anti-GFP IB. (F) HeLa cells transfected with CASP2pro-mVenus for 48 h, then lysed in RIPA Buffer and immunoprecipitated with GFP-Trap. Bacterial-produced MBP-TRAF2 or MBP control were added to the GFP-Trap precipitate for 2h and incubated on ice, followed by MBP purification and IB. mVenus and MBP tags were detected with anti-GFP and anti-MBP IB, respectively.

To further study the function of these sites, the 3KR mutations were introduced into the caspase-2 BiFC system. Interestingly, we did not observe a significant difference in the percentage of BiFC positive cells when comparing the wild type and 3KR mutant (Figure 3.8A). However, we found that when we attempted to immunoprecipitate the BiFC dimers, GFP-Trap pulled down significantly less caspase-2(3KR) BiFC dimers than the non-mutant caspase-2, suggesting that the mutant caspase-2 forms a weaker dimer (Figure 3.8B). To further investigate this possibility, we co-expressed Myc-caspase-2pro and caspase-2pro-mVenus in HeLa cells, immunoprecipitated the resulting heterodimers with GFP-Trap, and then subjected them to salt washes of increasing stringencies. This assay revealed that caspase-2(3KR) dimers are less stable and more easily disrupted while wild type caspase-2 dimers remain stable even under high concentrations of salt wash up to 750 mM NaCl (Figure 3.8C).

We then examined how the loss of these three ubiquitination sites affects caspase-2 function. When we expressed increasing amounts of catalytically active caspase-2, we found that wild type caspase-2 exhibited higher activity than the 3KR mutant, as evidenced by autoprocessing (Figure 3.8D). This effect on catalytic activity was validated in an enzymatic assay, which showed that the 3KR mutations significantly reduced the ability of caspase-2 to cleave the artificial substrate VDVAD-pNA (Figure 3.8E).

Moreover, cisplatin-induced cleavage of the 3KR mutant was less than the wild type when caspase-2 was expressed at near endogenous level (Figure 3.8F). And finally, the 3KR mutation significantly retarded the induction of apoptosis by cisplatin (Figure 3.8G). Together these data indicate that K15, K152, and K153, which are subject to ubiquitination, play a critical role in stabilizing caspase-2 dimerization to promote its full pro-apoptotic activation.

3.3 Discussion

The ability to study protein complexes is often hampered by a lack of precise tools. In this study, we demonstrated that the combination of BiFC with GFP-Trap nanobodies produces a powerful tool for isolating and characterizing protein complexes and their interactomes. Although we only used this method to investigate caspase-2 complexes, the modular nature of the BiFC system indicates that it should be broadly

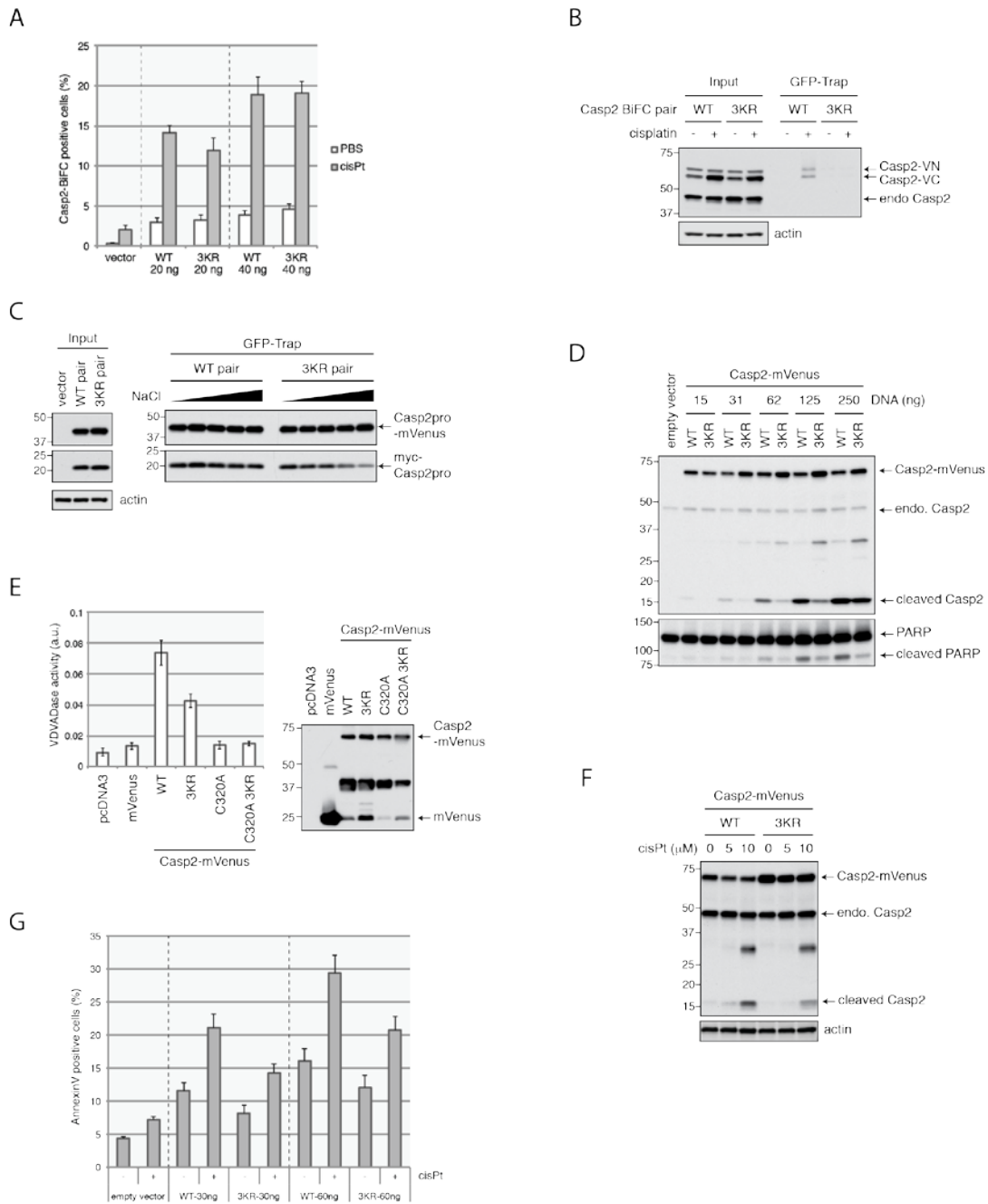


Figure 3.8 Caspase-2 prodomain ubiquitination appears to be necessary for dimer stability and activity.

(A) Various amounts of the indicated CASP2 (full length, catalytically inactive) BiFC constructs were transfected into HeLa cells, allowed to express for 24 h, and then treated

with cisplatin for 24 h in the presence of Q-VD(OMe)-OPh (10 μ M). BiFC was detected by flow cytometry. (B) GFP-Trap IP then IB of 20 ng CASP2pro BiFC samples from (A). (C) Indicated CASP2pro-mVenus and Myc-CASP2pro constructs co-expressed in HeLa cells, then dimerization was induced by cisplatin (20 μ M) and Q-VD(OMe)-OPh (10 μ M) for 24 h. This was followed by GFP-Trap IP and salt washes at increasing stringencies. (D) Catalytically active full length CASP2-mVenus constructs expressed in HEK293T cells for 48 h, followed by IB. (E) Catalytically active full length CASP2-mVenus constructs expressed in HEK293T cells for 24 h, followed by GFP-Trap IP and VDADase assay. Expression was assessed by anti-GFP IB. (F) Catalytically active full length CASP2-mVenus constructs expressed in HeLa cells for 24 h, followed by cisplatin (20 μ M) for 24 h and then IB. (G) Catalytically active full length CASP2-mVenus constructs expressed in HeLa cells for 24 h, followed by cisplatin (20 μ M) for 24 h and then stained with annexin V and assayed by flow cytometry.

useful. Indeed, as we were preparing this manuscript, another group published a report detailing the same approach, which they termed BiCAP, focusing on ERBB2 dimers (Croucher et al. 2016).

Using this approach, we showed that caspase-2 dimers specifically interacted with TRAF1, TRAF2, and TRAF3 but not other members of the TRAF family. This is the first time that TRAF3 has been shown to interact with caspase-2, while TRAF1 and TRAF2 had been previously identified by Lamkanfi and colleagues (Lamkanfi et al. 2005). In that study, caspase-2 and TRAF2, in complex with RIPK1, were found to positively regulate NF- κ B signaling, which is the canonical TRAF2 pathway. However, these complexes were characterized in the context of lysates that had been heated to 37°C. Although this *in vitro* technique was used in early studies to promote the formation of caspase-2 complexes (Read et al. 2002; Tinel and Tschopp 2004), it is unclear if it models a physiologically relevant stimulus. Furthermore, we were unable to

identify RIPK1 as a binding partner in either our proteomics experiments or through immunoblot analysis (data not shown). It is reasonable that different stimuli promote distinct caspase-2/TRAF2 complexes, with some perhaps functioning in a non-apoptotic capacity. Indeed, this might also be the case for TRAF1 or TRAF3, as they did not seem to be as critical for DNA damage-induced apoptosis.

In this study, we demonstrated that TRAF2 is required for DNA damage-induced caspase-2 dimerization and consequent cell death. Pathway analysis confirmed that TRAF2 acts upstream of the mitochondria to trigger cell death, confirming the role of the caspase-2/TRAF2 complex in initiating apoptosis. We observed that TRAF2 bound directly to caspase-2 at least in part through a TRAF interacting motif (TIM) and that this sequence is important for caspase-2 dimerization and cell death. This was somewhat puzzling since the TIM lies outside of the caspase-2 prodomain, and yet the caspase-2 prodomain still dimerized in a TRAF2-dependent manner in response to DNA damage. Interestingly, we found that full-length caspase-2 bound more strongly to TRAF2 than the prodomain alone (data not shown). This suggests that TRAF2 might bind to caspase-2 at more than one interface, with one being a canonical site (TIM) and the other novel (prodomain). Alternatively, it is possible that the TRAF2 interaction with the prodomain is indirect but still functionally critical.

TRAF2 is known to act as a scaffold that mediates the interaction of other proteins, such as TRAF3 and the ubiquitin E3 ligases cIAP1 and 2 (Borghetti, Verstrepen,

and Beyaert 2016). Thus, it is conceivable that TRAF2 is promoting caspase-2 dimerization as part of a caspase-2 activation platform. TRAF2 has also been found to act as a ubiquitin E3 ligase, a function that is attributed to its amino-terminal RING domain. Thus, TRAF2 might be directly responsible for ubiquitinating caspase-2 in a manner that promotes its activity. This is not unprecedented, as non-degradative K63-linked polyubiquitination has previously been shown to promote both caspase-8 and caspase-1 activation (Jin et al. 2009; Labbé et al. 2011). Active, dimerized caspase-2 has previously been demonstrated to form large cytoplasmic foci (Bouchier-Hayes et al. 2009), and ubiquitination could play a role in this oligomerization as it does caspase-8 (Jin et al. 2009). Alternatively, it might promote the binding of other activating factors or induce a localization change as occurs in NF- κ B regulation (Komander and Rape 2012).

We found that caspase-2 BiFC dimers were ubiquitinated in response to DNA damage. When we mutated prominent ubiquitination sites at K15, K152, and K153 (3KR) in the caspase-2 prodomain we found that caspase-2 could still dimerize, but the complex was unstable and had reduced catalytic activity. Of these three lysines, only K15 has been previously identified as a potential ubiquitination site, while its function was not determined (Mertins et al. 2013). K152 and K153 were previously identified to be part of a nuclear localization signal (NLS) in caspase-2 (Paroni et al. 2002; Baliga et al. 2003), and their mutation to alanine abolished nuclear import. The arginine substitutions used in this study are less disruptive than alanine mutations in that they maintain a

longer, basic residue at the position of interest (Hodel, Corbett, and Hodel 2001; Kosugi et al. 2008). Similarly to Paroni and colleagues, we found that mutation of K152 and K153 did not have a significant impact on caspase-2 activity induced by high overexpression (Paroni et al. 2002) and (Figure 3.8D). However, these mutations dampen activity when caspase-2 is expressed at lower levels (Figure 3.8D and 3.8E) and engaged by cisplatin (Figure 3.8F and 3.8G), indicating that ubiquitination plays an important role in stabilizing caspase-2 complexes. It is possible that ubiquitination of these lysines also blocks caspase-2 nuclear localization, which is in line with previous findings that caspase-2 dimerization occurs in the cytoplasm (Bouchier-Hayes et al. 2009).

It remains unclear if TRAF2 is the ubiquitin E3 ligase directly responsible for these modifications. Although knockdown of TRAF2 reduced caspase-2 ubiquitination, we have been unsuccessful in our attempts to ubiquitinate caspase-2 with TRAF2 in an *in vitro* assay. It is possible that TRAF2 engages another E3 ligase to promote caspase-2 ubiquitination, and further work will be important to shed light on this.. Regardless, we have shown that TRAF2 promotes caspase-2 activation and apoptosis in response to DNA damage. Further studies investigating this mechanism could yield insights into how to modulate caspase-2 as a therapeutic target, perhaps by targeting caspase-2 ubiquitination or TRAF2 activity.

4. Mitotic phosphatase activity is required for MCC maintenance during the spindle checkpoint

This chapter is adapted from a published co-first author manuscript (Foss et al. 2016).

4.1 Introduction

The spindle checkpoint is activated in early mitosis to protect chromosomal integrity by preventing entry into anaphase until all chromosomes are aligned and properly attached to the mitotic spindle. Defects in the spindle checkpoint may lead to missegregated chromosomes and aneuploidy, which could contribute to tumorigenesis (Kops, Weaver, and Cleveland 2005). Therefore the spindle checkpoint is essential for maintaining genomic stability (Chandhok and Pellman 2009; London and Biggins 2014b; Musacchio and Salmon 2007a).

The spindle checkpoint prevents cells from progressing into anaphase by inactivating the anaphase-promoting complex/cyclosome (APC/C), an E3 ubiquitin ligase required for mitotic progression (Pines 2011). The primary inhibitor of the APC/C during checkpoint operation is the mitotic checkpoint complex (MCC), which is composed of the APC/C coactivator CDC20 in complex with Mad2, BubR1, and Bub3 (Sudakin, Chan, and Yen 2001; Lara-Gonzalez, Westhorpe, and Taylor 2012a). Although sub-complexes of Mad2-CDC20 and BubR1-Bub3-CDC20 have some inhibitory effect on the APC/C, the complete MCC is a much stronger inhibitor (Sudakin, Chan, and Yen 2001; Fang 2002; Hein and Nilsson 2014; Chao et al. 2012). Once all chromosomes are properly engaged by the spindle, with one sister chromatid attached to microtubules

from one pole and the other sister chromatid to microtubules from the opposite pole, such that tension is applied at the kinetochores (bi-orientation), the checkpoint is satisfied and the MCC releases CDC20, which can in turn activate the APC/C (Rieder et al. 1994; Rieder et al. 1995; Li and Nicklas 1995). The activated APC/C then targets cyclin B and securin for degradation thereby leading to Cdk1 inactivation and sister chromatid segregation, respectively (London and Biggins 2014b). APC/C^{CDC20} is also responsible for cyclin A degradation, which occurs slightly earlier in mitosis than cyclin B degradation due in part to its high affinity for CDC20 (Di Fiore and Pines 2010).

Kinetochores lacking tension or attachment to the mitotic spindle form a platform for MCC formation (London and Biggins 2014b). This process occurs via sequential recruitment of MCC components to the kinetochore, and while there are still many unknowns regarding the molecular mechanisms regulating MCC assembly, it is well established that phosphorylation is essential for both MCC assembly and checkpoint activation (London and Biggins 2014b; Funabiki and Wynne 2013). One of the key mediators of MCC formation is the kinase MPS1, which is required for kinetochore localization of all known spindle checkpoint components (Tighe, Staples, and Taylor 2008; Abrieu et al. 2001; London and Biggins 2014b; Yamagishi et al. 2012; London and Biggins 2014a; Maciejowski et al. 2010a). Importantly, inhibition of MPS1 leads to disassembly of the MCC and a decrease in cyclin B and securin levels, indicating that the APC/C has been activated (Maciejowski et al. 2010a). MPS1 phosphorylation of

the kinetochore protein KNL1 forms a docking site for Bub1 and Bub3, which in turn recruit BubR1 and a heterodimer of Mad1 and Mad2 (Zhang, Lischetti, and Nilsson 2014; London et al. 2012). The Mad1-Mad2 complex recruits an additional Mad2 to the kinetochore where it undergoes a conformational change and binds CDC20 (Luo et al. 2002; Musacchio and Salmon 2007a). The Mad2-CDC20 complex then binds BubR1-Bub3 to form the functional MCC, which diffuses away from the kinetochore to inhibit the APC/C (London and Biggins 2014b; Funabiki and Wynne 2013). Aurora B kinase also contributes to the kinetochore recruitment of several essential checkpoint proteins (Ditchfield et al. 2003a). Additionally, Aurora B indirectly promotes spindle checkpoint maintenance by destabilizing improperly attached microtubules at the kinetochore (Ditchfield et al. 2003a; Morrow et al. 2005; Saurin et al. 2011; Santaguida et al. 2011; Kops and Shah 2012). Another important kinase for checkpoint signaling is Plk1, which was recently shown to enhance MPS1 activity and the localization of MCC components to kinetochores (von Schubert et al. 2015).

As the MPS1, Aurora B, and Plk1 kinases all promote spindle checkpoint activation, it is unsurprising that protein phosphatases have been implicated in checkpoint silencing. The two main phosphatases known to be involved in checkpoint silencing are PP1 and PP2A-B56. These phosphatases exist in both negative and positive feedback loops with the above-mentioned kinases to allow for robust checkpoint activation and also rapid inactivation and dissociation of the MCC upon proper

microtubule attachment (Nijenhuis et al. 2014a; Foley, Maldonado, and Kapoor 2011a; Liu et al. 2010; Espert et al. 2014). MPS1 phosphorylation of KNL1 recruits PP2A to kinetochores through its interaction with BubR1 (Kruse et al. 2013; Nijenhuis et al. 2014a; Xu et al. 2013; Yamagishi et al. 2012). PP1 is also recruited to KNL1, but its binding is inhibited early in prometaphase by strong Aurora B phosphorylation of KNL1 (Liu et al. 2010). Interestingly, BubR1-associated PP2A-B56 opposes Aurora B phosphorylation of KNL1 thereby promoting PP1 recruitment (Foley, Maldonado, and Kapoor 2011a; Nijenhuis et al. 2014a). In addition to PP2A-B56, PP1 has also been shown to oppose Aurora B at the kinetochore, thereby stabilizing kinetochore-microtubule attachments and promoting checkpoint silencing (Nijenhuis et al. 2014a; Liu et al. 2010; Meadows et al. 2011; Rosenberg, Cross, and Funabiki 2011; Emanuele et al. 2008). PP1 and PP2A-B56 have also both been implicated in dephosphorylating MPS1 phosphorylation sites on KNL1, which in turn dissociates PP2A-B56 and the MCC components from the kinetochore (Espert et al. 2014; Nijenhuis et al. 2014a). Taken together, these findings all indicate that PP1 and PP2A-B56 are essential for spindle checkpoint silencing and MCC disassembly. However, in examining the involvement of phosphatases in the spindle checkpoint, we found that their role is more complex: using two phosphoprotein phosphatase (PPP) inhibitors, calyculin A and okadaic acid, we demonstrate that a PPP family Ser/Thr phosphatase is required during the spindle checkpoint to prevent MCC disassembly and APC/C activation.

4.2 Results

4.2.1 Calyculin A and okadaic acid can override the spindle checkpoint to activate the APC/C

To test whether protein phosphatases are involved in APC/C inhibition during the spindle checkpoint, we treated synchronized nocodazole-arrested cells with a panel of phosphatase inhibitors and then measured cyclin B levels in cell lysates (Figure 4.1A). Cells treated with okadaic acid (0.1 μM), fostriecin, or the calcineurin inhibitors FK506 and cyclosporin A retained high levels of cyclin B, indicating the APC/C was still being inactivated by the spindle checkpoint. However, in cells treated with the phosphatase inhibitors calyculin A or a high concentration of okadaic acid (1 μM), cyclin B levels were dramatically reduced, indicating that the APC/C had been activated as a result of phosphatase inhibition. We also measured cyclin A levels in these cells and observed that levels were high in nocodazole-arrested cells but were reduced following calyculin A or okadaic acid (1 μM) treatment similar to cyclin B. Furthermore, calyculin A treatment accelerated cyclin B degradation during mitotic exit as compared to control cells or cells treated with fostriecin or cyclosporin A (Figure 4.1B). As calyculin A and okadaic acid are both inhibitors of the PPP family of Ser/Thr phosphatases, we deduced that a PPP phosphatase must be required during the spindle checkpoint to prevent cyclin A and B degradation.

During normal mitotic exit, cyclin A and B are both degraded via the proteasome after being targeted by the APC/C. To determine whether the calyculin A-induced

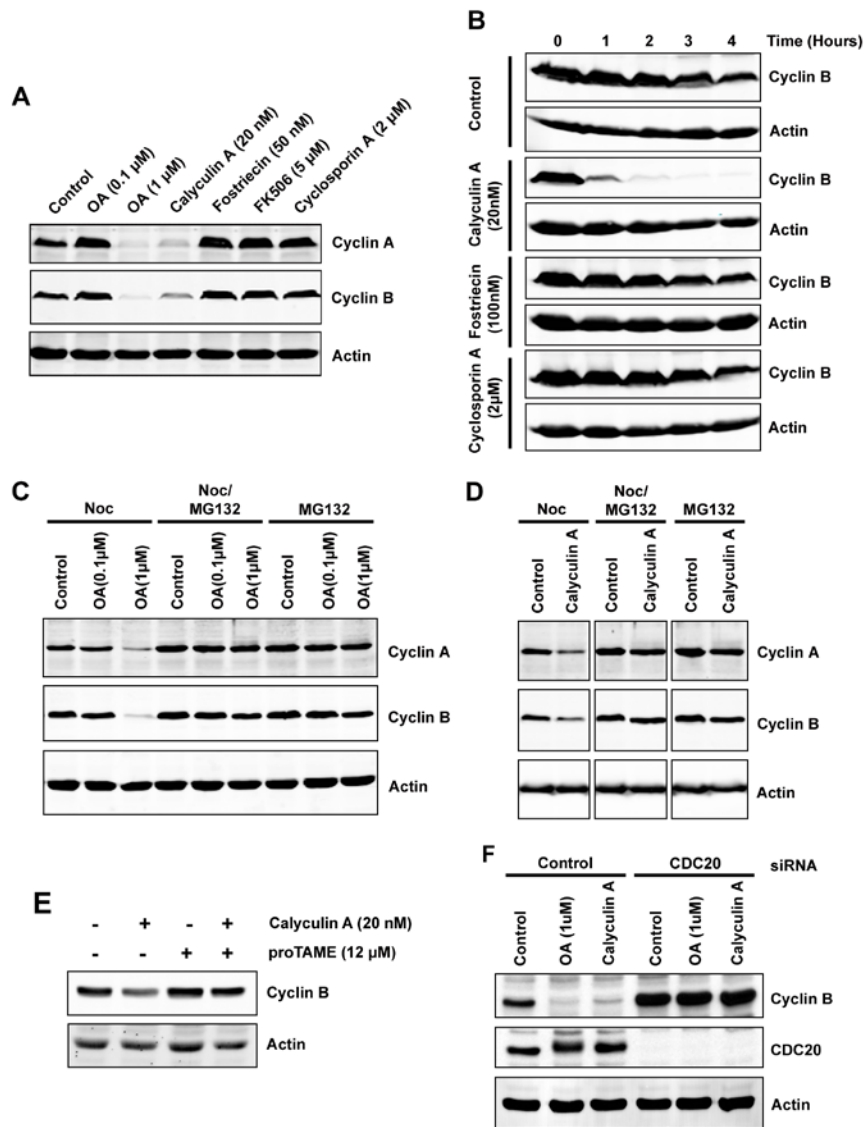


Figure 4.1 Calyculin A and okadaic acid (1 μ M) induce cyclin B degradation in spindle checkpoint-arrested cells via the APC/C^{CDC20}.

(A) Synchronized nocodazole-arrested HeLa Tet-Off cells were treated with the indicated phosphatase inhibitors for 2 hours. Protein levels were detected by immunoblotting with the indicated antibodies. (B) Synchronized nocodazole-arrested HeLa Tet-Off cells were treated with the indicated phosphatase inhibitors for 30 minutes prior to washing out nocodazole. Fresh media containing the phosphatase inhibitors was then added, and cells were harvested at indicated time points post nocodazole

release. Protein levels were detected by immunoblotting with the indicated antibodies. (C and D) Synchronized HeLa-Tet-Off cells were treated with nocodazole for 16 hours and then treated with MG132 (20 μ M) for 1 additional hour before the indicated phosphatase inhibitors were added for 2 hours. Protein levels were detected by immunoblotting with the indicated antibodies. (E) Synchronized nocodazole-arrested HeLa Tet-Off cells were pretreated with proTAME (12 μ M) for 1 hour and then treated with calyculin A (20 nM) for 2 hours. Protein levels were detected by immunoblotting with the indicated antibodies. (F) HeLa Tet-Off cells were transfected with CDC20 or control siRNA, synchronized with a double thymidine block, and released into nocodazole. Cells were then treated with the indicated inhibitors for 2 hours. Protein levels were detected by immunoblotting with the indicated antibodies. OA: okadaic acid; Noc: nocodazole.

decrease in cyclin levels was also mediated by the proteasome, synchronized nocodazole-arrested cells were treated with the proteasome inhibitor MG132 prior to treatment with the phosphatase inhibitors. Pre-treatment with MG132 rescued cyclin A and B levels in okadaic acid and calyculin A-treated cells, confirming that okadaic acid and calyculin A induce proteasomal degradation of cyclin A and B (Figure 4.1C and 4.1D). Furthermore, directly inhibiting the APC/C with the small molecule inhibitor proTAME or depleting CDC20 using siRNA also restored cyclin B levels following calyculin A treatment (Figure 4.1E and 4.1F). Therefore, calyculin A-induced cyclin degradation appears to occur via the pathway normally activated upon mitotic exit and is dependent on both the APC/C^{CDC20} and the proteasome. Taken together, these results demonstrate that a PPP phosphatase is necessary for APC/C inactivation during the spindle checkpoint.

4.2.2 Phosphatase activity is required for MCC maintenance during the spindle checkpoint

The MCC is the major inhibitor of the APC/C during the spindle checkpoint, we hypothesized that calyculin A and okadaic acid (1 μ M) may induce MCC disassembly. This dissociation would free CDC20 to activate the APC/C such that it could ubiquitinate cyclin A and B to target them for degradation. To test this hypothesis, endogenous CDC20 was immunoprecipitated from synchronized taxol-arrested mitotic cells treated with our panel of phosphatase inhibitors. In control cells, CDC20 co-immunoprecipitated with the other components of the MCC (Mad2, BubR1, and Bub3), but the binding between CDC20 and the other MCC components was greatly reduced in calyculin A and okadaic acid (1 μ M) treated cells (Figure 4.2A). Similar results were found when CDC20 was immunoprecipitated from cells arrested by nocodazole (Figure 4.2C). Additionally, CDC20 still disassociated from the MCC in the presence of MG132, which rescued cyclin A and B degradation (Figure 4.2B). This result indicates that calyculin A and okadaic acid-induced MCC disassembly is upstream of the proteasomal degradation of cyclin A and B.

To investigate the timing of MCC dissociation with respect to cyclin A and B degradation, nocodazole-arrested cells were treated with calyculin A for varying amounts of time, followed by CDC20 immunoprecipitation and immunoblot analysis of the MCC components and cyclin A and B. CDC20 interaction with BubR1 and Bub3 began to weaken after just 15 minutes of calyculin A treatment while binding with Mad2

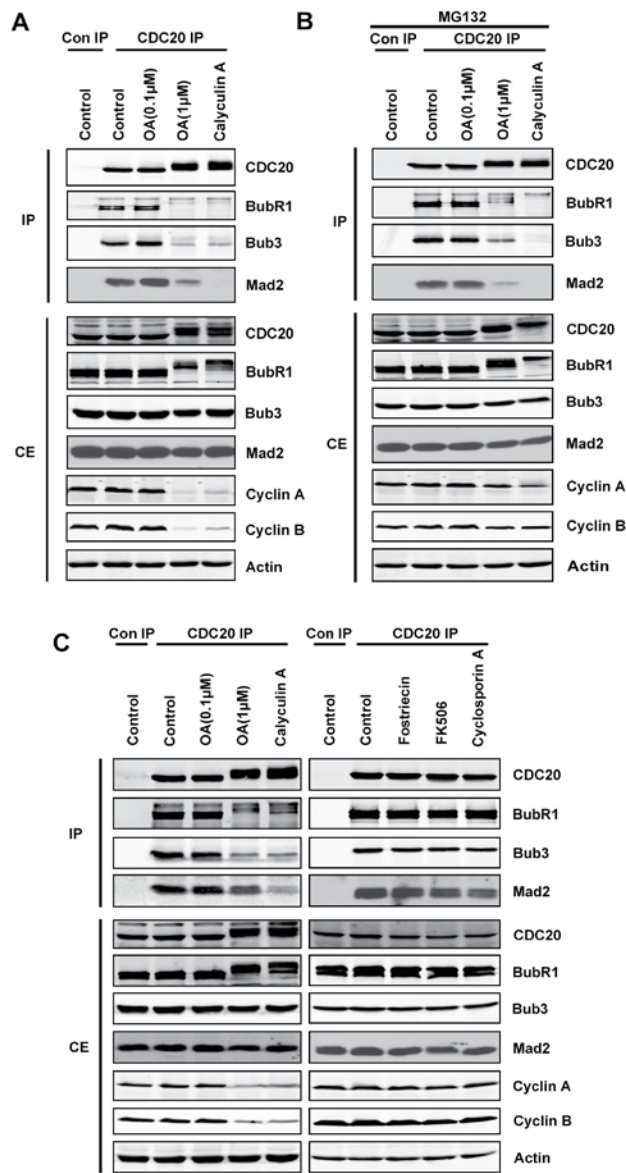


Figure 4.2 Calyculin A and okadaic acid (1 μ M) induce MCC dissociation during the spindle checkpoint.

(A and B) Synchronized taxol-arrested HeLa Tet-Off cells were treated for 2 hours with the indicated inhibitors before cells were harvested and lysed. CDC20 was immunoprecipitated from lysates, and protein levels were detected by immunoblotting with the indicated antibodies. (B) Cells were treated with MG132 (20 μ M) for 1 hour prior to phosphatase inhibitor treatment. Synchronized nocodazole-arrested HeLa Tet-

Off cells were treated for 2 hours with the indicated inhibitors before cells were harvested and lysed. CDC20 was immunoprecipitated from lysates, and protein levels were detected by immunoblotting with the indicated antibodies. Con: control IgG; OA: okadaic acid; IP: immunoprecipitation; CE: cell extract.

was noticeably decreased by 30 minutes and almost completely abolished by 60 minutes (Figure 4.3C). Strikingly, the degradation of cyclin A and B began to occur shortly after CDC20 lost its interaction with the MCC components. These data further support our hypothesis that calyculin A-induced cyclin degradation is the result of MCC dissociation and subsequent APC/C activation.

In carrying out these experiments, we observed a dramatic SDS-PAGE mobility shift of both CDC20 and BubR1 after treating with calyculin A. We verified these two proteins were hyperphosphorylated following calyculin A treatment by treating cell lysates with lambda phosphatase, which caused both CDC20 and BubR1 to downshift to their normal point of migration in the gel (Figure 4.4A and 4.4B). We speculated that the increased phosphorylation of CDC20 or BubR1 may be responsible for the MCC disassembly following calyculin A treatment. To test this hypothesis, we performed mass spectrometry analysis of overexpressed CDC20 and BubR1 in nocodazole-arrested

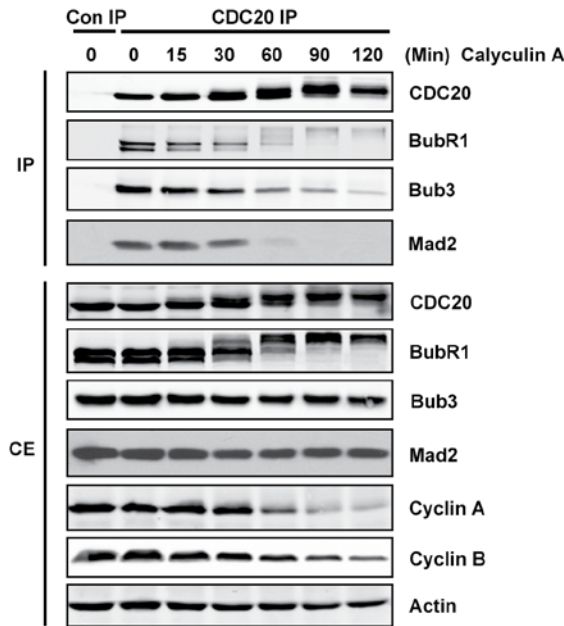


Figure 4.3 MCC dissociation precedes the degradation of cyclin A and B.

Synchronized nocodazole-arrested HeLa Tet-Off cells were treated with calyculin A (20 nM) and harvested at the indicated time points. CDC20 was immunoprecipitated from lysates, and protein levels were detected by immunoblotting with the indicated antibodies. Con: control IgG; OA: okadaic acid; IP: immunoprecipitation; CE: cell extract.

293T cells and identified several new phosphorylation sites on both proteins in calyculin A-treated samples versus control samples (Figure 4.4C). Non-phosphorylatable mutants of CDC20 and BubR1, in which the identified serine and threonine sites were mutated to alanine, were transfected into cells to determine the importance of these phosphorylation events for calyculin A-induced cyclin degradation during the spindle checkpoint. However, no significant differences in cyclin levels were observed between

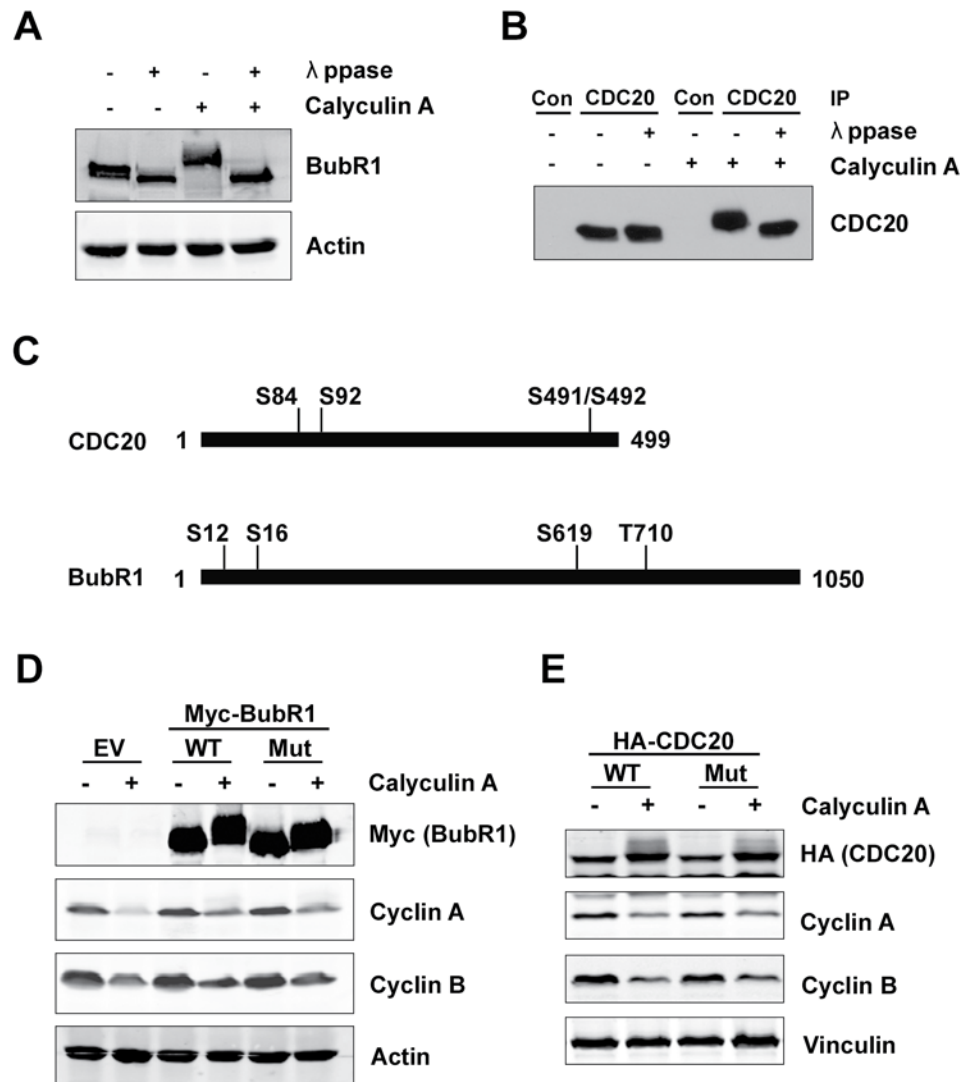


Figure 4.4 Calyculin A-induced phosphorylation of CDC20 and BubR1 at mass spectrometry-identified sites is not necessary for MCC dissociation.

(A) Synchronized nocodazole-arrested HeLa Tet-Off cells were treated with calyculin A (20 nM) for 2 hours. Cells were harvested, lysed in Co-IP buffer, and then treated with lambda phosphatase for 1 hour. Protein levels and mobility shift were detected by immunoblotting with the indicated antibodies. (B) Synchronized nocodazole-arrested HeLa Tet-Off cells were treated with calyculin A (20 nM) for 2 hours. Cells were harvested, and CDC20 was immunoprecipitated from lysates. Immunoprecipitated CDC20 was then treated with lambda phosphatase for 1 hour. Protein levels and mobility shift were detected by immunoblotting with the indicated antibodies. (C)

Schematic representation of the calyculin A-induced phosphorylation sites on CDC20 and BUBR1 that were identified by mass spectrometry in 293T cells. (D and E) The 4 identified phosphorylation sites on BUBR1 and CDC20 were mutated to alanine and the wild-type (WT) and mutant (Mut) constructs were transfected into 293T cells. The cells were arrested at the spindle checkpoint with nocodazole and then treated with calyculin A (20 nM) for 2 hours. Cells were harvested 48 hours post transfection, and protein levels were detected by immunoblotting with the indicated antibodies. Note: Actin immunoblot was cut in half in (D). Con: control IgG; EV: empty vector.

cells expressing wild type protein and those expressing mutant proteins (Figure 4.4D and 4.4E). This result suggests that hyperphosphorylation of BubR1 and CDC20 may not be responsible for the MCC inactivation induced by calyculin A. However, it should be noted that these mutations did not completely abolish the observed electrophoretic shift of BuBR1 and CDC20 proteins following calyculin A treatment, so it remains possible that unidentified phosphorylation sites on these proteins are responsible for the observed effects of calyculin A.

4.2.3 Calyculin A and okadaic acid-induced APC/C activation does not lead to mitotic exit

We have shown that treating mitotic cells with calyculin A and okadaic acid (1 μ M) causes cyclin B degradation. Degradation of cyclin B leads to Cdk1 inactivation, which is typically followed by dephosphorylation of Cdk1 mitotic substrates and rapid exit from mitosis. However, as phosphatases (notably PP1 and PP2A) are necessary for Cdk1 substrate dephosphorylation at mitotic exit, inhibiting PP1 and PP2A with calyculin A or okadaic acid prevents cells from exiting mitosis even though cyclin B has been

degraded. To demonstrate that calyculin A and okadaic acid treated cells remain in mitosis, cell lysates from inhibitor-treated, nocodazole-arrested cells were immunoblotted with the MPM2 antibody to determine Cdk1 substrate phosphorylation. As predicated, the MPM2 signal was present in all conditions, indicating that the cells remained arrested in mitosis (Figure 4.5A). The MPM2 signal was greatly enhanced in cells treated with calyculin A or okadaic acid (1 μ M), despite the fact that cyclin A and B were degraded, highlighting the necessity of phosphatases for mitotic exit. As a positive control for mitotic exit, we treated cells with the Cdk1 inhibitor roscovitine, which induced robust Cdk1 substrate dephosphorylation (Figure 4.5B). We also visualized chromosome condensation using chromosome spreading to further assess the mitotic state of the cells treated with phosphatase inhibitors. Using this technique, we could clearly see condensed chromosomes in the nocodazole-arrested cells treated with calyculin A and okadaic acid (1 μ M) further confirming the cells remained in mitosis (Figure 4.5C). Taken together, our data demonstrate that while calyculin A and okadaic acid (1 μ M) lead to MCC disassembly and APC/C activation, the cells are not able to fully exit mitosis.

Lastly, in an effort to identify the specific phosphatase(s) required for MCC maintenance during the spindle checkpoint, we used siRNA or shRNA to knockdown

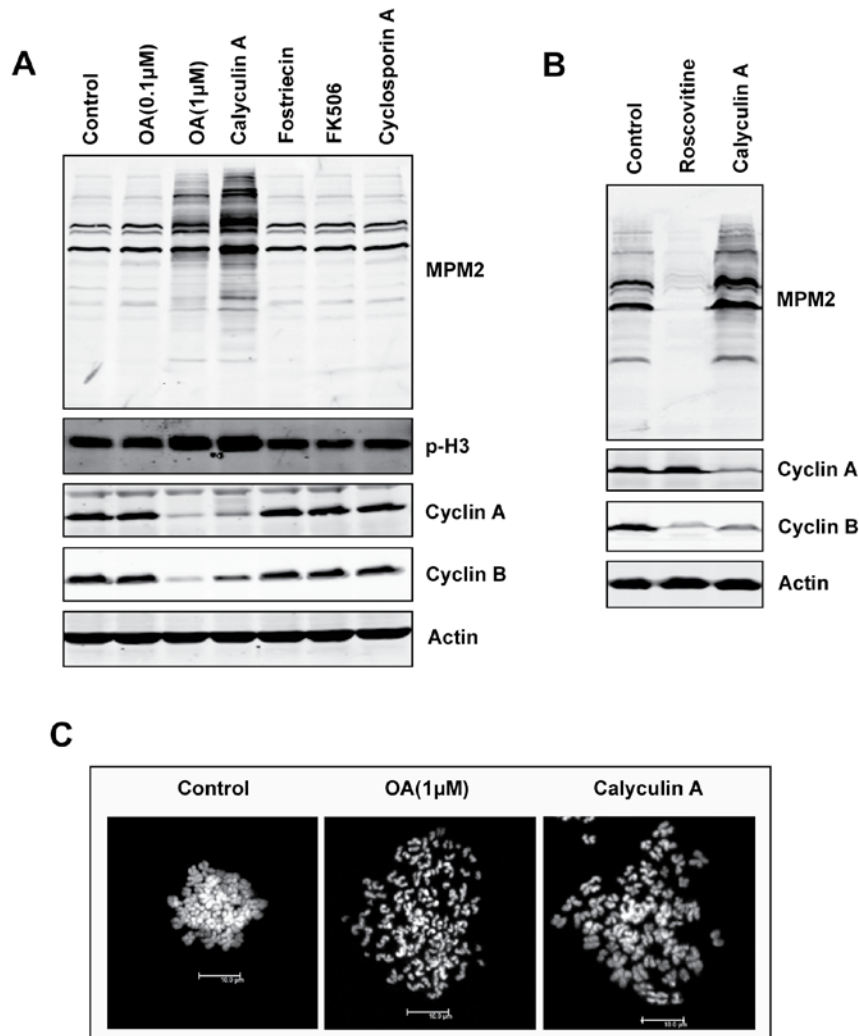


Figure 4.5 Calyculin A and okadaic acid (1 μM) do not induce mitotic exit despite APC/C activation.

(A and B) Synchronized nocodazole-arrested HeLa Tet-Off cells were treated for 2 hours with the indicated inhibitors. Protein levels were detected by immunoblotting with the indicated antibodies. (C) Synchronized nocodazole-arrested HeLa Tet-Off cells were treated with for 2 hours with the indicated inhibitors. Cells were then harvested and chromosome spreads were performed. OA: okadaic acid.

the PPP family phosphatases that are inhibited by calyculin A and okadaic acid (PP1, PP2A, PP4, PP5, and PP6) (Swingle, Ni, and Honkanen 2007) and have a potential role in the spindle checkpoint, and then measured cyclin levels in the nocodazole-arrested cells. Low concentrations of okadaic acid (0.1 μ M) are known to inhibit PP2A and PP4 (and likely PP6 based on sequence similarity to PP2A and PP4 (Swingle, Ni, and Honkanen 2007)), but as we did not observe any changes in cyclin A or B levels at low okadaic acid concentrations, we hypothesized that the phosphatase involved in MCC maintenance during the spindle checkpoint would likely be PP1, which is only inhibited by higher concentrations of okadaic acid. (Swingle, Ni, and Honkanen 2007) PP5's okadaic acid sensitivity is in between PP1 and PP2A, but its sensitivity to calyculin A is several fold higher than PP1 and PP2A (Swingle, Ni, and Honkanen 2007), which further supports our hypothesis that PP1 is the relevant phosphatase for MCC maintenance. However, none of the PPP phosphatase siRNAs or shRNAs decreased cyclin B levels in synchronized nocodazole-arrested cells (Figure 4.6A-H). We actually observed increased levels of cyclin A and B when knocking down each of the three isoforms of PP1 (α , β , and γ), indicating that PP1 knockdown cells may have arrested in mitosis prior to nocodazole treatment. To test if there is redundancy between the three PP1 isoforms, all three isoforms were knocked down together, but cyclin A and B levels were still slightly elevated in the nocodazole-arrested cells (Figure 4.6D).

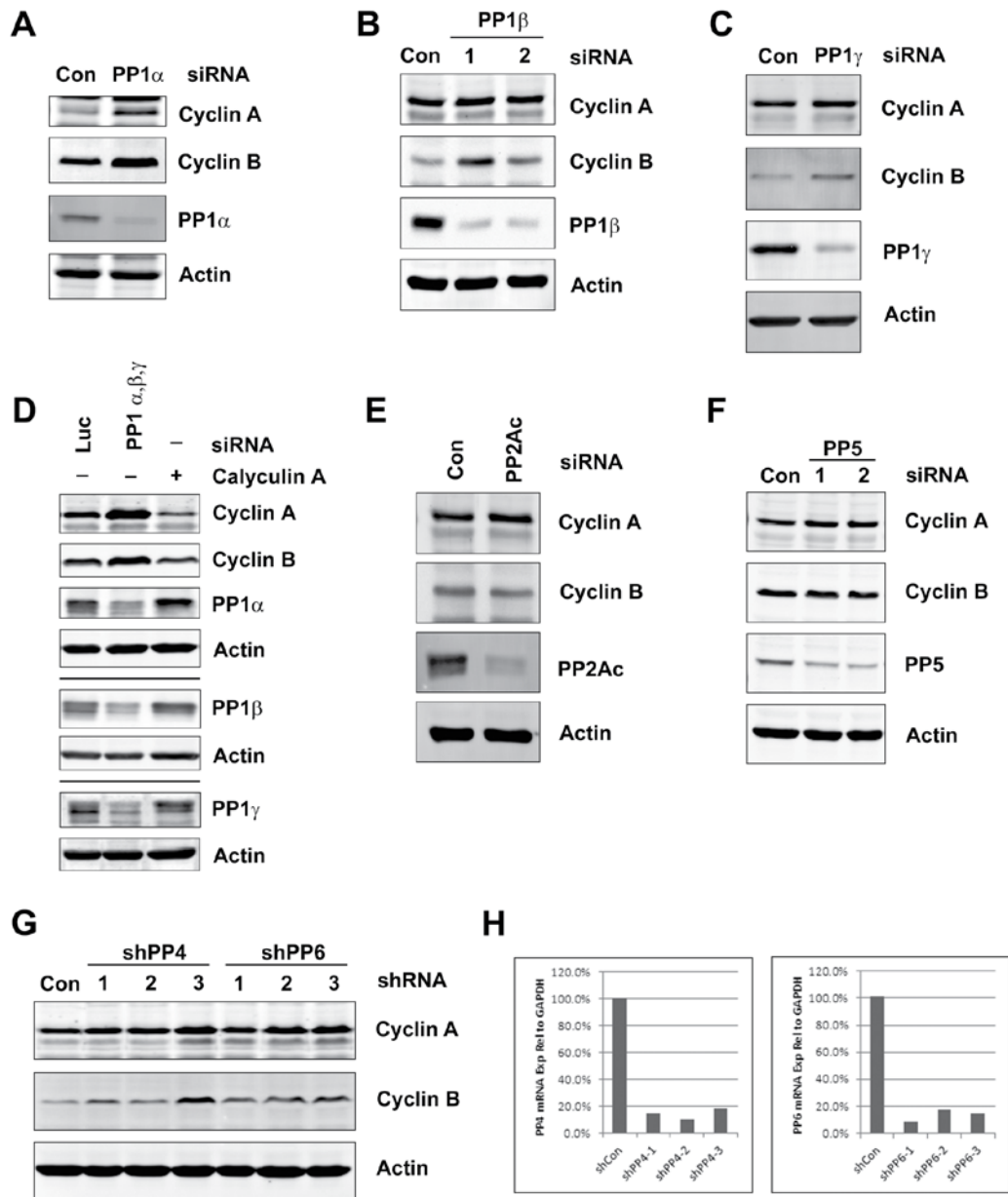


Figure 4.6 Knockdown of PPP family phosphatases did not induce cyclin degradation.

(A-F) HeLa Tet-Off cells were transfected with siRNA, synchronized for 24 hours in thymidine, and released into nocodazole for 16 hours. Mitotic cells were harvested, and protein levels were detected by immunoblotting with the indicated antibodies. Where indicated, calyculin A (20 nM) was added for 2 hours prior to harvesting. (G) HeLa Tet-Off cells stably expressing control shRNA or shRNA targeting PP4 or PP6 were

synchronized as described above. Three different shRNA sequences were used for PP4 and PP6. (H) mRNA levels of PP4 and PP6 were measured by qPCR in shRNA expressing HeLa Tet-Off cells. Expression levels are shown relative to GAPDH and normalized to control cells. Con: control.

To further investigate which phosphatase is responsible for MCC maintenance during the spindle checkpoint, we sought to identify MCC interacting phosphatases using mass spectrometry. Myc-tagged Mad2 and BubR1 were transfected into cells and then immunoprecipitated from nocodazole-arrested cell lysates following DSP crosslinking to stabilize protein interactions. Mass spectrometry was then used to identify the MCC-binding proteins. CDC20 and Bub3 were co-immunoprecipitated with both proteins, confirming that our overexpressed proteins were binding with other MCC components. Thirteen phosphatases and phosphatase regulatory subunits were identified by mass spectrometry, including PP1 α , PP2Ac, PP5, one PP1 regulatory subunit, and three PP2A regulatory subunits (Table 4.1). We also identified PP2c-gamma, but we did not investigate this phosphatase because it is not inhibited by calyculin A. As we already tested the knockdown effect of PP1, PP2A, and PP5, we used siRNA to test the effect of knocking down the remaining phosphatases and regulatory subunits. However, there were no detectable differences in cyclin A or B levels during the spindle checkpoint following knockdown of each of these phosphatases (Figure 4.7A and 4.7B). It is possible that residual levels of phosphatase activity following knockdown were responsible for persistence of the MCC or that multiple phosphatases

contribute to this activity. Nonetheless, our results clearly indicate that phosphatases, as well as kinases, are required for maintenance of the MCC during spindle checkpoint function.

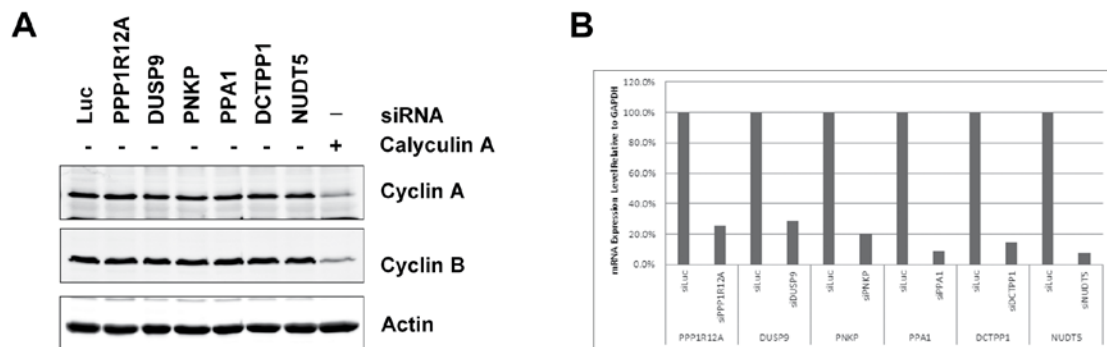


Figure 4.7 Knockdown of mass spectrometry-identified phosphatases did not induce cyclin degradation.

(A) HeLa Tet-Off cells were transfected with siRNA, synchronized for 24 hours in thymidine, and released into nocodazole for 16 hours. Mitotic cells were harvested and split in half for immunoblot (A) and qPCR (B) analysis. Protein levels were detected by immunoblotting with the indicated antibodies. Where indicated, calyculin A (20 nM) was added for 2 hours prior to harvesting. (B) qPCR was used to measure mRNA levels of the indicated phosphatases. mRNA levels are relative to GAPDH and normalized to control cells. Luc: luciferase.

4.3 Discussion

In previous reports examining the phosphoregulation of spindle checkpoint signaling, phosphatases have solely been implicated in activities promoting checkpoint silencing (e.g., microtubule-kinetochore stabilization and dephosphorylation of MPS1

Table 4.1 Mass spectrometry results showing Myc-Mad2 and Myc-BubR1 binding proteins.

293T cells were transfected with pCS2-Myc-Mad2 or pcDNA3-Myc-BubR1 and arrested at the spindle checkpoint with nocodazole. Cells were harvested 48 hours after transfection, DSP crosslinking was performed, and Myc-Mad2 and Myc-BubR1 were immunoprecipitated from cell lysates. Binding proteins were identified by mass spectrometry, and Scaffold Proteome Software was used to analyze the data. NT: No Treatment, EUPC: Exclusive Unique Peptide Count

Protein ID	Accession ID	EUPC NT	EUPC Mad2	EUPC BubR1
Cell division cycle protein 20 homolog OS=Homo sapiens GN=CDC20 PE=1 SV=2	CDC20_HUMAN	0	4	4
Mitotic checkpoint protein BUB3 OS=Homo sapiens GN=BUB3 PE=1 SV=1	BUB3_HUMAN	0	3	9
Serine/threonine-protein phosphatase 2A 65 kDa regulatory subunit A alpha isoform OS=Homo sapiens GN=PPP2R1A PE=1 SV=4	2AAA_HUMAN	0	4	10
Serine/threonine-protein phosphatase 2A 56 kDa regulatory subunit gamma isoform OS=Homo sapiens GN=PPP2R5C PE=1 SV=3	2A5G_HUMAN	0	0	1
Serine/threonine-protein phosphatase 2A 55 kDa regulatory subunit B alpha isoform OS=Homo sapiens GN=PPP2R2A PE=1 SV=1	2ABA_HUMAN	0	2	2
Serine/threonine-protein phosphatase 2A catalytic subunit alpha isoform OS=Homo sapiens GN=PPP2CA PE=1 SV=1	PP2AA_HUMAN	0	2	4
Serine/threonine-protein phosphatase PP1-alpha catalytic subunit OS=Homo sapiens GN=PPP1CA PE=1 SV=1	PP1A_HUMAN	0	2	3
Protein phosphatase 1 regulatory subunit 12A OS=Homo sapiens GN=PPP1R12A PE=1 SV=1	MYPT1_HUMAN	0	0	1
Serine/threonine-protein phosphatase 5 OS=Homo sapiens GN=PPP5C PE=1 SV=1	PPP5_HUMAN	0	0	1
Protein phosphatase 1G OS=Homo sapiens GN=PPM1G PE=1 SV=1 (PP2C-gamma)	PPM1G_HUMAN	0	2	0
Inorganic pyrophosphatase OS=Homo sapiens GN=PPA1 PE=1 SV=2	IPYR_HUMAN	0	1	3
dCTP pyrophosphatase 1 OS=Homo sapiens GN=DCTPP1 PE=1 SV=1	DCTP1_HUMAN	0	1	1
ADP-sugar pyrophosphatase OS=Homo sapiens GN=NUDT5 PE=1 SV=1	NUDT5_HUMAN	0	4	0
Dual specificity protein phosphatase 9 OS=Homo sapiens GN=DUSP9 PE=1 SV=1	DUS9_HUMAN	0	0	1
Bifunctional polynucleotide phosphatase/kinase OS=Homo sapiens GN=PNKP PE=1 SV=1	PNKP_HUMAN	0	1	0

targets), while the counteracting kinases have clearly been shown to be critical for checkpoint activation and maintenance.(Funabiki and Wynne 2013; London and Biggins 2014b) Using phosphatase inhibitors in cells arrested at the spindle checkpoint, we specifically explored the role of phosphatases during the checkpoint as opposed to entry or exit. Here we have demonstrated a novel role for phosphatases in maintaining the MCC during the spindle checkpoint. These findings also reveal that an as yet unknown kinase may be required for dissolving the MCC once the spindle checkpoint has been satisfied. This apparent role reversal of kinases and phosphatases highlights the complexity of spindle checkpoint signaling.

Our results clearly demonstrate that phosphorylation of an unknown target leads to MCC disassembly; therefore, we attempted to identify the relevant phosphatase substrate(s) that becomes phosphorylated and drives MCC dissociation following calyculin A and okadaic acid (1 μ M) treatment. Two attractive potential substrates were the MCC components CDC20 and BubR1 because phosphorylation of both proteins is significantly increased following calyculin A treatment. However, despite identifying a number calyculin A-induced phosphorylation sites on these two proteins by mass spectrometry and performing mutational analysis of these sites, we were unable to observe any reversal of calyculin A's ability to cause cyclin degradation during the spindle checkpoint. Nevertheless, we cannot rule out these two proteins as relevant phosphatase targets during the checkpoint because it is possible there are other calyculin

A-induced phosphorylation sites that were not identified by mass spectrometry but that promote MCC disassembly. It is also possible that phosphorylation of multiple substrates contributes to MCC dissociation following calyculin A treatment.

Lastly, we attempted to identify the relevant phosphatase required for MCC maintenance by using siRNA or shRNA to systematically deplete cells of the PPP family phosphatases that are inhibited by calyculin A and okadaic acid. Based on the phosphatases known to be inhibited by 1 μ M okadaic acid and calyculin A but not 0.1 μ M okadaic acid or fostriecin, we speculated that PP1 would likely be the responsible phosphatase. Given that PP1 is required for checkpoint silencing, the notion that it may also be required for checkpoint maintenance may seem contradictory. However, PP1 does not appear to be heavily recruited to kinetochores until metaphase, where it promotes stable kinetochore-microtubule attachments.(Liu et al. 2010) An interesting possibility to consider is that during prometaphase when the spindle checkpoint is highly active, a pool of PP1 not localized at the kinetochores may be responsible for maintaining the MCC in an intact complex so it can effectively inhibit the APC/C. However, we did not detect any decreases in cyclin A or B levels following knockdown of any of the phosphatases, including all three isoforms of PP1 in tandem, in nocodazole-arrested cells. It is possible there is redundancy among the phosphatases and that calyculin A and okadaic acid cause such a dramatic decrease in cyclin A and B levels because they inhibit multiple phosphatases at once. Future studies investigating

the precise phosphatase(s) responsible for MCC maintenance along with the specific targets of the phosphatase will be important to improve our understanding of MCC maintenance and spindle checkpoint signaling.

5. Conclusions and future directions

5.1 BiFC combined with GFP-Trap for the identification of novel regulators of active caspase-2

For the study detailed in chapter 3, we set out to develop a new method for studying caspase-2 activation, building on previous work developed by Bouchier-Hayes and colleagues (Bouchier-Hayes et al. 2009). Caspase-2 bears the unique honor of being both perhaps the most studied caspase and the least understood. Unfortunately, a lot of the extensive body of research conducted on caspase-2 has drawn improper or at least premature conclusions on the function of caspase-2 based on imprecise methodologies, particularly in relation to studying caspase-2 as an initiator caspase. Too many studies have made improper conclusions based on caspase-2 cleavage products or the supposedly caspase-2 specific artificial substrate, neither of which is exclusive to caspase-2 activity. It is for that reason that more rigorous efforts need to be combined with new methodologies that allow the proper monitoring of caspase-2 activity. This is especially important as caspase-2 has begun to emerge as a tumor suppressor and regulator of the aging process and obesity-related disorders.

In chapter 3, we demonstrated that the caspase-2 BiFC technique developed by Bouchier-Hayes and colleagues could be developed further to directly study physiologically relevant caspase-2 dimers. The keys to the success of this study were the identification of GFP-Trap as a tool that can differentiate between BiFC dimers and monomers, as well as the development of a cell system that expressed near endogenous

levels of the caspase-2 BiFC constructs. While overexpression of caspase-2 is able to drive spontaneous activation, it is difficult to say whether this occurs via a similar mechanism to endogenous caspase-2 activation.

Once we demonstrated that we could specifically isolate near endogenous levels of dimerized caspase-2, we were able to analyze the active caspase-2 interactome by mass spectrometry technique. This revealed a number of caspase-2 interactors, to include RAIDD, TRAF1-3, cIAP1, and HtrA2/Omi. Interestingly, although RAIDD is the most well-known caspase-2 interactor, we found that it was dispensible both for apoptosis and caspase-2 dimerization in response to DNA damage (data not shown). Furthermore, BiFC pulldown by GFP-Trap found that RAIDD binding actually went down after treatment with caspase-2 stimuli. However, we only studied a subset of caspase-2 activating stimuli, so we speculate that a more systematic survey would identify scenarios where RAIDD plays a critical role in caspase-2 activation.

We went on to demonstrate that TRAF2 especially plays a critical role in DNA damage-induced activation of caspase-2 and the downstream intrinsic apoptotic pathway. As far as we are aware, this is the first study to ascribe a directly pro-apoptotic function to TRAF2, which is normally associated with pro-survival signaling like promoting activation of the NF- κ B pathway. It is unclear how TRAF2 would switch between these roles, but hopefully further work will shed light on this. Furthermore, it

has been shown before that TRAF2 can play a role in promoting caspase-1 activation (Labbé et al. 2011).

While TRAF2 was critical for DNA damage-induced caspase-2 activation, TRAF3 appeared to be only partially involved, and TRAF1 was dispensable. TRAF2 is known to form heterotrimers with both of these proteins, so it is possible that their interaction with caspase-2 was non-functional. However, our lab has seen in other scenarios, such as lipopoptosis, that TRAF3 is critical for caspase-2 activation. As was mentioned above for RAIDD, it is possible that the role played by each of these TRAFs in caspase-2 regulation is context-dependent. As a side note, while we chose to focus on the TRAF proteins due to prevalence and early success in our studies, it would also be interesting to explore the role of cIAP1 and HtrA2/Omi in caspase-2 activation.

We went on to demonstrate that caspase-2 possesses a TRAF-interacting motif in its p19 catalytic domain, and that this sequence is critical for full length caspase-2 interaction with TRAF proteins and activation. This was unexpected because the free caspase-2 prodomain was also found to interact with TRAF1, 2, and 3. However, the interaction of TRAF2 with the free caspase-2 prodomain was found to be weaker than its interaction with the full length caspase-2 protein (data not shown). It is possible that TRAF2 interaction with the free caspase-2 prodomain is indirect and mediated by other proteins, perhaps even endogenous caspase-2. Another possible explanation is that the prodomain of the full length caspase-2 protein is unable to bind TRAF2 because it is

inaccessible, perhaps because it assumes a conformation different from the free prodomain, or perhaps because of the binding of other interacting partners. Finally, it is also possible that the TIM mutation disrupted caspase-2 folding to a degree that prevented binding of TRAF2 to the prodomain. However, we do not favor this explanation as the prodomain is separated from the catalytic domains by a relatively unstructured linker region, so it is difficult to see how this mutation would negatively affect the prodomain structure (Pop and Salvesen 2009).

Finally, we demonstrated that dimerized caspase-2 undergoes ubiquitination in the prodomain, and this ubiquitination is dependent on K15, K152, and K153. Expression of triple arginine (non-ubiquitinatable) mutants at low, near-endogenous levels revealed a subtle and unexpected phenotype: these proteins could still dimerize, but the dimers were relatively unstable and had reduced catalytic activity. This suggests that ubiquitination of the caspase-2 prodomain serves to promote a stable and more active complex. This is reminiscent of previous studies of caspase-1 and -8 that found nondegradative K63-linked polyubiquitination led to increased activity (Labbé et al. 2011; Jin et al. 2009). In the case of caspase-8, the authors demonstrated that this modification led to the recruitment of other proteins, which in turn promoted complex stability, recruitment into larger aggregates, and full caspase-8 activation and commitment to apoptosis (Jin et al. 2009). Further study of the caspase-2 ubiquitination described in this study is needed to determine how it promotes stability of the caspase-2

complex. Also, although we found that TRAF2 was important for ubiquitination of the caspase-2 prodomain, we were unable to show that TRAF2 is the direct E3 ligase of caspase-2. More detailed work should help to resolve this question.

Looking forward, it would be especially interesting to combine this technique with the knock-in capabilities of CRISPR/Cas9 or other genome editing tools. Knocking the BiFC system into an endogenous locus would likely enable even more faithful representation of the physiological regulation of caspase-2. However, even without using such genome editing techniques, this tool could be easily applied across a wide array of cell types to study various caspase-2 stimuli, so long as care is taken to titrate the BiFC constructs. Furthermore, this technique can be easily adapted to other interacting proteins and would be especially useful for studying those complexes that do not have antibodies suitable for co-immunoprecipitation assays. In fact, another group independently developed the same technique in parallel for the study of ErbB2 dimers, which they named bimolecular complementation affinity purification (BiCAP) (Croucher et al. 2016). However, their study was conducted in the context of overexpressed BiFC constructs, which could diminish the ability to detect relevant binding partners and post-translational modifications, or even produce artifactual results. Future studies utilizing this technique should take care to use appropriate controls, such as physiological expression of the BiFC constructs.

5.2 An unexpected role for protein phosphatase activity: promoting the MCC

In chapter 4 we detailed a study of phosphatase regulation of the spindle checkpoint when engaged by microtubule inhibitors. Kinases like CDK1 and Greatwall are known to drive a mitotic phenotype while phosphatases like PP1 and PP2A both oppose mitotic entry and promote exit. Over the last decade this paradigm has expanded to include the spindle (mitotic) checkpoint, with kinases being responsible for checkpoint activation and maintenance and phosphatases responsible for checkpoint silencing. We sought to expand the understanding of this regulation by treating checkpoint-arrested cells with a range of phosphatase inhibitors. Surprisingly, we found that treating with the serine/threonine phosphatase inhibitors calyculin A and okadaic acid (1 μ M) resulted in the degradation of cyclin A and B. Interestingly, we found that CDC20 knockdown or inhibition of the APC/C^{CDC20} rescued this loss. This indicated that the spindle checkpoint was no longer active: indeed, we found that phosphatase inhibitor treatment led directly to dissociation of the APC/C^{CDC20}-inhibiting MCC in a manner independent of CDC20. Together, these data showed that an unknown serine/threonine phosphatase plays a crucial role in maintaining the MCC.

We thus sought to determine the identity of the relevant phosphatase using siRNA and shRNA against the PPP family of serine/threonine phosphatases. Due to the high concentration of okadaic acid required to silence the checkpoint, we speculated that PP1 was the relevant phosphatase. However, we found that none of the knockdown

experiments were able to phenocopy the calyculin A and okadaic acid-induced checkpoint silencing. We also conducted an unbiased screen for the relevant phosphatase using co-immunoprecipitation of the MCC coupled with mass spectrometry analysis. However, although we were able to identify a number of phosphatases (some novel) that interacted with the MCC, knockdown again failed to replicate the inhibitor studies.

It is possible that siRNA transfection did not result in a robust enough knockdown to ablate the relevant enzyme, or that multiple phosphatases are involved. Regardless, though, this study requires a shift in the prevailing paradigm that phosphatases only participate in silencing of the checkpoint. It also indicated that a kinase is required for checkpoint silencing. We attempted to identify the protein targeted by this phosphoregulation. Two proteins that appeared likely candidates were BubR1 and CDC20, as they are both components of the MCC and both appeared to become phosphorylated after phosphatase inhibitor treatment. Unfortunately, despite identifying multiple phosphorylation sites on both proteins, we found that the non-phosphorylatable mutants were unable to rescue the MCC dissociation. However, it is still possible that other, unidentified phosphorylation sites on these proteins or other regulators of the MCC are responsible for the silencing of the checkpoint. Further studies will be required to identify the relevant enzymes and targets of this novel signaling event.

5.3 Concluding remarks

This dissertation presents two separate efforts to study the regulation of cellular processes that impinge on genetic stability. We developed a novel, modular technique for studying protein complexes that we used to identify a novel molecular mechanism of caspase-2 activation in response to DNA damage. We also identified a novel regulation of a critical cell cycle checkpoint that shifts the current signaling paradigm regarding this checkpoint. Further investigation of these signaling pathways should reveal biologically and potentially clinically important discoveries. Hopefully this work will provide a foundation for future research into the spindle checkpoint and caspase-2, as well as any pathologies impacted by these signaling pathways.

References

- Abrieu, A., L. Magnaghi-Jaulin, J. A. Kahana, M. Peter, A. Castro, S. Vigneron, T. Lorca, D. W. Cleveland, and J. C. Labbe. 2001. 'Mps1 is a kinetochore-associated kinase essential for the vertebrate mitotic checkpoint', *Cell*, 106: 83-93.
- Alnemri, E S, D J Livingston, D W Nicholson, G Salvesen, N A Thornberry, W W Wong, and J Yuan. 1996. 'Human ICE/CED-3 protease nomenclature.', *Cell*, 87: 171.
- Alvarez, Sergio E, Kuzhuvelil B Harikumar, Nitai C Hait, Jeremy Allegood, Graham M Strub, Eugene Y Kim, Michael Maceyka, Hualiang Jiang, Cheng Luo, Tomasz Kordula, Sheldon Milstien, and Sarah Spiegel. 2010. 'Sphingosine-1-phosphate is a missing cofactor for the E3 ubiquitin ligase TRAF2.', *Nature*, 465: 1084-88.
- Baliga, B C, S H Read, and S Kumar. 2004. 'The biochemical mechanism of caspase-2 activation.', *Cell death and differentiation*, 11: 1234-41.
- Baliga, Belinda C, Paul A Colussi, Stuart H Read, Manisha M Dias, David A Jans, and Sharad Kumar. 2003. 'Role of prodomain in importin-mediated nuclear localization and activation of caspase-2.', *The Journal of biological chemistry*, 278: 4899-905.
- Bergeron, L, G I Perez, G Macdonald, L Shi, Y Sun, A Jurisicova, S Varmuza, K E Latham, J A Flaws, J C Salter, H Hara, M A Moskowitz, E Li, A Greenberg, J L Tilly, and J Yuan. 1998. 'Defects in regulation of apoptosis in caspase-2-deficient mice.', *Genes & development*, 12: 1304-14.
- Bergsbaken, T., S. L. Fink, and B. T. Cookson. 2009. 'Pyroptosis: host cell death and inflammation', *Nat Rev Microbiol*, 7: 99-109.
- Billen, L P, A Shamas-Din, and D W Andrews. 2008. 'Bid: a Bax-like BH3 protein.', *Oncogene*, 27 Suppl 1: S93-104.
- Bonzon, Christine, Lisa Bouchier-Hayes, Lisa J Pagliari, Douglas R Green, and Donald D Newmeyer. 2006. 'Caspase-2-induced apoptosis requires bid cleavage: a physiological role for bid in heat shock-induced death.', *Molecular biology of the cell*, 17: 2150-57.
- Borghi, Alice, Lynn Verstrepen, and Rudi Beyaert. 2016. 'TRAF2 multitasking in TNF receptor-induced signaling to NF- κ B, MAP kinases and cell death.', *Biochemical pharmacology*, 116: 1-10.

- Bouchier-Hayes, L, and D R Green. 2012. 'Caspase-2: the orphan caspase.', *Cell death and differentiation*, 19: 51-57.
- Bouchier-Hayes, Lisa, Andrew Oberst, Gavin P McStay, Samuel Connell, Stephen W G Tait, Christopher P Dillon, Jonathan M Flanagan, Helen M Beere, and Douglas R Green. 2009. 'Characterization of cytoplasmic caspase-2 activation by induced proximity.', *Molecular cell*, 35: 830-40.
- Butt, A J, N L Harvey, G Parasivam, and S Kumar. 1998. 'Dimerization and autoprocessing of the Nedd2 (caspase-2) precursor requires both the prodomain and the carboxyl-terminal regions.', *The Journal of biological chemistry*, 273: 6763-68.
- Cecconi, F, G Alvarez-Bolado, B I Meyer, K A Roth, and P Gruss. 1998. 'Apaf1 (CED-4 homolog) regulates programmed cell death in mammalian development.', *Cell*, 94: 727-37.
- Chandhok, N. S., and D. Pellman. 2009. 'A little CIN may cost a lot: revisiting aneuploidy and cancer', *Curr Opin Genet Dev*, 19: 74-81.
- Chao, W. C., K. Kulkarni, Z. Zhang, E. H. Kong, and D. Barford. 2012. 'Structure of the mitotic checkpoint complex', *Nature*, 484: 208-13.
- Chen, Z. J., and L. J. Sun. 2009. 'Nonproteolytic functions of ubiquitin in cell signaling', *Mol Cell*, 33: 275-86.
- Cheung, Herman H, N Lynn Kelly, Peter Liston, and Robert G Korneluk. 2006. 'Involvement of caspase-2 and caspase-9 in endoplasmic reticulum stress-induced apoptosis: a role for the IAPs.', *Experimental cell research*, 312: 2347-57.
- Chipuk, Jerry E, Tudor Moldoveanu, Fabien Llambi, Melissa J Parsons, and Douglas R Green. 2010. 'The BCL-2 family reunion.', *Molecular cell*, 37: 299-310.
- Chou, J J, H Matsuo, H Duan, and G Wagner. 1998. 'Solution structure of the RAIDD CARD and model for CARD/CARD interaction in caspase-2 and caspase-9 recruitment.', *Cell*, 94: 171-80.
- Chung, Jee Y, Young Chul Park, Hong Ye, and Hao Wu. 2002. 'All TRAFs are not created equal: common and distinct molecular mechanisms of TRAF-mediated signal transduction.', *Journal of cell science*, 115: 679-88.

- Colussi, P A, N L Harvey, and S Kumar. 1998. 'Prodomain-dependent nuclear localization of the caspase-2 (Nedd2) precursor. A novel function for a caspase prodomain.', *The Journal of biological chemistry*, 273: 24535-42.
- Colussi, P A, N L Harvey, L M Shearwin-Whyatt, and S Kumar. 1998. 'Conversion of procaspase-3 to an autoactivating caspase by fusion to the caspase-2 prodomain.', *The Journal of biological chemistry*, 273: 26566-70.
- Crawford, E. D., and J. A. Wells. 2011. 'Caspase substrates and cellular remodeling', *Annu Rev Biochem*, 80: 1055-87.
- Croucher, D R, M Iconomou, J F Hastings, S P Kennedy, J Z R Han, R F Shearer, J McKenna, A Wan, J Lau, S Aparicio, and D N Saunders. 2016. 'Bimolecular complementation affinity purification (BiCAP) reveals dimer-specific protein interactions for ERBB2 dimers', *Science signaling*, 9: ra69-ra69.
- Datta, S R, H Dudek, X Tao, S Masters, H Fu, Y Gotoh, and M E Greenberg. 1997. 'Akt phosphorylation of BAD couples survival signals to the cell-intrinsic death machinery.', *Cell*, 91: 231-41.
- de Zoete, M R, N W Palm, S Zhu, and R A Flavell. 2014. 'Inflammasomes', *Cold Spring Harbor Perspectives in Biology*.
- del Peso, L, M González-García, C Page, R Herrera, and G Nuñez. 1997. 'Interleukin-3-induced phosphorylation of BAD through the protein kinase Akt.', *Science*, 278: 687-89.
- Dhanasekaran, D. N., and E. P. Reddy. 2008. 'JNK signaling in apoptosis', *Oncogene*, 27: 6245-51.
- Di Fiore, B., and J. Pines. 2010. 'How cyclin A destruction escapes the spindle assembly checkpoint', *J Cell Biol*, 190: 501-9.
- Ditchfield, C., V. L. Johnson, A. Tighe, R. Ellston, C. Haworth, T. Johnson, A. Mortlock, N. Keen, and S. S. Taylor. 2003a. 'Aurora B couples chromosome alignment with anaphase by targeting BubR1, Mad2, and Cenp-E to kinetochores', *J Cell Biol*, 161: 267-80.
- Ditchfield, Claire, Victoria L Johnson, Anthony Tighe, Rebecca Ellston, Carolyn Haworth, Trevor Johnson, Andrew Mortlock, Nicholas Keen, and Stephen S Taylor. 2003b. 'Aurora B couples chromosome alignment with anaphase by

- targeting BubR1, Mad2, and Cenp-E to kinetochores.', *The Journal of cell biology*, 161: 267-80.
- Donovan, Nicole, Esther B E Becker, Yoshiyuki Konishi, and Azad Bonni. 2002. 'JNK phosphorylation and activation of BAD couples the stress-activated signaling pathway to the cell death machinery.', *The Journal of biological chemistry*, 277: 40944-49.
- Dorstyn, L, J Puccini, C H Wilson, S Shalini, M Nicola, S Moore, and S Kumar. 2012. 'Caspase-2 deficiency promotes aberrant DNA-damage response and genetic instability', 19: 1288-98.
- Droin, N, F Bichat, C Rébé, A Wotawa, O Sordet, A Hammann, R Bertrand, and E Solary. 2001. 'Involvement of caspase-2 long isoform in Fas-mediated cell death of human leukemic cells.', *Blood*, 97: 1835-44.
- Duan, H, and V M Dixit. 1997. 'RAIDD is a new 'death' adaptor molecule.', *Nature*, 385: 86-89.
- Ellis, H. 1986. 'Genetic control of programmed cell death in the nematode *C. elegans*', *Cell*, 44: 817-29.
- Elmore, Susan. 2007. 'Apoptosis: A Review of Programmed Cell Death', *Toxicologic Pathology*, 35: 495-516.
- Emanuele, M. J., W. Lan, M. Jwa, S. A. Miller, C. S. Chan, and P. T. Stukenberg. 2008. 'Aurora B kinase and protein phosphatase 1 have opposing roles in modulating kinetochore assembly', *J Cell Biol*, 181: 241-54.
- Enari, M, H Sakahira, H Yokoyama, K Okawa, A Iwamatsu, and S Nagata. 1998. 'A caspase-activated DNase that degrades DNA during apoptosis, and its inhibitor ICAD.', *Nature*, 391: 43-50.
- Espert, A., P. Uluocak, R. N. Bastos, D. Mangat, P. Graab, and U. Gruneberg. 2014. 'PP2A-B56 opposes Mps1 phosphorylation of Knl1 and thereby promotes spindle assembly checkpoint silencing', *J Cell Biol*, 206: 833-42.
- Fadok, V A, D R Voelker, P A Campbell, J J Cohen, D L Bratton, and P M Henson. 1992. 'Exposure of phosphatidylserine on the surface of apoptotic lymphocytes triggers specific recognition and removal by macrophages.', *Journal of immunology (Baltimore, Md. : 1950)*, 148: 2207-16.

- Fang, G. 2002. 'Checkpoint protein BubR1 acts synergistically with Mad2 to inhibit anaphase-promoting complex', *Mol Biol Cell*, 13: 755-66.
- Foley, E. A., M. Maldonado, and T. M. Kapoor. 2011a. 'Formation of stable attachments between kinetochores and microtubules depends on the B56-PP2A phosphatase', *Nat Cell Biol*, 13: 1265-71.
- Foley, Emily A, and Tarun M Kapoor. 2013. 'Microtubule attachment and spindle assembly checkpoint signalling at the kinetochore.', *Nature Reviews Molecular cell biology*, 14: 25-37.
- Foley, Emily A, Maria Maldonado, and Tarun M Kapoor. 2011b. 'Formation of stable attachments between kinetochores and microtubules depends on the B56-PP2A phosphatase.', *Nature cell biology*, 13: 1265-71.
- Foss, Kristen M, Alexander Robeson, Sally Kornbluth, and Liguozhang. 2016. 'Mitotic phosphatase activity is required for MCC maintenance during the spindle checkpoint.', *Cell cycle (Georgetown, Tex.)*, 15: 225-33.
- Funabiki, H., and D. J. Wynne. 2013. 'Making an effective switch at the kinetochore by phosphorylation and dephosphorylation', *Chromosoma*, 122: 135-58.
- Ghavami, Saeid, Shahla Shojaei, Behzad Yeganeh, Sudharsana R Ande, Jaganmohan R Jangamreddy, Maryam Mehrpour, Jonas Christoffersson, Wiem Chaabane, Adel Rezaei Moghadam, Hessam H Kashani, Mohammad Hashemi, Ali A Owji, and Marek J Łos. 2014. 'Autophagy and apoptosis dysfunction in neurodegenerative disorders.', *Progress in neurobiology*, 112: 24-49.
- Gonzalvez, Francois, David Lawrence, Becky Yang, Sharon Yee, Robert Pitti, Scot Marsters, Victoria C Pham, Jean-Philippe Stephan, Jennie Lill, and Avi Ashkenazi. 2012. 'TRAF2 Sets a Threshold for Extrinsic Apoptosis by Tagging Caspase-8 with a Ubiquitin Shutoff Timer', *Molecular cell*, 48: 888-99.
- Green, Douglas R. 2003. 'Introduction: apoptosis in the development and function of the immune system.', *Seminars in immunology*, 15: 121-23.
- Guo, Y., S. M. Srinivasula, A. Druilhe, T. Fernandes-Alnemri, and E. S. Alnemri. 2002. 'Caspase-2 induces apoptosis by releasing proapoptotic proteins from mitochondria', *J Biol Chem*, 277: 13430-7.

- Harvey, N L, A J Butt, and S Kumar. 1997. 'Functional activation of Nedd2/ICH-1 (caspase-2) is an early process in apoptosis.', *The Journal of biological chemistry*, 272: 13134-39.
- Harvey, N L, J A Trapani, T Fernandes-Alnemri, G Litwack, E S Alnemri, and S Kumar. 1996. 'Processing of the Nedd2 precursor by ICE-like proteases and granzyme B.', *Genes to cells : devoted to molecular & cellular mechanisms*, 1: 673-85.
- Hein, J. B., and J. Nilsson. 2014. 'Stable MCC binding to the APC/C is required for a functional spindle assembly checkpoint', *EMBO Rep*, 15: 264-72.
- Ho, L H, S H Read, L Dorstyn, L Lambrusco, and S Kumar. 2008. 'Caspase-2 is required for cell death induced by cytoskeletal disruption.', *Oncogene*, 27: 3393-404.
- Ho, Lien Ha, Robyn Taylor, Loretta Dorstyn, Dimitrios Cakouros, Philippe Bouillet, and Sharad Kumar. 2009. 'A tumor suppressor function for caspase-2.', *Proceedings of the National Academy of Sciences of the United States of America*, 106: 5336-41.
- Hodel, M. R., A. H. Corbett, and A. E. Hodel. 2001. 'Dissection of a nuclear localization signal', *J Biol Chem*, 276: 1317-25.
- Horvitz, H R. 1999. 'Genetic control of programmed cell death in the nematode *Caenorhabditis elegans*.' , *Cancer research*, 59: 1701s-06s.
- J F R Kerr, A H Wyllie A R Currie. 1972. 'Apoptosis: A Basic Biological Phenomenon with Wide-ranging Implications in Tissue Kinetics', *British Journal of Cancer*, 26: 239.
- Janssens, Sophie, Antoine Tinel, Saskia Lippens, and Jurg Tschopp. 2005. 'PIDD mediates NF-kappaB activation in response to DNA damage.', *Cell*, 123: 1079-92.
- Jin, Zhaoyu, Yun Li, Robert Pitti, David Lawrence, Victoria C Pham, Jennie R Lill, and Avi Ashkenazi. 2009. 'Cullin3-Based Polyubiquitination and p62-Dependent Aggregation of Caspase-8 Mediate Extrinsic Apoptosis Signaling', *Cell*, 137: 721-35.
- Johnson, Erika Segear, and Sally Kornbluth. 2012. 'Phosphatases driving mitosis: pushing the gas and lifting the brakes.', *Progress in molecular biology and translational science*, 106: 327-41.

- Joselin, Alvin P, Klaus Schulze-Osthoff, and Christian Schwerk. 2006. 'Loss of Acinus inhibits oligonucleosomal DNA fragmentation but not chromatin condensation during apoptosis.', *The Journal of biological chemistry*, 281: 12475-84.
- Jost, Philipp J, Stephanie Grabow, Daniel Gray, Mark D McKenzie, Ueli Nachbur, David C S Huang, Philippe Bouillet, Helen E Thomas, Christoph Borner, John Silke, Andreas Strasser, and Thomas Kaufmann. 2009. 'XIAP discriminates between type I and type II FAS-induced apoptosis.', *Nature*, 460: 1035-39.
- Kim, Ira R, Kiichi Murakami, Nien-Jung Chen, Samuel D Saibil, Elzbieta Matysiak-Zablocki, Alisha R Elford, Madeleine Bonnard, Samuel Benchimol, Andrea Jurisicova, Wen-Chen Yeh, and Pamela S Ohashi. 2009. 'DNA damage- and stress-induced apoptosis occurs independently of PIDD.', *Apoptosis : an international journal on programmed cell death*, 14: 1039-49.
- Komander, D., and M. Rape. 2012. 'The ubiquitin code', *Annu Rev Biochem*, 81: 203-29.
- Konishi, Yoshiyuki, Maria Lehtinen, Nicole Donovan, and Azad Bonni. 2002. 'Cdc2 phosphorylation of BAD links the cell cycle to the cell death machinery.', *Molecular cell*, 9: 1005-16.
- Kops, G. J., and J. V. Shah. 2012. 'Connecting up and clearing out: how kinetochore attachment silences the spindle assembly checkpoint', *Chromosoma*, 121: 509-25.
- Kops, G. J., B. A. Weaver, and D. W. Cleveland. 2005. 'On the road to cancer: aneuploidy and the mitotic checkpoint', *Nat Rev Cancer*, 5: 773-85.
- Kosugi, S., M. Hasebe, T. Entani, S. Takayama, M. Tomita, and H. Yanagawa. 2008. 'Design of peptide inhibitors for the importin alpha/beta nuclear import pathway by activity-based profiling', *Chem Biol*, 15: 940-9.
- Krumschnabel, G, B Sohm, F Bock, C Manzl, and A Villunger. 2008. 'The enigma of caspase-2: the laymen's view', *Cell death and differentiation*, 16: 195-207.
- Kruse, T., G. Zhang, M. S. Larsen, T. Lischetti, W. Streicher, T. Kragh Nielsen, S. P. Bjorn, and J. Nilsson. 2013. 'Direct binding between BubR1 and B56-PP2A phosphatase complexes regulate mitotic progression', *J Cell Sci*, 126: 1086-92.
- Kubala, M. H., O. Kovtun, K. Alexandrov, and B. M. Collins. 2010. 'Structural and thermodynamic analysis of the GFP:GFP-nanobody complex', *Protein Sci*, 19: 2389-401.

- Kuida, K, T S Zheng, S Na, C Kuan, D Yang, H Karasuyama, P Rakic, and R A Flavell. 1996. 'Decreased apoptosis in the brain and premature lethality in CPP32-deficient mice.', *Nature*, 384: 368-72.
- Kumar, S, M Kinoshita, M Noda, N G Copeland, and N A Jenkins. 1994. 'Induction of apoptosis by the mouse Nedd2 gene, which encodes a protein similar to the product of the *Caenorhabditis elegans* cell death gene *ced-3* and the mammalian IL-1 beta-converting enzyme.', *Genes & development*, 8: 1613-26.
- Kumar, S, Y Tomooka, and M Noda. 1992. 'Identification of a set of genes with developmentally down-regulated expression in the mouse brain.', *Biochemical and biophysical research communications*, 185: 1155-61.
- Labbé, K, and M Saleh. 2008. 'Cell death in the host response to infection', *Cell death and differentiation*, 15: 1339-49.
- Labbé, Katherine, Christian R McIntire, Karine Doiron, Philippe M Leblanc, and Maya Saleh. 2011. 'Cellular inhibitors of apoptosis proteins cIAP1 and cIAP2 are required for efficient caspase-1 activation by the inflammasome.', *Immunity*, 35: 897-907.
- Lamkanfi, Mohamed, Kathleen D'Amico, Lieselotte Vande Walle, Marjan van Gurp, Geertrui Denecker, Jill Demeulemeester, Michael Kalai, Wim Declercq, Xavier Saelens, and Peter Vandenaebroeck. 2005. 'A novel caspase-2 complex containing TRAF2 and RIP1.', *The Journal of biological chemistry*, 280: 6923-32.
- Lara-Gonzalez, P., F. G. Westhorpe, and S. S. Taylor. 2012a. 'The spindle assembly checkpoint', *Curr Biol*, 22: R966-80.
- Lara-Gonzalez, Pablo, Frederick G Westhorpe, and Stephen S Taylor. 2012b. 'The Spindle Assembly Checkpoint', *CURBIO*, 22: R966-R80.
- Lavrik, Inna N, Alexander Golks, Simone Baumann, and Peter H Krammer. 2006. 'Caspase-2 is activated at the CD95 death-inducing signaling complex in the course of CD95-induced apoptosis.', *Blood*, 108: 559-65.
- Leber, Brian, Jialing Lin, and David W Andrews. 2007. 'Embedded together: The life and death consequences of interaction of the Bcl-2 family with membranes', *Apoptosis : an international journal on programmed cell death*, 12: 897-911.
- Letai, Anthony G. 2008. 'Diagnosing and exploiting cancer's addiction to blocks in apoptosis.', *Nature Publishing Group*, 8: 121-32.

- Ley, Rebecca, Kathryn Balmanno, Kathryn Hadfield, Claire Weston, and Simon J Cook. 2003. 'Activation of the ERK1/2 signaling pathway promotes phosphorylation and proteasome-dependent degradation of the BH3-only protein, Bim.', *The Journal of biological chemistry*, 278: 18811-16.
- Li, H, H Zhu, C J Xu, and J Yuan. 1998. 'Cleavage of BID by caspase 8 mediates the mitochondrial damage in the Fas pathway of apoptosis.', *Cell*, 94: 491-501.
- Li, X., and R. B. Nicklas. 1995. 'Mitotic forces control a cell-cycle checkpoint', *Nature*, 373: 630-2.
- Lindsten, T, A J Ross, A King, W X Zong, J C Rathmell, H A Shiels, E Ulrich, K G Waymire, P Mahar, K Frauwirth, Y Chen, M Wei, V M Eng, D M Adelman, M C Simon, A Ma, J A Golden, G Evan, S J Korsmeyer, G R MacGregor, and C B Thompson. 2000. 'The combined functions of proapoptotic Bcl-2 family members bak and bax are essential for normal development of multiple tissues.', *Molecular cell*, 6: 1389-99.
- Liu, D., M. Vleugel, C. B. Backer, T. Hori, T. Fukagawa, I. M. Cheeseman, and M. A. Lampson. 2010. 'Regulated targeting of protein phosphatase 1 to the outer kinetochore by KNL1 opposes Aurora B kinase', *J Cell Biol*, 188: 809-20.
- London, N., and S. Biggins. 2014a. 'Mad1 kinetochore recruitment by Mps1-mediated phosphorylation of Bub1 signals the spindle checkpoint', *Genes Dev*, 28: 140-52.
- — —. 2014b. 'Signalling dynamics in the spindle checkpoint response', *Nat Rev Mol Cell Biol*, 15: 736-47.
- London, N., S. Ceto, J. A. Ranish, and S. Biggins. 2012. 'Phosphoregulation of Spc105 by Mps1 and PP1 regulates Bub1 localization to kinetochores', *Curr Biol*, 22: 900-6.
- Luo, X, I Budihardjo, H Zou, C Slaughter, and X Wang. 1998. 'Bid, a Bcl2 interacting protein, mediates cytochrome c release from mitochondria in response to activation of cell surface death receptors.', *Cell*, 94: 481-90.
- Luo, X., Z. Tang, J. Rizo, and H. Yu. 2002. 'The Mad2 spindle checkpoint protein undergoes similar major conformational changes upon binding to either Mad1 or Cdc20', *Mol Cell*, 9: 59-71.
- Luthi, A. U., and S. J. Martin. 2007. 'The CASBAH: a searchable database of caspase substrates', *Cell Death Differ*, 14: 641-50.

- Machado, M V, G A Michelotti, M L Jewell, T A Pereira, G Xie, R T Premont, and A M Diehl. 2016. 'Caspase-2 promotes obesity, the metabolic syndrome and nonalcoholic fatty liver disease', 7: e2096-12.
- Machado, M V, G A Michelotti, T de Almeida Pereira, J Boursier, L Kruger, M Swiderska-Syn, G Karaca, G Xie, C D Guy, B Bohinc, K R Lindblom, E Johnson, S Kornbluth, and A M Diehl. 2015. 'Reduced lipoapoptosis, hedgehog pathway activation and fibrosis in caspase-2 deficient mice with non-alcoholic steatohepatitis.', *Gut*, 64: 1148-57.
- Maciejowski, J., K. A. George, M. E. Terret, C. Zhang, K. M. Shokat, and P. V. Jallepalli. 2010a. 'Mps1 directs the assembly of Cdc20 inhibitory complexes during interphase and mitosis to control M phase timing and spindle checkpoint signaling', *J Cell Biol*, 190: 89-100.
- Maciejowski, John, Kelly A George, Marie-Emilie Terret, Chao Zhang, Kevan M Shokat, and Prasad V Jallepalli. 2010b. 'Mps1 directs the assembly of Cdc20 inhibitory complexes during interphase and mitosis to control M phase timing and spindle checkpoint signaling.', *The Journal of cell biology*, 190: 89-100.
- Malumbres, M., and M. Barbacid. 2009. 'Cell cycle, CDKs and cancer: a changing paradigm', *Nat Rev Cancer*, 9: 153-66.
- Malumbres, Marcos. 2014. 'Cyclin-dependent kinases', *Genome Biology*, 15: 122.
- Manchado, Eusebio, María Guillamot, Guillermo de Cárcer, Manuel Eguren, Michelle Trickey, Irene García-Higuera, Sergio Moreno, Hiroyuki Yamano, Marta Cañamero, and Marcos Malumbres. 2010. 'Targeting Mitotic Exit Leads to Tumor Regression In Vivo: Modulation by Cdk1, Mastl, and the PP2A/B55α,δ Phosphatase', *Cancer cell*, 18: 641-54.
- Mancini, M, C E Machamer, S Roy, D W Nicholson, N A Thornberry, L A Casciola-Rosen, and A Rosen. 2000. 'Caspase-2 is localized at the Golgi complex and cleaves golgin-160 during apoptosis.', *The Journal of cell biology*, 149: 603-12.
- Manzl, C, G Krumschnabel, F Bock, B Sohm, V Labi, F Baumgartner, E Logette, J Tschopp, and A Villunger. 2009. 'Caspase-2 activation in the absence of PIDDosome formation', *The Journal of cell biology*, 185: 291-303.
- Manzl, C, L Peintner, G Krumschnabel, F Bock, V Labi, M Drach, A Newbold, R Johnstone, and Andreas Villunger. 2012. 'PIDDosome-independent tumor suppression by Caspase-2.', *Cell death and differentiation*.

- McIlwain, D. R., T. Berger, and T. W. Mak. 2013. 'Caspase functions in cell death and disease', *Cold Spring Harb Perspect Biol*, 5: a008656.
- Meadows, J. C., L. A. Shepperd, V. Vanoosthuysse, T. C. Lancaster, A. M. Sochaj, G. J. Buttrick, K. G. Hardwick, and J. B. Millar. 2011. 'Spindle checkpoint silencing requires association of PP1 to both Spc7 and kinesin-8 motors', *Dev Cell*, 20: 739-50.
- Mertins, P., J. W. Qiao, J. Patel, N. D. Udeshi, K. R. Clauser, D. R. Mani, M. W. Burgess, M. A. Gillette, J. D. Jaffe, and S. A. Carr. 2013. 'Integrated proteomic analysis of post-translational modifications by serial enrichment', *Nat Methods*, 10: 634-7.
- Metzger, M. B., V. A. Hristova, and A. M. Weissman. 2012. 'HECT and RING finger families of E3 ubiquitin ligases at a glance', *J Cell Sci*, 125: 531-7.
- Morgan, David O. 1997. 'CYCLIN-DEPENDENT KINASES: Engines, Clocks, and Microprocessors', *Annual review of cell and developmental biology*, 13: 261-91.
- Morrow, C. J., A. Tighe, V. L. Johnson, M. I. Scott, C. Ditchfield, and S. S. Taylor. 2005. 'Bub1 and aurora B cooperate to maintain BubR1-mediated inhibition of APC/CCdc20', *J Cell Sci*, 118: 3639-52.
- Musacchio, A., and E. D. Salmon. 2007a. 'The spindle-assembly checkpoint in space and time', *Nat Rev Mol Cell Biol*, 8: 379-93.
- Musacchio, Andrea, and Edward D Salmon. 2007b. 'The spindle-assembly checkpoint in space and time', *Nature Reviews Molecular cell biology*, 8: 379-93.
- Nagai, Takeharu, Keiji Iyata, Eun Sun Park, Mie Kubota, Katsuhiko Mikoshiba, and Atsushi Miyawaki. 2002. 'A variant of yellow fluorescent protein with fast and efficient maturation for cell-biological applications.', *Nature biotechnology*, 20: 87-90.
- Nagata, Shigekazu, Rikinari Hanayama, and Kohki Kawane. 2010. 'Autoimmunity and the Clearance of Dead Cells', *Cell*, 140: 619-30.
- Nakano, Katsunori, and Karen H Vousden. 2001. 'PUMA, a Novel Proapoptotic Gene, Is Induced by p53', *Molecular cell*, 7: 683-94.
- Nijenhuis, W., G. Vallardi, A. Teixeira, G. J. Kops, and A. T. Saurin. 2014a. 'Negative feedback at kinetochores underlies a responsive spindle checkpoint signal', *Nat Cell Biol*, 16: 1257-64.

- Nijenhuis, Wilco, Giulia Vallardi, Antoinette Teixeira, Geert J P L Kops, and Adrian T Saurin. 2014b. 'Negative feedback at kinetochores underlies a responsive spindle checkpoint signal.', *Nature cell biology*, 16: 1257-64.
- Nutt, Leta K, Marisa R Buchakjian, Eugene Gan, Rashid Darbandi, Sook-Young Yoon, Judy Q Wu, Yuko J Miyamoto, Jennifer A Gibbons, Jennifer A Gibbon, Josh L Andersen, Christopher D Freel, Wanli Tang, Changli He, Manabu Kurokawa, Yongjun Wang, Seth S Margolis, Rafael A Fissore, and Sally Kornbluth. 2009. 'Metabolic control of oocyte apoptosis mediated by 14-3-3zeta-regulated dephosphorylation of caspase-2.', *Developmental cell*, 16: 856-66.
- Nutt, Leta K, Seth S Margolis, Mette Jensen, Catherine E Herman, William G Dunphy, Jeffrey C Rathmell, and Sally Kornbluth. 2005. 'Metabolic regulation of oocyte cell death through the CaMKII-mediated phosphorylation of caspase-2.', *Cell*, 123: 89-103.
- Oda, E, R Ohki, H Murasawa, J Nemoto, T Shibue, T Yamashita, T Tokino, T Taniguchi, and N Tanaka. 2000. 'Noxa, a BH3-only member of the Bcl-2 family and candidate mediator of p53-induced apoptosis.', *Science*, 288: 1053-58.
- Oeckinghaus, A, and S Ghosh. 2009. 'The NF- κ B Family of Transcription Factors and Its Regulation', *Cold Spring Harbor Perspectives in Biology*, 1: a000034-a34.
- Oeckinghaus, Andrea, Matthew S Hayden, and Sankar Ghosh. 2011. 'Crosstalk in NF- κ B signaling pathways', *Nature Immunology*, 12: 695-708.
- Olsson, M, H Vakifahmetoglu, P M Abruzzo, K Högstrand, A Grandien, and B Zhivotovsky. 2009. 'DISC-mediated activation of caspase-2 in DNA damage-induced apoptosis.', *Oncogene*, 28: 1949-59.
- Paroni, G, C Henderson, C Schneider, and C Brancolini. 2001. 'Caspase-2-induced apoptosis is dependent on caspase-9, but its processing during UV- or tumor necrosis factor-dependent cell death requires caspase-3.', *The Journal of biological chemistry*, 276: 21907-15.
- Paroni, Gabriela, Clare Henderson, Claudio Schneider, and Claudio Brancolini. 2002. 'Caspase-2 can trigger cytochrome C release and apoptosis from the nucleus.', *The Journal of biological chemistry*, 277: 15147-61.
- Parrish, A. B., C. D. Freel, and S. Kornbluth. 2013. 'Cellular mechanisms controlling caspase activation and function', *Cold Spring Harb Perspect Biol*, 5.

- Parsons, M J, L McCormick, L Janke, A Howard, L Bouchier-Hayes, and D R Green. 2013. 'Genetic deletion of caspase-2 accelerates MMTV/c-neu-driven mammary carcinogenesis in mice', *Cell death and differentiation*: 1-9.
- Peintner, L, L Dorstyn, S Kumar, T Aneichyk, A Villunger, and C Manzl. 2015. 'The tumor-modulatory effects of Caspase-2 and Pidd1 do not require the scaffold protein Raidd', *Cell death and differentiation*: 1-9.
- Pines, J. 2011. 'Cubism and the cell cycle: the many faces of the APC/C', *Nat Rev Mol Cell Biol*, 12: 427-38.
- Pinsky, Benjamin A, and Sue Biggins. 2005. 'The spindle checkpoint: tension versus attachment.', *Trends in Cell Biology*, 15: 486-93.
- Pop, C, and G S Salvesen. 2009. 'Human Caspases: Activation, Specificity, and Regulation', *Journal of Biological Chemistry*, 284: 21777-81.
- Poreba, M., A. Strozzyk, G. S. Salvesen, and M. Drag. 2013. 'Caspase substrates and inhibitors', *Cold Spring Harb Perspect Biol*, 5: a008680.
- Puccini, Joseph, Sonia Shalini, Anne K Voss, Magtouf Gatei, Claire H Wilson, Devendra K Hiwase, Martin F Lavin, Loretta Dorstyn, and Sharad Kumar. 2013. 'Loss of caspase-2 augments lymphomagenesis and enhances genomic instability in Atm-deficient mice.', *Proceedings of the National Academy of Sciences of the United States of America*.
- Read, Stuart H, Belinda C Baliga, Paul G Ekert, David L Vaux, and Sharad Kumar. 2002. 'A novel Apaf-1-independent putative caspase-2 activation complex.', *The Journal of cell biology*, 159: 739-45.
- Ribe, Elena M, Ying Y Jean, Rebecca L Goldstein, Claudia Manzl, Leonidas Stefanis, Andreas Villunger, and Carol M Troy. 2012a. 'Neuronal caspase 2 activity and function requires RAIDD, but not PIDD', *The Biochemical journal*, 444: 591-99.
- — —. 2012b. 'Neuronal caspase-2 activity and function requires RAIDD but not PIDD.', *The Biochemical journal*.
- Rieder, C. L., R. W. Cole, A. Khodjakov, and G. Sluder. 1995. 'The checkpoint delaying anaphase in response to chromosome monoorientation is mediated by an inhibitory signal produced by unattached kinetochores', *J Cell Biol*, 130: 941-8.

- Rieder, C. L., A. Schultz, R. Cole, and G. Sluder. 1994. 'Anaphase onset in vertebrate somatic cells is controlled by a checkpoint that monitors sister kinetochore attachment to the spindle', *J Cell Biol*, 127: 1301-10.
- Riedl, S. J., and Y. Shi. 2004. 'Molecular mechanisms of caspase regulation during apoptosis', *Nat Rev Mol Cell Biol*, 5: 897-907.
- Riento, K., and A. J. Ridley. 2003. 'Rocks: multifunctional kinases in cell behaviour', *Nat Rev Mol Cell Biol*, 4: 446-56.
- Rosenberg, J. S., F. R. Cross, and H. Funabiki. 2011. 'KNL1/Spc105 recruits PP1 to silence the spindle assembly checkpoint', *Curr Biol*, 21: 942-7.
- Sahara, S, M Aoto, Y Eguchi, N Imamoto, Y Yoneda, and Y Tsujimoto. 1999. 'Acinus is a caspase-3-activated protein required for apoptotic chromatin condensation.', *Nature*, 401: 168-73.
- Santaguida, S., C. Vernieri, F. Villa, A. Ciliberto, and A. Musacchio. 2011. 'Evidence that Aurora B is implicated in spindle checkpoint signalling independently of error correction', *EMBO J*, 30: 1508-19.
- Saurin, A. T., M. S. van der Waal, R. H. Medema, S. M. Lens, and G. J. Kops. 2011. 'Aurora B potentiates Mps1 activation to ensure rapid checkpoint establishment at the onset of mitosis', *Nat Commun*, 2: 316.
- Schweizer, Andreas, Christophe Briand, and Markus G Grütter. 2003. 'Crystal structure of caspase-2, apical initiator of the intrinsic apoptotic pathway.', *The Journal of biological chemistry*, 278: 42441-47.
- Segawa, Katsumori, Sachiko Kurata, and Shigekazu Nagata. 2016. 'Human Type IV P-type ATPases That Work as Plasma Membrane Phospholipid Flippases and Their Regulation by Caspase and Calcium', *Journal of Biological Chemistry*, 291: 762-72.
- Segawa, Katsumori, Sachiko Kurata, Yuichi Yanagihashi, Thijn R Brummelkamp, Fumihiko Matsuda, and Shigekazu Nagata. 2014. 'Caspase-mediated cleavage of phospholipid flippase for apoptotic phosphatidylserine exposure.', *Science*, 344: 1164-68.
- Segear Johnson, Erika, Kelly R Lindblom, Alexander Robeson, Robert D Stevens, Olga R Ilkayeva, Christopher B Newgard, Sally Kornbluth, and Joshua L Andersen. 2013. 'Metabolomic profiling reveals a role for caspase-2 in lipoapoptosis.', *The Journal of biological chemistry*.

- Shalini, S, A Nikolic, C H Wilson, J Puccini, N Sladojevic, J Finnie, L Dorstyn, and S Kumar. 2016. 'Caspase-2 deficiency accelerates chemically induced liver cancer in mice': 1-10.
- Shi, Jianjin, Yue Zhao, Kun Wang, Xuyan Shi, Yue Wang, Huanwei Huang, Yinghua Zhuang, Tao Cai, Fengchao Wang, and Feng Shao. 2015. 'Cleavage of GSDMD by inflammatory caspases determines pyroptotic cell death.', *Nature*.
- Shi, Jianjin, Yue Zhao, Yupeng Wang, Wenqing Gao, Jingjin Ding, Peng Li, Liyan Hu, and Feng Shao. 2014. 'Inflammatory caspases are innate immune receptors for intracellular LPS', *Nature*: 1-18.
- Sidi, Samuel, Takaomi Sanda, Richard D Kennedy, Andreas T Hagen, Cicely A Jette, Raymond Hoffmans, Jennifer Pascual, Shintaro Imamura, Shuji Kishi, James F Amatrudda, John P Kanki, Douglas R Green, Alan A D'Andrea, and A Thomas Look. 2008. 'Chk1 suppresses a caspase-2 apoptotic response to DNA damage that bypasses p53, Bcl-2, and caspase-3.', *Cell*, 133: 864-77.
- Silva, Manuel T. 2010. 'Secondary necrosis: the natural outcome of the complete apoptotic program.', *FEBS letters*, 584: 4491-99.
- Sivakumar, Sushama, and Gary J Gorbsky. 2015. 'Spatiotemporal regulation of the anaphase-promoting complex in mitosis', *Nature Reviews Molecular cell biology*, 16: 82-94.
- Slee, E A, M T Harte, R M Kluck, B B Wolf, C A Casiano, D D Newmeyer, H G Wang, J C Reed, D W Nicholson, E S Alnemri, D R Green, and S J Martin. 1999. 'Ordering the cytochrome c-initiated caspase cascade: hierarchical activation of caspases-2, -3, -6, -7, -8, and -10 in a caspase-9-dependent manner.', *The Journal of cell biology*, 144: 281-92.
- Sodhi, R. K., N. Singh, and A. S. Jaggi. 2010. 'Poly(ADP-ribose) polymerase-1 (PARP-1) and its therapeutic implications', *Vascul Pharmacol*, 53: 77-87.
- Sudakin, V., G. K. Chan, and T. J. Yen. 2001. 'Checkpoint inhibition of the APC/C in HeLa cells is mediated by a complex of BUBR1, BUB3, CDC20, and MAD2', *J Cell Biol*, 154: 925-36.
- Swatek, K. N., and D. Komander. 2016. 'Ubiquitin modifications', *Cell Res*, 26: 399-422.

- Swingle, M., L. Ni, and R. E. Honkanen. 2007. 'Small-molecule inhibitors of ser/thr protein phosphatases: specificity, use and common forms of abuse', *Methods Mol Biol*, 365: 23-38.
- Tait, S. W., and D. R. Green. 2010. 'Mitochondria and cell death: outer membrane permeabilization and beyond', *Nat Rev Mol Cell Biol*, 11: 621-32.
- — —. 2013. 'Mitochondrial regulation of cell death', *Cold Spring Harb Perspect Biol*, 5.
- Talanian, R V, C Quinlan, S Trautz, M C Hackett, J A Mankovich, D Banach, T Ghayur, K D Brady, and W W Wong. 1997. 'Substrate specificities of caspase family proteases.', *The Journal of biological chemistry*, 272: 9677-82.
- Tan, K O, K M Tan, and V C Yu. 1999. 'A novel BH3-like domain in BID is required for intramolecular interaction and autoinhibition of pro-apoptotic activity.', *The Journal of biological chemistry*, 274: 23687-90.
- Tang, Hong-Wen, Hsiao-Man Liao, Wen-Hsin Peng, Hong-Ru Lin, Chun-Hong Chen, and Guang-Chao Chen. 2013. 'Atg9 Interacts with dTRAF2/TRAF6 to Regulate Oxidative Stress-Induced JNK Activation and Autophagy Induction.', *Developmental cell*.
- Tighe, A., O. Staples, and S. Taylor. 2008. 'Mps1 kinase activity restrains anaphase during an unperturbed mitosis and targets Mad2 to kinetochores', *J Cell Biol*, 181: 893-901.
- Tinel, Antoine, Sophie Janssens, Saskia Lippens, Solange Cuenin, Emmanuelle Logette, Bastienne Jaccard, Manfredo Quadroni, and Jurg Tschopp. 2007. 'Autoproteolysis of PIDD marks the bifurcation between pro-death caspase-2 and pro-survival NF-kappaB pathway.', *The EMBO journal*, 26: 197-208.
- Tinel, Antoine, and Jurg Tschopp. 2004. 'The PIDDosome, a protein complex implicated in activation of caspase-2 in response to genotoxic stress.', *Science*, 304: 843-46.
- Tu, Shine, Gavin P McStay, Louis-Martin Boucher, Tak Mak, Helen M Beere, and Douglas R Green. 2006. 'In situ trapping of activated initiator caspases reveals a role for caspase-2 in heat shock-induced apoptosis.', *Nature cell biology*, 8: 72-77.
- Turk, B., and V. Stoka. 2007. 'Protease signalling in cell death: caspases versus cysteine cathepsins', *FEBS Lett*, 581: 2761-7.

- van Loo, G., X. Saelens, F. Matthijssens, P. Schotte, R. Beyaert, W. Declercq, and P. Vandenabeele. 2002. 'Caspases are not localized in mitochondria during life or death', *Cell Death Differ*, 9: 1207-11.
- Vanoosthuysse, Vincent, and Kevin G Hardwick. 2009a. 'A novel protein phosphatase 1-dependent spindle checkpoint silencing mechanism.', *Current biology : CB*, 19: 1176-81.
- — —. 2009b. 'Overcoming inhibition in the spindle checkpoint.', *Genes & development*, 23: 2799-805.
- Vermeulen, Katrien, Dirk R Van Bockstaele, and Zwi N Berneman. 2003. 'The cell cycle: a review of regulation, deregulation and therapeutic targets in cancer.', *Cell proliferation*, 36: 131-49.
- von Schubert, C., F. Cubizolles, J. M. Bracher, T. Sliedrecht, G. J. Kops, and E. A. Nigg. 2015. 'Plk1 and Mps1 Cooperatively Regulate the Spindle Assembly Checkpoint in Human Cells', *Cell Rep*, 12: 66-78.
- Walczak, Henning. 2013. 'Death receptor-ligand systems in cancer, cell death, and inflammation.', *Cold Spring Harbor Perspectives in Biology*, 5: a008698.
- Wang, L, M Miura, L Bergeron, H Zhu, and J Yuan. 1994. 'Ich-1, an Ice/ced-3-related gene, encodes both positive and negative regulators of programmed cell death.', *Cell*, 78: 739-50.
- Wei, M C, W X Zong, E H Cheng, T Lindsten, V Panoutsakopoulou, A J Ross, K A Roth, G R MacGregor, C B Thompson, and S J Korsmeyer. 2001. 'Proapoptotic BAX and BAK: a requisite gateway to mitochondrial dysfunction and death.', *Science*, 292: 727-30.
- Wolf, B B, M Schuler, F Echeverri, and D R Green. 1999. 'Caspase-3 is the primary activator of apoptotic DNA fragmentation via DNA fragmentation factor-45/inhibitor of caspase-activated DNase inactivation.', *The Journal of biological chemistry*, 274: 30651-56.
- Xie, Ping. 2013. 'TRAF molecules in cell signaling and in human diseases', *Journal of Molecular Signaling*, 8: 1-1.
- Xu, P., E. A. Raetz, M. Kitagawa, D. M. Virshup, and S. H. Lee. 2013. 'BUBR1 recruits PP2A via the B56 family of targeting subunits to promote chromosome congression', *Biol Open*, 2: 479-86.

- Yamagishi, Y., C. H. Yang, Y. Tanno, and Y. Watanabe. 2012. 'MPS1/Mph1 phosphorylates the kinetochore protein KNL1/Spc7 to recruit SAC components', *Nat Cell Biol*, 14: 746-52.
- Yang, C S, K Matsuura, N-J Huang, A C Robeson, B Huang, L Zhang, and S Kornbluth. 2014. 'Fatty acid synthase inhibition engages a novel caspase-2 regulatory mechanism to induce ovarian cancer cell death.', *Oncogene*.
- Ye, H, Y C Park, M Kreishman, E Kieff, and H Wu. 1999. 'The structural basis for the recognition of diverse receptor sequences by TRAF2.', *Molecular cell*, 4: 321-30.
- Yu, J, L Zhang, P M Hwang, K W Kinzler, and B Vogelstein. 2001. 'PUMA induces the rapid apoptosis of colorectal cancer cells.', *Molecular cell*, 7: 673-82.
- Zhang, G., T. Lischetti, and J. Nilsson. 2014. 'A minimal number of MELT repeats supports all the functions of KNL1 in chromosome segregation', *J Cell Sci*, 127: 871-84.
- Zhang, L., N. J. Huang, C. Chen, W. Tang, and S. Kornbluth. 2012. 'Ubiquitylation of p53 by the APC/C inhibitor Trim39', *Proc Natl Acad Sci U S A*, 109: 20931-6.
- Zhang, Yingpei, Susan S Padalecki, Asish R Chaudhuri, Eric De Waal, Beth A Goins, Barry Grubbs, Yuji Ikeno, Arlan Richardson, Gregory R Mundy, and Brian Herman. 2007. 'Caspase-2 deficiency enhances aging-related traits in mice.', *Mechanisms of ageing and development*, 128: 213-21.
- Zlatic, S. A., P. V. Ryder, G. Salazar, and V. Faundez. 2010. 'Isolation of labile multi-protein complexes by in vivo controlled cellular cross-linking and immunomagnetic affinity chromatography', *J Vis Exp*.

Biography

Alex Robeson was born April 16, 1984. He attended Covenant College from August 2002 – May 2006, when he graduated cum laude with a BA in Biology and a minor in Chemistry. He worked at the Translational Genomics Research Institute in Phoenix, AZ from May 2007 – July 2009 under Michael T. Barrett, studying the clonal evolution of cancer and profiling tumor genomes using aCGH in search of common cancer driver mutations. In 2009 Alex entered the Duke Cell and Molecular Biology Program, from which he entered the Program in Molecular Cancer Biology and joined the lab of Sally Kornbluth. Alex has presented his work at Gordon Research Conference: Cell Death (2014).

Foss, Kristen M*, **Alexander Robeson***, Sally Kornbluth, and Liguozhang. 2016. 'Mitotic phosphatase activity is required for MCC maintenance during the spindle checkpoint.', *Cell cycle*, 15: 225-33.

***Authors contributed equally to this work.**